MEASUREMENT AND SIMULATION OF SOIL WATER STATUS UNDER FIELD CONDITIONS

By

KENNETH COY STONE

A DISSERTATION PRESENTED TO THE GRADUATE SCHOOL
OF THE UNIVERSITY OF FLORIDA IN
PARTIAL FULFILLMENT OF THE REQUIREMENTS
FOR THE DEGREE OF DOCTOR OF PHILOSOPHY

UNIVERSITY OF FLORIDA

1987

ACKNOWLEDGEMENTS

The author would like to express his appreciation to Dr. Allen G. Smajstrla for his guidance, assistance and encouragement throughout this research. The author would like to thank his other committee members for their support and guidance throughout this research and in coursework taken under their supervision.

The author also expresses his appreciation to the Agricultural Engineering Department for the use of its research and computing facilities. Appreciation is also expressed to other faculty and staff members in the department for their assistance.

Special gratitude is expressed to the authors family for their continuous support and encouragement throughout his studies.

Finally, the author would like to express his very special graditude to his wife, Carol, for her drafting expertise, patience and continuous support and encouragement.

TABLE OF CONTENTS

Page

ACKNOWLEDGEMENTS ii

LIST OF TABLES v

LIST OF FIGURES vi

ABSTRACT x

CHAPTERS

I INTRODUCTION 1

II REVIEW OF LITERATURE 4

Measurement of Soil Water Status 4
Soil Water Content Measurement 4
Soil Water Potential Measurement 8
Automation of
Soil Water Potential Measurements 11
Water Movement in Soils 15
Soil Water Extraction 20

III METHODS AND MATERIALS 26

Equipment 26
Instrumentation Development 27
Field Data Collection 30
Model Development 33
One-Dimensional Model 36
Two-Dimensional Model 41
Soil Water Extraction 50

IV RESULTS AND DISCUSSION 54
Instrumentation Performance 54
Field Data Collection 60
Model Verification 70
Model Operation with Field Data 94
One-Dimensional Model 102
Two-Dimensional Model 109
Model Application 116

V SUMMARY AND CONCLUSIONS 124

Microcomputer-based Data Acquisition System 124
Field Data 124

Modeling Soil Water Movement and Extraction 125
Model Applications 125
APPENDICES

A. Alternating Direction Implicit Finite Differencing. . 126
B. Listing of Soil Water Movement and Extraction Model. .137

REFERENCES 163

BIOGRAPHICAL SKETCH 167

LIST OF TABLES

Table 3-1. Microcomputer-based data acquisition system components and approximate costs 28

Table 4-1. One-dimensional distribution of water extraction for a 15 day drying cycle for young citrus trees with and without grass cover 68

Table 4-2. Two-dimensional distribution of water extraction for a 15 day drying cycle for young citrus trees with grass cover 69

Table 4-3. Two-dimensional distribution of water extraction for a 4 day drying cycle for young citrus trees with and without grass cover 73

Table 4-4. One-dimensional distribution of water extraction for a 4 day drying cycle for a grass cover crop at water depletion levels of 20 kPa and 40 kPa 76

LIST OF FIGURES

Figure 2-1. A typical soil water characteristic curve 5

Figure 3-1. Layout of lysimeter system. 31

Figure 3-2. Details of individual lysimeter soil water status monitoring system. 32

Figure 3-3. Location of tensiometers in 1985 field experiment for young citrus trees in grassed and bare soil lysimeters. 34

Figure 3-4. Location of tensiometers in 1986 field experiment for young citrus trees in grassed and bare soil lysimeters. 35

Figure 3-5. Schematic diagram of the finite-difference grid system for the one-dimensional model of water movement and extraction. 38

Figure 3-6. Schematic diagram of the finite-difference grid system for the two-dimensional model of water movement and extraction. 44

Figure 3-7. Effect of the relative available soil water and potential soil water extraction rate on the soil water extraction rate. 53

Figure 4-1. Calibration curve of output voltage versus pressure applied for pressure transducer No. 1. . . 55

Figure 4-2. Calibration curve of digital units versus voltage applied for the analog-to-digital circuit used. 57

Figure 4-3. Comparisons of mercury manometer manually-read and pressure transducer automatically-read tensiometer water potentials during drying cycles for 2 tensiometers in the laboratory. 58

Figure 4-4. Comparisons of mercury manometer manually-read and pressure transducer automatically-read tensiometer water potentials for all laboratory data. 59

Figure 4-5. Evaluation of pressure transducer-tensiometer No. 1 by comparison of mercury manometer manually-read and pressure transducer automatically-read water potentials in the field. 61

Figure 4-6. Evaluation of pressure transducer-tensiometer No. 2 by comparison of mercury manometer manually-read and pressure transducer automatically-read water potentials in the field. 62

Figure 4-7. Evaluation of pressure transducer-tensiometer No. 3 by comparison of mercury manometer manually-read and pressure transducer automatically-read water potentials in the field. 63

Figure 4-8. Evapotranspiration rate from the 1985 field experiment with a 20 kPa soil water potential treatment young citrus tree with grass cover. . . . 66

Figure 4-9. Evapotranspiration rate from the 1985 field experiment with a 20 kPa soil water potential treatment young citrus tree with bare soil. 67

Figure 4-10. Evapotranspiration rate from the 1986 field experiment with a 20 kPa soil water potential treatment young citrus tree with grass cover. . . . 71

Figure 4-11. Evapotranspiration rate from the 1986 field experiment with a 20 kPa soil water potential treatment young citrus tree with bare soil. 72

Figure 4-12. Evapotranspiration rate from the 1986 field experiment with a 20 kPa soil water potential treatment with a grass cover. 74

Figure 4-13. Evapotranspiration rate from the 1986 field experiment with a 40 kPa soil water potential treatment with a grass cover. 75

Figure 4-14. Soil water potential-soil water content relationship for Rehovot sand. 79

Figure 4-15. Hydraulic conductivity-soil water content relationship for Rehovot sand. 80

Figure 4-16. Simulated results of soil water content profiles for infiltration into a Rehovot sand under constant rain intensity of 12.7 mm/hr. 81

Figure 4-17. Simulated results of soil water content profiles for infiltration into a Rehovot sand under constant rain intensity of 47 mm/hr. 82

Figure 4-18. Soil water potential-soil water content relationship for Yolo light clay. 83

Figure 4-19. Hydraulic conductivity-soil water content relationship for Yolo light clay. 84

Figure 4-20. Soil water potential-soil water content relationship for Adelanto loam. 85

Figure 4-21. Hydraulic conductivity-soil water content relationship for Adelanto loam. 86

Figure 4-22. Simulated results of soil water content profiles for infiltration into a Yolo light clay with initial pressure potential at -66 kPa. 87

Figure 4-23. Simulated results of soil water content profiles for infiltration into a Yolo light clay with initial pressure potential at -200 kPa. 88

Figure 4-24. Simulated results of soil water content profiles for infiltration into a Adelanto loam with initial pressure potential at -66 kPa. 89

Figure 4-25. Soil water potential-soil water content relationship for Nahal Sinai sand. 90

Figure 4-26. Hydraulic conductivity-soil water content relationship for Nahal Sinai sand. 91

Figure 4-27. Simulated results of dimensionless soil water content distribution for infiltration into a Nahal Sinai sand at 57 min of infiltration time. . 92

Figure 4-28. Simulated results of dimensionless soil water content distribution for infiltration into a Nahal Sinai sand at 297 min of infiltration time. . 93

Figure 4-29. Two-dimensional model simulated results of soil water content profiles for infiltration into a Rehovot sand under constant rain intensity of 12.7 mm/hr. 95

Figure 4-30. Two-dimensional model simulated results of soil water content profiles for infiltration into a Rehovot sand under constant rain intensity of 47 mm/hr. 96

Figure 4-31. Evapotranspiration rate from the second drying cycle of the 1985 field experiment with a 20 kPa soil water potential treatment young citrus tree with grass cover. 98

Figure 4-32. Distribution of evapotranspiration through the daylight hours. 99

Figure 4-33. Soil water potential-soil water content relationship for Arredondo fine sand. 100

Figure 4-34. Hydraulic conductivity-soil water potential relationship for Arredondo fine sand. 101

Figure 4-35. Simulation results for the one-dimensional model with field data for the 150 mm depth. 104

Figure 4-36. Simulation results for the one-dimensional model with field data for the 300 mm depth. 105

Figure 4-37. Simulation results for the one-dimensional model with field data for the 450 mm depth. 106

Figure 4-38. Simulation results for the one-dimensional model with field data for the 600 mm depth. 107

Figure 4-39. Simulation results for the one-dimensional model with field data for the 900 mm depth. 108

Figure 4-40. Simulation results for the two-dimensional model with field data for the 150 mm depth. 111

Figure 4-41. Simulation results for the two-dimensional model with field data for the 300 mm depth. 112

Figure 4-42. Simulation results for the two-dimensional model with field data for the 450 mm depth. 113

Figure 4-43. Simulation results for the two-dimensional model with field data for the 600 mm depth. 114

Figure 4-44. Simulation results for the two-dimensional model with field data for the 900 mm depth. 115

Figure 4-45. Soil water potentials for the three irrigation treatments at the 300 mm depth. 118

Figure 4-46. Soil water potentials for the three irrigation treatments at the 900 mm depth. 119

Figure 4-47. Soil water storage for the three irrigation treatments. 120

Figure 4-48. Cumulative irrigation for the three irrigation treatments. 121

Figure 4-49. Cumulative drainage from the soil profile for the three irrigation treatments. 122

Abstract of Dissertation Presented to the Graduate School
of the University of Florida in Partial Fulfillment of the
Requirements for the Degree of Doctor of Philosophy

MEASUREMENT AND SIMULATION OF SOIL WATER STATUS UNDER FIELD CONDITIONS

By

KENNETH COY STONE

May 1987

Chairman: Allen G. Smajstrla
Major Department: Agricultural Engineering

Irrigation of agricultural crops is one of the major uses of fresh water in Florida. Supplemental irrigation is required in Florida because the predominant sandy soils have very low water holding capacities, up to 70% of the annual rainfall occurs during months when many crops are not grown, and rainfall is not uniformly distributed. Under these conditions the scheduling of irrigation becomes extremely important. The timely application of irrigation water can result in increased yields and greater profits, while untimely applications could result in decreased yields and profits, and leaching of nutrients.

A low cost microcomputer-based data acquisition system for continuous soil water potential measurements was developed. The system consisted of tensiometer-mounted pressure transducers, an analog-to-digital converter and a portable microcomputer. The data acquisition system was evaluated under laboratory and field conditions. Excellent

agreement was obtained between soil water potentials read with the data acquisition system and those read manually using mercury manometers.

Experiments were conducted utilizing the data acquisition system to monitor soil water potentials of young citrus trees in field lysimeters to determine model parameters and to evaluate model performance. Evapotranspiration, soil water extraction rates and relative soil water extractions were calculated from the soil water potential measurements.

Two numerical models were developed to study the movement and extraction of soil water. A one-dimensional model was developed to describe a soil profile which is uniformly irrigated such as one which is sprinkler irrigated. The model was used to simulate soil water movement and extraction from a young citrus tree with grass cover in a field lysimeter. Simulated results were in excellent agreement with field observations.

A two-dimensional model was developed to describe a nonuniformly irrigated soil profile as in trickle irrigation. The model was used to simulate the two-dimensional movement and extraction of soil water from a young citrus tree with grass cover in a field lysimeter. The model results were in excellent agreement with field observations.

CHAPTER I
INTRODUCTION

Irrigation of agricultural crops is one of the major uses of fresh water in Florida. It was reported (Harrison et al., 1983) that in 1981, 41 percent of the fresh water use in Florida was for irrigation of more than 800,000 hectares of agricultural crops. Three reasons cited for supplemental irrigation in Florida were 1) sandy soils have very low water holding capacities, 2) up to 70 percent of the annual rainfall occurs during months when many crops are not grown, and 3) rainfall is not uniformly distributed even during months of high rainfall.

Because no control can be placed on when and where rainfall occurs, researchers must focus their attention on managing the soil water content in the plant root zone. One method of managing the water content in soils is to apply small amounts of irrigation water at frequent intervals. In the absence of rainfall, this provides agricultural plants with adequate water for growth and also minimizes losses from percolation below the root zone. With rainfall interactions, irrigation scheduling is more difficult; the objective is to minimize irrigation inputs (maximize effective rainfall) while optimizing production returns. Because of the complexity of these interactions, numerical models are useful tools to study them. Many researchers have developed models to use in the study of soil water management (Smajstrla, 1982; Zur and Jones, 1981). These models allow many different irrigation strategies to be investigated without the cost normally associated with field experiments. These models involve

analyses of infiltration, redistribution, evaporation and other factors which affect the movement and uptake of soil water by plants.

The objective of this research was to develop a data collection system and a numerical model which together will provide researchers with information needed for developing and validating models of soil water movement, crop water use and evapotranspiration. The instrumentation system developed will record soil water potentials on a real time basis in order to provide input data for model verification and validation. A microcomputer based instrumentation system will allow the computer to monitor inputs and make decisions based on the input data. The microcomputer will have the ability to monitor and control events in the field.

Two numerical models will be developed to study the movement and extraction of soil water. A one-dimensional model will be developed to describe the movement and extraction of soil water in a soil profile which is uniformly irrigated. A two-dimensional model will be developed to describe the movement and extraction of soil water from a soil profile which is not uniformly irrigated such as trickle irrigation.

The specific objectives of this research were:

1. To develop and test instrumentation for the real-time monitoring of soil water potential under agricultural crops.
2. To record the dynamics of soil water movement and water extraction under irrigated agricultural crops.
3. To develop a numerical model to simulate the soil water extraction patterns observed under agricultural crops as a function of irrigation management practices and climatic demands.

4. To demonstrate the use of the numerical model in evaluating and recommending irrigation strategies.

CHAPTER II
REVIEW OF LITERATURE

Measurement of Soil Water Status

The measurement of soil water can be classified into two catagories: (1) the amount of water held in a given amount of soil (soil water content), and (2) the potential, or tension with which the water is held by the soil (soil water potential). These properties are related to each other (Figure 2-1) and describe the ability of a soil to hold water available for plant growth.

Soil Water Content Measurement

Several methods are available to measure soil water content. The gravimetric method is the standard method of determining the soil water content. This method consist of physically collecting a soil sample from the field, weighing it, and oven drying the sample to constant weight at 105 C. The difference in weights before and after drying is the amount of water removed from the sample. Water contents can be calculated on a weight basis, or on a volume basis if the soil volume or bulk density was measured when the sample was taken. An advantage of the gravimetric method is that it requires no specialized equipment. Disadvantages are that it is laborious and time consuming. Destructive sampling is required and sampling may disturb a location sufficiently to distort results. This method does not lend itself to automation.

Neutron scattering allows the nondestructive measurement of soil water content. A neutron moisture meter may be used in the field to

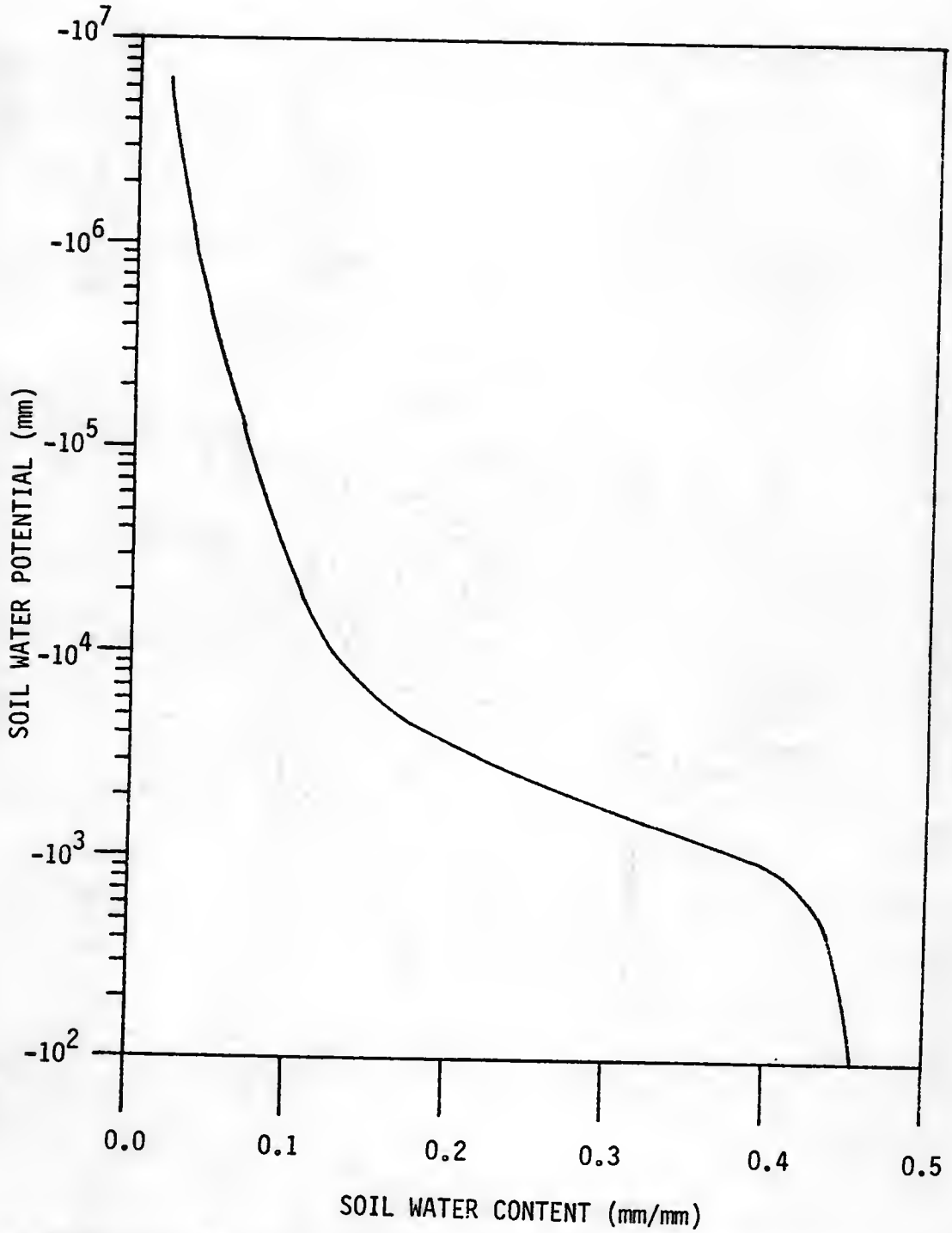

Figure 2-1. A typical soil water potential-soil water content curve.

rapidly and repeatably measure water contents in the same location and depth of soil. An access tube must be installed in the soil to allow a probe to be lowered to the desired soil depth for measurements.

The neutron scattering method operates on the principle of nuclear thermalization. Fast neutrons are emitted from a radiation source located on a probe which is lowered into the soil. These neutrons lose energy as they collide with hydrogen atoms in the soil and are slowed or thermalized. Thermalized neutrons are counted by a detector which is also located on the probe. The number of slow neutrons is an indirect measure of the quantity of water in the soil because of the hydrogen atoms present in water. Because the neutron method counts only hydrogen atoms, the method must be calibrated for each specific soil type and location. This is especially true for soils with variable quantities of organic matter because the neutron meter will also count hydrogen atoms in the organic matter and cause errors in the water content measurements.

With the neutron method, a spherical volume of soil is sampled as neutrons are emitted from the source. The radius of the sphere varies with the soil water content from a small radius for wet soils to 20 or 30 cm for very dry soils. This measurement over a relatively large volume is an advantage for homogenous soils with no discontinuities. However when discontinuities such as water tables exist, their exact locations cannot be detected accurately. Aribi et al. (1985) investigated the accuracies of neutron meters when measuring water contents near boundaries. They found that significant errors occurred when readings were taken within the top 0.4 meters in an unsaturated soil profile.

Another disadvantage of the neutron method is that the equipment cost is high. The radioactive material contained in the neutron meter is also a disadvantage because of the health hazards associated with radiation. The automation of a neutron meter would be very expensive and extremely complicated.

Gamma ray attenuation is a method which can be used to determine the soil water content. This method determines soil water content by measuring the amount of gamma radiation energy lost as a radiation beam is directed through a soil. The method depends on the fact that gamma rays lose part of their energy upon striking another substance, in this case soil water. As the water content changes, the amount of attenuation will also change.

Various types of gamma radiation instruments are available. One type is intended for laboratory or stationary use. This instrument has the source and detector parallel in line at a fixed distance apart, and a soil column is placed between them. The source and detector are then moved along the length of the soil column to determine the water content distribution in the column. This would not be practical for field application.

A second type of gamma radiation instrument has been developed for field application. This instrument requires that two parallel access tubes be installed into the soil. The source is placed in one access tube and the detector in the other. Radiation is focused into a narrow beam between the source and detector, and soil water content can be measured in very thin layers of soil.

Another type of gamma radiation instrument consists of a stationary detector located at the soil surface and a source located on a probe

which is lowered into the soil. The relationship between the source and detector is known, and thus changes in density with depth can be measured accurately with this instrument. Because the detector is located at the soil surface, the instrument is limited to the top 30 cm of the profile.

Gamma radiation instruments are expensive, and they can be hazardous due to the radioactive source. This type of instrument would be very difficult and expensive to automate.

Additional research has been conducted to utilize other soil properties which would lend themselves to rapid methods of soil water content determination. Fletcher (1939) conducted work on a dielectric method of estimating soil water content. He used a resonance method to determine the dielectric constant of the soil. This type of instrument consists of an ocillator circuit and a tuned receiving circuit. The instrument is placed in the soil and allowed to equilibrate. A variable capacitor in the receiving circuit is then tuned to resonance, and the capacitor reading is correlated with the soil water content. This instrument must be calibrated for each soil in which it is used. Such a device is not known to be commercially available.

Most of the methods discussed produce indirect measurements of soil water content. Soil water content is calibrated to other factors such as neutron thermalization, gamma ray attenuation or dielectric properties. Only the gravametric method yields a direct measure of soil water content.

Soil Water Potential Measurement

An alternative to the measurement of soil water content is the measurement of soil water potential. A tensiometer measures the

potential or tension of water in the soil. The tensiometer consists of a closed tube with a ceramic cup on the end which is inserted into the soil and a vacuum gage or manometer to measure the water potential in the tensiometer tube. The tube is filled with water, closed and allowed to equilibrate with the soil water potential. As the soil dries, water in the tensiometer is pulled through the ceramic cup. The soil water potential which pulls water through the ceramic cup is registered on the vacuum gage or manometer. This force is also the hydraulic potential that a plant would need to exert to extract water from the soil. Therefore, a tensiometer measures the energy status of water in the soil. Tensiometers left in the soil for a long period of time tend to follow the changes in the soil water potential.

The hydraulic resistance of the ceramic cup, the surrounding soil, and the contact between the cup and soil cause tensiometer readings to lag behind the actual tension changes in the soil. Lags are also caused by the volume of water needed to be moved through the cup to register on the measuring device. The useful range of tensiometers is from 0 to -80 kPa. Below -80 kPa air enters through the ceramic cup or the water column in the tensiometer breaks, causing the tensiometer to fail. This measurement limitation is not serious for irrigated crops on sandy soils because most of the available water for plant use occurs between 0 and -80 kPa.

Another method of measuring soil water potential is the thermal conductance method. The rate of heat dissipation in a porous material of low heat conductivity is sensitive to the water content in the porous material. When in contact with a soil, the water potential in the porous material tends to equilibrate with the soil water potential.

Phene et al. (1971) developed an instrument to measure soil water potential by sensing heat dissipaton within a porous ceramic. The water potential of the porous ceramic was measured by applying heat at a point centered within the ceramic and measuring the temperature rise at that point. Soil water potential measurements were obtained by taking two temperature readings. The first one was taken before the heating cycle and the second after the heating cycle. The difference between the two temperature measurements was the change in temperature at the center of the sensor due to the heat applied. The magnitude of the difference varies depending on the water content of the porous block. Phene stated that the sensor should measure the soil water potential regardless of the soil in which it is embedded.

In experimental applications of the heat pulse device, the accuracy of the sensor was $\pm$ 20 kPa over the range 0 to -200 kPa. In Florida sandy soils such a wide range of variability would not be acceptable because most of the available soil water is contained in the soil between field capacity and -20 kPa. Calibration for individual soils could improve the accuracy of the instrument. This instrument has the capability of allowing automated data collection and is nondestructive. The cost of the individual sensors and the associated data recording devices is relatively high.

Soil psychrometers are instruments which can be used to measure soil water potentials in the range of -1 to -15 bars. They operate by cooling a thermocouple junction which is in equilibrium with the soil to the point of water condensation on the junction, and then measuring the junction temperature as water is allowed to evaporate. Thus the temperature depression due to evaporation can be related to soil water

tension. Only small responses are obtained at potentials above -1 bar, making this instrument unsuitable for irrigation scheduling on sandy soils where irrigations would typically be scheduled at much greater potentials.

Electrical resistance blocks can be correlated with soil water potential. The blocks are placed in the soil and allowed to equilibrate with the soil water. Resistance blocks usually contain a pair of electrodes embedded in gypsum, nylon or fiberglass. Measurements with resistance blocks are sensitive to the electrolytic solutes in the fluid between the electrodes. Thus resistance blocks are sensitive to variations in salinity of soil water and to temperature changes. Temperatures must be measured and resistance readings appropriately corrected.

Resistance blocks are not uniformly sensitive over the entire range of soil water content. They are more accurate at low water contents than at water contents near field capacity. Because of this limitation, resistance blocks can be used to complement tensiometers to measure soil water potentials below the -80 kPa range. They are relatively inexpensive, and an automated data collection system may be built around these instruments for measuring water potentials in drier soils.

Automation of Soil Water Potential Measurements

The instruments discussed may all be used to measure the status of soil water. Most of the techniques relate a soil property to another property which is measured by the instrument. Two of the methods allow a direct measure of a soil property. The gravimeteric method gives a direct measure of soil water content and tensiometers give direct measurement of soil water potential. The gravimetric measurement method

requires destructive sampling and does not lend itself to automation. Tensiometers may be automated by recording the changes in soil water potential, and they do not require destructive sampling. Therefore, to measure the status of soil water under a growing crop, an automated data collection system using tensiometers to measure soil water potential was chosen.

To determine the soil water potential, the water potential within the tensiometer is measured. The tensiometer water potential is assumed to be in equilibrium with the soil water potential. Early methods of measuring tensiometer water potentials used mercury manometers. Later, mechanical vacuum gauges were used. Both methods functioned well for manual applications. Neither, however, was readily automated.

Recent interest in better understanding the dynamics of soil water movement, and in the development of numerical models to simulate this process, has resulted in the need for an automated system of recording tensiometer readings on a continuous real time basis.

Van Bavel et al. (1968) used a camera to take periodic photographs of a tensiometer manometer board. By analyzing the photographs they were able to record changes in potentials. This procedure was, however, laborious and did not provide continuous soil water potential records.

Enfield and Gillaspy (1980) developed a transducer which measured the level of mercury in a mercury manometer tensiometer. The principle of operation of their transducer was the same as a concentric capacitor. The level of mercury in the manometer corresponds directly to the length of a capacitor plate. A steel tube was used as the outer capacitor plate around a column of mercury. The nylon tube which contained the mercury column acted as the dielectric material. The capacitance of the

transducer was measured and converted to length of the column of mercury. This instrument was found to be very sensitive to temperature fluctuations. Further research is needed on this transducer to make it suitable for applications in automated data collection systems.

Fitzsimmons and Young (1972) used a tensiometer-pressure transducer system to study infiltration. Their system consisted of a pressure transducer which was connected to many tensiometers by a system of fluid switches. This system required substantial time lags after switching a tensiometer to the transducer before an accurate reading could be made. This was primarily due to changes in volume due to the elasticity of the system. This resulted in a large scanning time in order to read all tensiometers. Long and Hulk (1980) used a similar system.

Bottcher and Miller (1982) developed an automatic manometer scanning device which read and recorded mercury levels in manometer-type tensiometers. The system consisted of a computer-controlled chain-drive mechanism which moved photocells and light sources up and down the manometer tubes. When the scanner passed a mercury-water interface, a change in voltage was detected by the computer. This system is expensive, uses specially constructed rather than commercially-available components, and is not readily expandable. It also requires the use of a central manometer board with connecting tubing from the various tensiometers. It has the advantage of easy verification of computer readings by manual reading of the manometers.

Marthaler et al. (1983) used a pressure transducer to read individual tensiometers. The upper end of the tensiometers was closed off with septum stoppers to provide air-tight seals through which a needle connected to a pressure transducer was inserted. The needle was

inserted into a pocket of entrapped air in the tensiometer, and the pressure transducer output was obtained immediately. This method introduced an error because the air pocket was compressible and was affected by the addition of air at atmospheric pressure in the needle, transducer, and connectors. This system was designed to minimize errors by minimizing the volume of air introduced into the tensiometer. The tensiometer air pockets were, however, temperature sensitive and introduced diurnal time lags because of expansion and contraction due to diurnal temperature changes. Also, to read several instruments, the pressure transducer was required to be moved manually. Thus, this type of system does not lend itself to automation.

Thomson et al. (1982) used individual pressure transducers on tensiometers with all air purged from the system to monitor soil water potentials. Thus, they were able to avoid lag times associated with air pockets in the tensiometers. They were able to read pressure transducers very rapidly by electronic rather than hydraulic switching.

A soil water potential monitoring system that used pressure transducers as used by Thomson et al. (1982) would be able to record data from a number of sensors very rapidly. A continuous data acquisition system based on tensiometer-mounted pressure transducers would provide data necessary for models of movement of water in soils, crop water use, and evapotranspiration. The use of a microcomputer to monitor the pressure transducers would allow the system to be programmed to make decisions based on the input data (Zazueta et al., 1984). Also, the cost of a dedicated data acquisiton system would be greater than that of a microcomputer-based system because of current microcomputer costs and availability.

Water Movement in Soils

The general equations governing unsaturated flow in porous media are the continuity equation and Darcy's Law. Hillel (1980) presented a combined flow equation which incorporates the continuity equation

$$\frac{\partial \theta}{\partial t} = - \nabla \cdot q - S \tag{1}$$

where q = flux density of water,

θ = volumetric water content,

∇ = differential operator,

t = time, and

S = a sink or source term,

with Darcy's equation for unsaturated flow

$$q = - K(h) \nabla H \tag{2}$$

where K = hydraulic conductivity,

H = the total hydraulic head and defined as

$H = h - z$, and

h = capillary pressure head.

The resulting combined flow equation for both steady and transient flows is also known as Richards equation

$$\frac{\partial \theta}{\partial t} = \nabla \cdot (K(h) \nabla H) - S \tag{3}$$

For one-dimensional vertical flow, equation (3) becomes

$$\frac{\partial \theta}{\partial t} = \frac{\partial}{\partial z} \left(K(h) \frac{\partial h}{\partial z} \right) - \frac{\partial K(h)}{\partial z} - S(z,t) \tag{4}$$

where z = the vertical dimension.

The sink term is used to represent the loss or gain of water from the soil by root extraction or by application of irrigation water from a point source.

For implicit solutions, equation (4) must be written in terms of only one variable, soil water content or potential. By introducing the specific water capacity, C, defined as

$$C = \frac{d\theta}{dh} \tag{5}$$

and using the chain rule of calculus, equation (4) may be written in terms of the soil water potential as

$$C \frac{\partial h}{\partial t} = \frac{\partial}{\partial z}\left(K(h) \frac{\partial h}{\partial z}\right) - \frac{\partial K(h)}{\partial z} - S(z,t) \tag{6}$$

For two-dimensional flow, equation (3) becomes

$$C \frac{\partial h}{\partial t} = \frac{\partial}{\partial x}\left(K(h) \frac{\partial h}{\partial x}\right) + \frac{\partial}{\partial z}\left(K(h) \frac{\partial h}{\partial z}\right) - \frac{\partial K(h)}{\partial z} - S(x,z,t) \tag{7}$$

The two-dimensional flow equation written in radial coordinates with radial symmetry may be written as

$$C \frac{\partial h}{\partial t} = \frac{1}{r} \frac{\partial}{\partial r}\left(r\, K(h) \frac{\partial h}{\partial r}\right) + \frac{\partial}{\partial z}\left(K(h) \frac{\partial h}{\partial z}\right) - \frac{\partial K(h)}{\partial z} - S(x,z,t) \tag{8}$$

The two-dimensional flow equation in radial coordinates may be used to describe water movement and extraction of soil water from nonuniform water applications such as trickle irrigation.

Due to the variable nature of K(h), equations (6), (7) and (8) are highly nonlinear, and analytical solutions are extremely complex or

impossible to obtain. The nonlinearity of equations (6) and (7), and the typical variable boundary conditions, have led to the use of numerical methods to solve practical problems of soil-plant-water relationships, such as irrigation management for agricultural crops.

For one-dimensional flow, equation (6) has been successfully solved using explicit finite difference methods by many researchers. Hanks and Bowers (1962) developed a numerical model for infiltration into layered soils. They solved the Richards equation for the hydraulic potential using implicit finite difference equations with a Crank-Nicholson technique which averages the finite differences over two successive time steps. Rubin and Steinhardt (1963) developed a numerical model to study the soil water relationships during rainfall infiltration. They used a Crank-Nicholson technique to solve Richards equation for the water content. Rubin (1967) developed a numerical model which analyzed the hysteresis effects on post-infiltration redistribution of soil water.

Haverkamp et al. (1977) reviewed six numerical models of one-dimensional infiltration. Each model employed different discretization techniques for the nonlinear infiltration equation. The models reviewed were solved using both the water content based equation and the water potential based equation. They found that implicit models which solved the potential based infiltration equation had the widest range of applicability for predicting water movement in soil, either saturated or nonsaturated.

Clark and Smajstrla (1983) developed an implicit model of soil water flow to study the distribution of water in soils as influenced by various irrigation depths and intensities. The model simulated water application rates from center-pivot irrigation systems with intensities

of application typical of low and high pressure irrigation systems. Their model also simulated post-infiltration redistribution.

Rubin (1968) developed a two-dimensional numerical model of transient water flow in unsaturated and partly unsaturated soils. He utilized alternating-direction implicit (ADI) finite difference methods. He studied horizontal infiltration and ditch drainage with the numerical model. Hornberger et al. (1969) developed a two-dimensional model to study water movement in a composite soil moisture groundwater system. They modeled the two-dimensional response of falling water tables. They considered both saturated and unsaturated zones in their model. The solution method used was a Gauss-Sidel iterative technique.

A two-dimensional model to simulate the drawdown in a pumped unconfined aquifer was developed by Taylor and Luthin (1969). The model gave simultaneous solutions in both the saturated and unsaturated zones. They used a Gauss-Sidel iterative method to solve the flow equations.

Amerman (1969) developed two-dimensional numerical models to simulate steady state saturated flow, drainage and furrow irrigation. He used ADI methods to solve both the steady state saturated flow model and the furrow irrigation model. He also used an explicit method to solve the drainage model.

A study of the sensivity of the grid spacing for finite difference models was reported on by Amerman and Monke (1977). Two finite difference models of two-dimensional infiltration were analyzed. They solved the two-dimensional flow equations with successive overrelaxation (SOR) and alternating direction implicit (ADI) methods. They found that smaller grid sizes were needed in regions where the hydraulic gradients

changed rapidly. Considerable computational savings without appreciable loss of accuracy was achieved using irregular grid sizes.

Perrens and Watson (1977) developed a two-dimensional numerical model of water movement to analyze infiltration and redistribution. They used an iterative alternating direction implicit technique to solve the flow equation. Two soil types, a sand and a sandy loam, were simulated. Nonuniform surface fluxes were applied along the horizontal soil surface in a step type distribution pattern. They also incorporated hysteresis of soil hydraulic characteristics into the model to be used in the redistribution phase of the simulations.

Researchers have also utilized two-dimensional models to study soil water movement from trickle irrigation systems. Brandt et al. (1971) solved the flow equation in two dimensions to analyze infiltration from a trickle source. They developed a plane flow model in cartesian coordinates to analyze infiltration from a line source of closely spaced emitters with overlapping wetting patterns. They also developed a cylinderical flow model to analyze infiltration from a single emitter when its wetting pattern is not affected by other emitters. Both models were solved using noniterative ADI finite difference procedures with Newton's iterative method. The results were compared to an analytical solution of steady infiltration and a one-dimensional solution with good results.

Armstrong and Wilson (1983) developed a model for moisture distribution under a trickle source. They utilized the Continuous System Modeling Program (CMSP) to simulate the soil moisture movement. The model calculated the net flow rates into each grid. It then calculated the change in water content by dividing the net flow rate

by the volume of soil in each grid and then multiplying by the time step. Finally, the model calculated the new water contents from the previous water contents plus the calculated water content changes. Model results compared favorably with field measurements.

Zazueta et al. (1985) developed a simple explicit numerical model for the prediction of soil water movement from trickle sources. The model was based on the mass balance equation and an integrated form of Darcy's law. The model produced good agreement with other results obtained with more complicated numerical methods and analytical solutions.

Soil Water Extraction

Water uptake by plant roots has been investigated by many researchers. Among the first researchers to attempt to describe plant water relations were Gradmann (1928) and van den Honert (1948). Two approaches to modeling water extraction have been utilized to describe the water extraction by plant roots. The first, called the microscopic approach, describes water movement to individual roots. The second approach, called the macroscopic water extraction model, describes water uptake by the whole root zone, and the flow to individual roots is ignored.

Gardner (1960) developed a microscopic water uptake model. He described the root as an infinitely long cylinder of uniform radius and water-absorbing properties, assuming that water moves in the radial direction only. The flow equation for such a system is

$$\frac{\partial \theta}{\partial t} = \frac{1}{r}\frac{\partial}{\partial r}\left(r D \frac{\partial \theta}{\partial r} \right) \qquad (9)$$

where θ = the volumetric water content,

D = the diffusivity,

t = the time and

r = the radial distance from the axis of the root.

He then obtained a solution at the boundary between the plant root and the soil in order to maintain a constant rate of water movement to the plant, subject to the following boundary conditions:

$$\theta = \theta_o, \quad h = h_o, \quad \text{at } t = t_o, \quad \text{and}$$

$$2 \pi r_1 k\left(\frac{dh}{dr}\right) = 2 \pi r_1 D \left(\frac{d\theta}{dr}\right) = q \quad \text{at } r = r_1 \tag{10}$$

where k = the hydraulic conductivity of the soil,

r_1 = the radius of the root, and

q = the rate of water uptake by the root.

The solution of (9) subject to the initial and boundary conditions in (10) is

$$h - h_o = dh = \frac{q}{4 \pi k}\left(\ln \frac{4Dt}{r^2} - g\right) \tag{11}$$

where $g = 0.57722$ is Euler's constant. The diffusivity and conductivity were assumed to be constant, this assumption was justified because D, r and t are all in the logarithmic term, and dh is thus not very sensitive to these variables.

Gardner (1960) also noted that the solution will behave as though infinite for only very short times or for very low values of hydraulic conductivity. Exact solutions of the problem for finite systems would require taking the dependence of D and k upon the soil water potential into account. Gardner also compared equation (11) with the steady-state solution for flow in a hollow cylinder:

$$h - h_o = dr = \frac{q}{4 \pi k} \left(\ln \frac{b^2}{a^2} \right) \qquad (12)$$

where h_o = the potential at the outer radius of the hollow cylinder,

b = one half the distance between neighboring roots, and

h = the potential at the inner radius a.

If $b = 2\sqrt{Dt}$, then equation (12) is identical to equation (11) except for the g term which is small compared to the logarithmic term and may be ignored.

Gardner and Ehlig (1962) presented a macroscopic water uptake equation in which the rate of water uptake is proportional to the potential energy gradient and inversely proportional to the impedance to water movement within the soil and the plant. The potential energy was expressed as the difference between the diffusion pressure deficit and the soil suction. The impedance was expressed as the sum of plant impedance and soil impedance. They analyzed greenhouse experiments and obtained results consistent with the uptake equation.

Molz and Remson (1970) developed a mathematical model describing moisture removal from soil by plant roots. The model described one-dimensional water movement and extraction. The model used a macroscopic water extraction term to describe moisture removal by plants. Their formula for the extraction term was given as

$$S(z,t) = T \left(\frac{R(z)\ D(\theta)}{\int R(z)\ D(\theta)\ dz} \right) \qquad (13)$$

where $D(\theta)$ = diffusivity,

$R(z)$ = the effective root density,

T = the transpiration rate per unit area and

v = the root depth.

The model gave results that compared reasonably with experimental results. The numerical solution of the Richards equation with the extraction function was obtained using the Douglas-Jones predictor-corrector method.

Nimah and Hanks (1973) developed a numerical model to predict water content profiles, evapotranspiration, water flow in the soil, root extraction, and root water potential under field conditions. Their extraction term had the form

$$A(z,t) = \frac{(Hroot + (1.05\ z) - h(z,t) - s(z,t))\ RDF(z)\ K(\Theta)}{\Delta x\ \ \Delta z} \qquad (14)$$

where $A(z,t)$ = the soil water extraction rate,

$Hroot$ = the effective water potential in the root at the soil surface,

$h(z,t)$ = the soil matric potential,

$s(z,t)$ = the osmotic potential,

$RDF(z)$ = proportion of total active roots in depth increment DZ,

$K(\Theta)$ = the hydraulic conductivity and

Δx = the distance between the plant roots at the point where $h(z,t)$ and $s(z,t)$ are measured.

Tollner and Molz (1983) developed a macrocopic water uptake model. The extraction function assumed that water uptake rate per unit volume of soil is proportional to the product of contact length per unit soil volume, root permeability per unit length and water potential difference between soil and root xylem potential. A factor which accounts for reduced root-soil-water contact as water is removed was included in the

extraction function. Their model predictions were comparable with results of a greenhouse experiment.

Slack et al. (1977) developed a mathematical model of water extraction by plant roots as a function of leaf and soil water potentials. The model used a microscopic model to calculate water uptake which was input into a macroscopic model of water movement and water uptake. Water movement was described by a two-dimensional radial flow model. The model was used to estimate transpiration from corn grown in a controlled environment under soil drying conditions. The model predicted daily transpiration adequately for the period modeled.

Feddes et al. (1978) developed an implicit finite difference model to describe water flow and extraction in a non-homogeneous soil root system under the influence of groundwater. Their extraction term assumed the extraction rate to be maximum when the soil water potential was above a set limit. When the soil water potential fell below this limit, the water uptake, S(h), was decreased linearly with the soil water potential

$$S(h) = Smax \frac{(h - h3)}{(h2 - h3)} \qquad (15)$$

where h2 is the set limit below which the water uptake decreases linearly to h3. Below h3 it was assumed that no water is extracted, then h3 may be assumed to be the wilting point. The maximum possible transpiration rate divided by the effective rooting depth is Smax. The model yielded satisfactory results in predicting both cumulative transpiration and distribution of soil moisture content with depth.

Zur and Jones (1981) developed a model for studying the integrated effects of soil, crop and climatic conditions on the expansive growth, photosynthesis and water use of agricultural crops. The model utilized Penman's equation modified by Monteith to calculate the water vapor transport from the plant to the atmosphere. It utilized a macroscopic soil water extraction term to calculate water uptake from the soil. The model assumed the water uptake from the soil was the difference between the total water potential at the root surface and the soil water potential divided by the sum of the resistance to radial water flow inside the roots and resistance of water flow in the soil. The model treated the water relations in plants in considerable detail. It was successfully tested on soybeans. However the model did not take into consideration infiltration, drainage, evaporation from the soil surface or upward movement of water in the soil.

CHAPTER III
MATERIALS AND METHODS

Equipment

The data acquisition system developed in this research was based on tensiometer-mounted pressure transducers. Pressure transducers used were Micro Switch model 141PC15D. These transducers measured pressures from 0 to -100 kPa. They produced an analog electrical output from 1 to 6 volts which was proportional to the vacuum exerted on a membrane in the transducers. The transducers operated much like strain gages. One side of the membrane was open to the atmosphere and the other side was in contact with water in the tensiometer. As pressure on the water changed, the membrane was deformed and the voltage across the membrane changed.

The pressure transducers required an 8-volt direct current (VDC) power supply at 8 mA each. Because a multiple-transducer system was developed, a separate regulated power supply was used rather than the microcomputer power supply. This assured adequate power for the transducers.

The pressure transducers were temperature-compensated. Outputs varied less than 1% of full scale output in the range of 5 C to 45 C.

The output voltages from the pressure transducers were interfaced to a microcomputer through an analog-to-digital (A/D) board. The A/D board was a Mico World MW-311 general purpose Input/Output Board. This device had 8-bit resolution and measured input voltages from 0 to 5 volts. It had 16-channel multiplexing capability.

The microcomputer used was a Commodore 64. It was selected for its programmability, its availability at local electronics supply companies, and its low cost. An overall goal in component selection was to be able to replace any component individually with as little down-time as possible, and thus to assure the reliability of the system.

The microcomputer output was to a video screen, a printer, and a cassette recorder. The cassette recorder provided storage of data for later computations and easy transfer to other computer systems. The printer provided a hard copy backup of data. The video screen provided immediate interaction with the computer for programming and monitoring.

The microcomputer was programmed in the BASIC computer language. It had approximately 32 kilobytes of programmable memory (RAM) when using the BASIC computer language. This was sufficient to store the calibration equations and calculated outputs from the transducer inputs. The microcomputer also had an internal 24-hour clock which was required for real-time data acquisition. Data acquisition system components and approximate costs are given in Table 3-1.

Instrumentation Test Procedure

Pressure transducers were individually calibrated using a regulated vacuum source and a mercury manometer. Measurements of transducer voltages and mercury column heights were made at decreasing pressure increments of approximately -10 kPa from 0 to approximately -80 kPa. To determine whether the transducers displayed hysteretic behavior, calibrations were continued at increasing pressure increments from -80 kPa to 0 kPa.

Table 3-1. Microcomputer-based data acquisition system components and approximate costs.

Component	Cost($)
Microcomputer	100
Printer	100
Cassette Recorder	60
Pressure Transducer	68
Tensiometer	40
Analog-to-Digital and Multiplexing Circuit	200
Transducer Power Supply	50

A/D boards were calibrated while interfaced with the microcomputer. Known voltages were applied to the boards and the digital outputs read by the computer were recorded.

Calibrated pressure transducers were interfaced to the tensiometers by drilling small holes into the walls of the tensiometers. Access ports on the transducers were inserted into the tensiometers and the connections were sealed with silicone sealant. The pressure transducer-equipped tensiometers were connected to the computer using 3-lead 22 gauge electrical hookup wire.

Two tests of the functioning of the microcomputer-based tensiometer pressure transducer system were conducted. The first was conducted in the laboratory. Three mercury manometer tensiometers were equipped with pressure transducers and interfaced with the microcomputer. The tensiometers were serviced to remove air from the system. The ceramic cups were then exposed to the atmosphere and allowed to dry for several hours. Microcomputer readings and mercury manometer readings were taken for comparison at random intervals during drying. Data collection continued throughout the tensiometer range. Three replications were taken.

The second test of the tensiometer-pressure transducer system was conducted under field conditions. Three instrumented mercury manometer tensiometers were installed in a field lysimeter system with grass cover. The microcomputer was located in the field laboratory office 25 m from the sensors. Tensiometers were serviced and allowed to equilibrate with the soil water potential. The microcomputer was programmed to read the pressure transducers hourly. Mercury manometers were read manually at random intervals, typically 2 or 3 times per day

during the field evaluation. Manual mercury manometer readings were compared with the microcomputer readings to assess the accuracy of the instrumentation under field conditions. Instrumentation was evaluated for 3 1-week periods. Tensiometers were serviced to remove entrapped air between 1-week analysis periods.

Field Data Collection

A field lysimeter system was used to monitor soil water status and water uptake from young citrus trees. The field lysimeter system was located at the Irrigation Research and Education Park in Gainesville, Fl. Layout of the lysimeters is shown in Figure 3-1. The lysimeters were cylindrical steel tanks with one end open. Tanks were installed with the open end upward, exposing a circular surface production area of 2 m^2. Soil profiles were 1.8 m deep. The soil in the lysimeters was Arredondo Fine Sand, (hyperthermic, coated, Typic Quartzipsamment), which was hand packed to approximate the physical characteristics of an undisturbed soil profile. Drainage of excess water from the bottom of each lysimeter was accomplished using either a porous stone or porous ceramic cup located in the bottom of the tank as shown in Figure 3-2. A vacuum pump removed the water from the lysimeters and the water was trapped in PVC cylinders. The PVC cylinders were used to measure the drainage from each lysimeter. Automated rainfall shelters were used to cover the lysimeters in the event of rainfall. Additional details of the construction and operation of the lysimeters were given by Smajstrla (1985).

Data collection was conducted in two phases. In 1985 two lysimeters were instrumented, and data were collected as described earlier. Each lysimeter contained a young citrus tree approximately 3

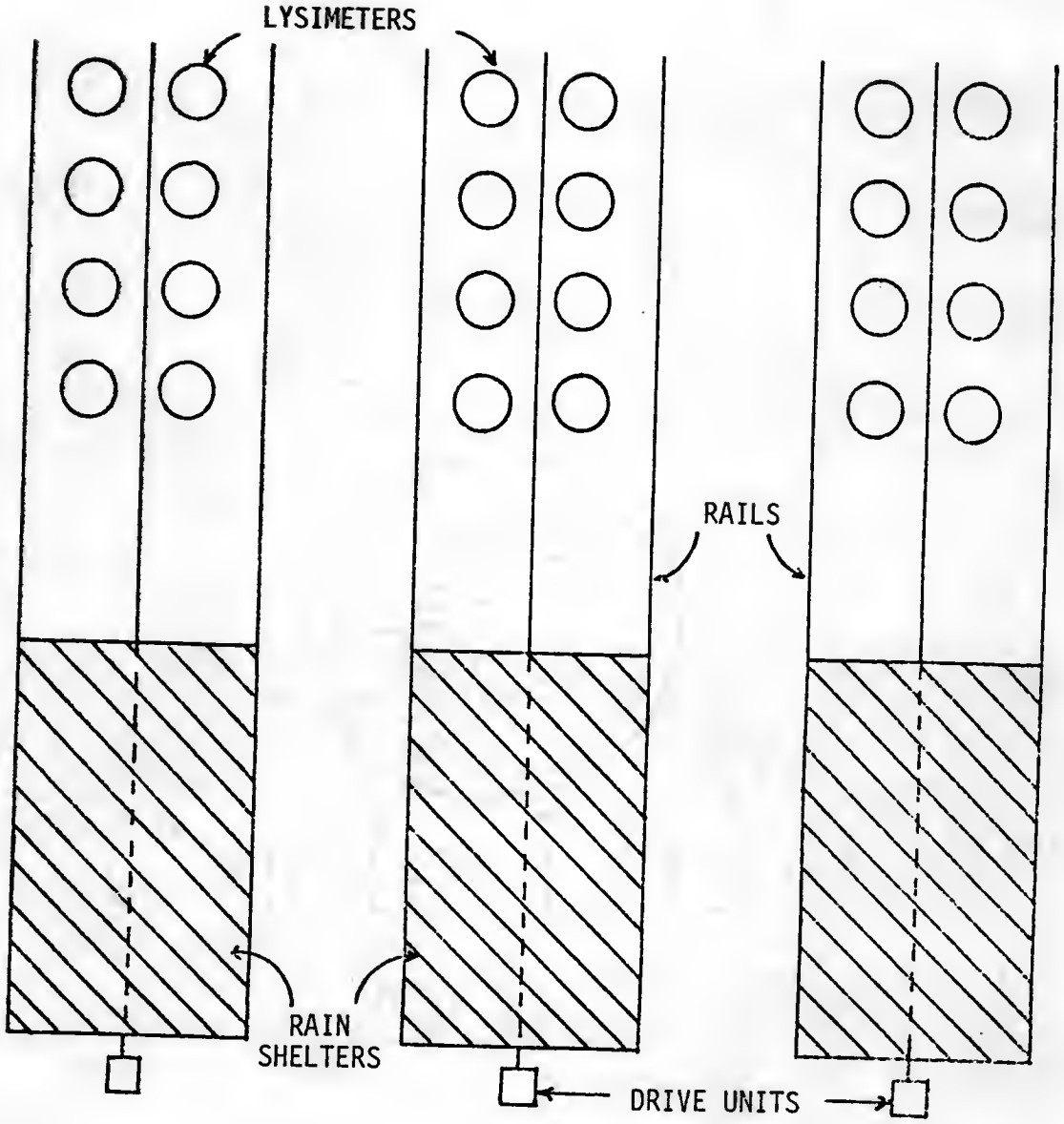

Figure 3-1. Layout of lysimeter system.

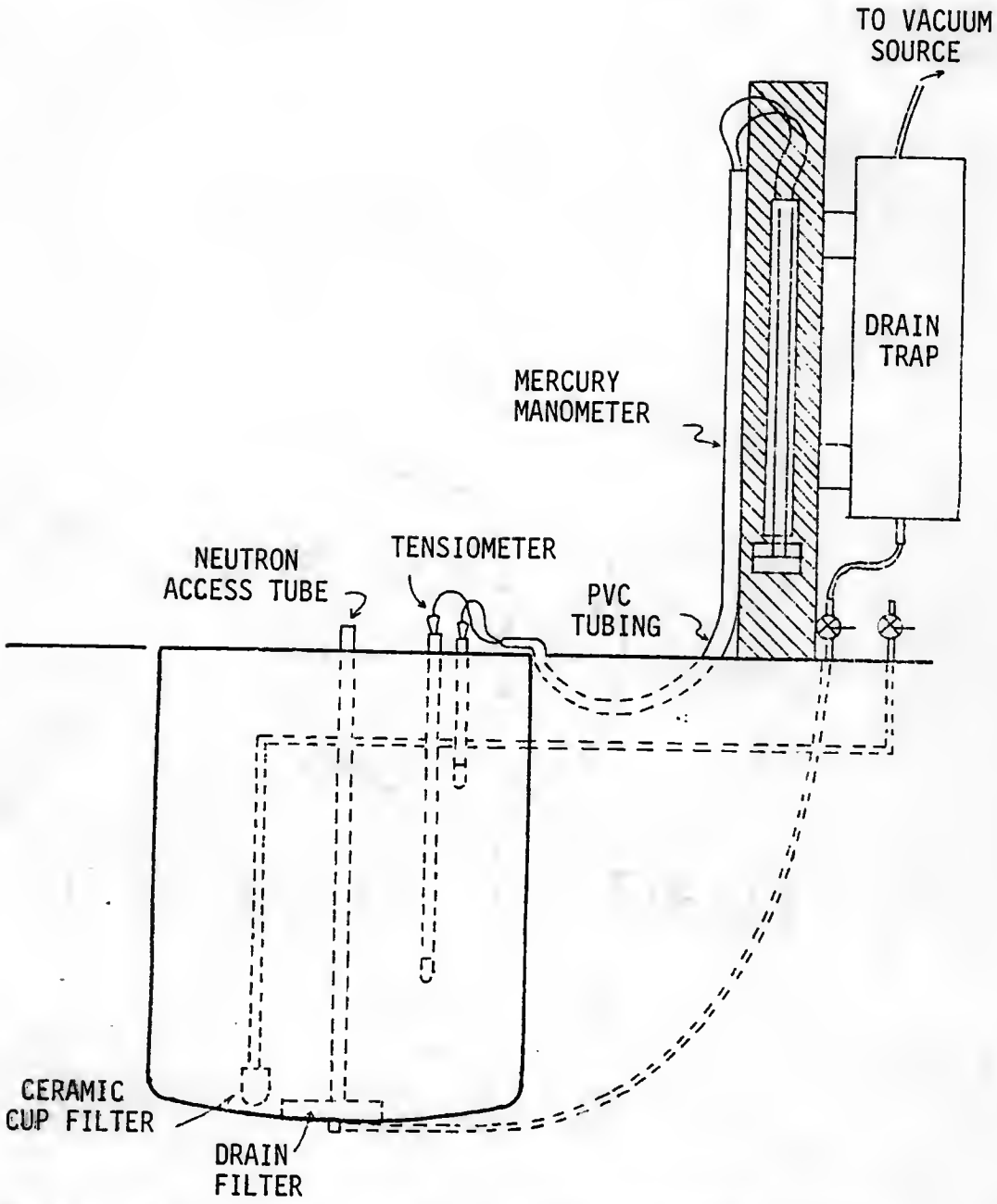

Figure 3-2. Details of individual lysimeter soil water status monitoring system.

years old. Both lysimeters were irrigated when the water potential in the lysimeter dropped below -20 kPa. The -20 kPa water potential corresponded to approximately a 44% water depletion from field capacity. One lysimeter had a grass cover crop and the second had bare soil. These two cover practices were used to simulate different cultural practice effects upon the young citrus in a related experiment.

Tensiometers were installed at radii of 100, 300, 500 and 700 mm from the center of the lysimeter, and at depths of 150, 300, 450, 600 and 900 mm as shown in Figure 3-3. Data were collected with the microcomputer based data acquisition system at 10 minute intervals and averaged over hourly periods.

In 1986 two lysimeters with young citrus trees were instrumented with the same water and cover treatments as in 1985. Tensiometers were installed in the lysimeters at radii of 130, 380 and 630 mm and at depths of 150, 300, 450, 600, 900 and 1020 mm as shown in Figure 3-4. In addition to the two lysimeters with young citrus trees, two lysimeters with only grass cover were instrumented. The water potential treatments for the two grassed lysimeters were -20 kPa and -40 kPa. The -40 kPa water potential corresponded to approximately a 50% water depletion from field capacity.

Model Development

A computer program describing the infiltration, redistribution and extraction of soil water was written in the FORTRAN computer language. A Prime 550 computer was used for all computations.

Several assumptions were employed in the development and use of the numerical models to ease the complexities associated with mathematically describing water movement in unsaturated porous media. These

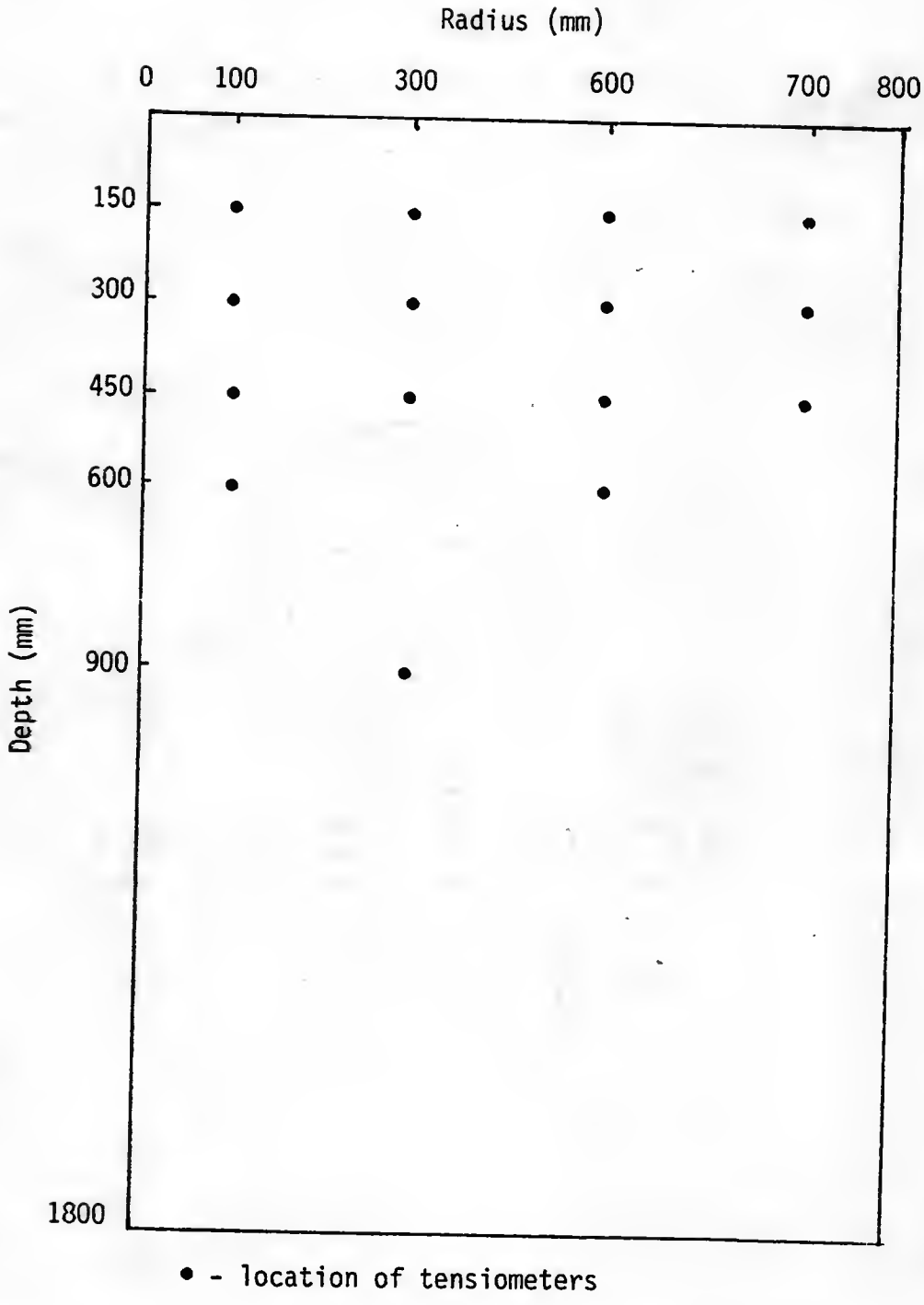

Figure 3-3. Location of tensiometers in 1985 field experiment for young citrus trees in grassed and bare soil lysimeters.

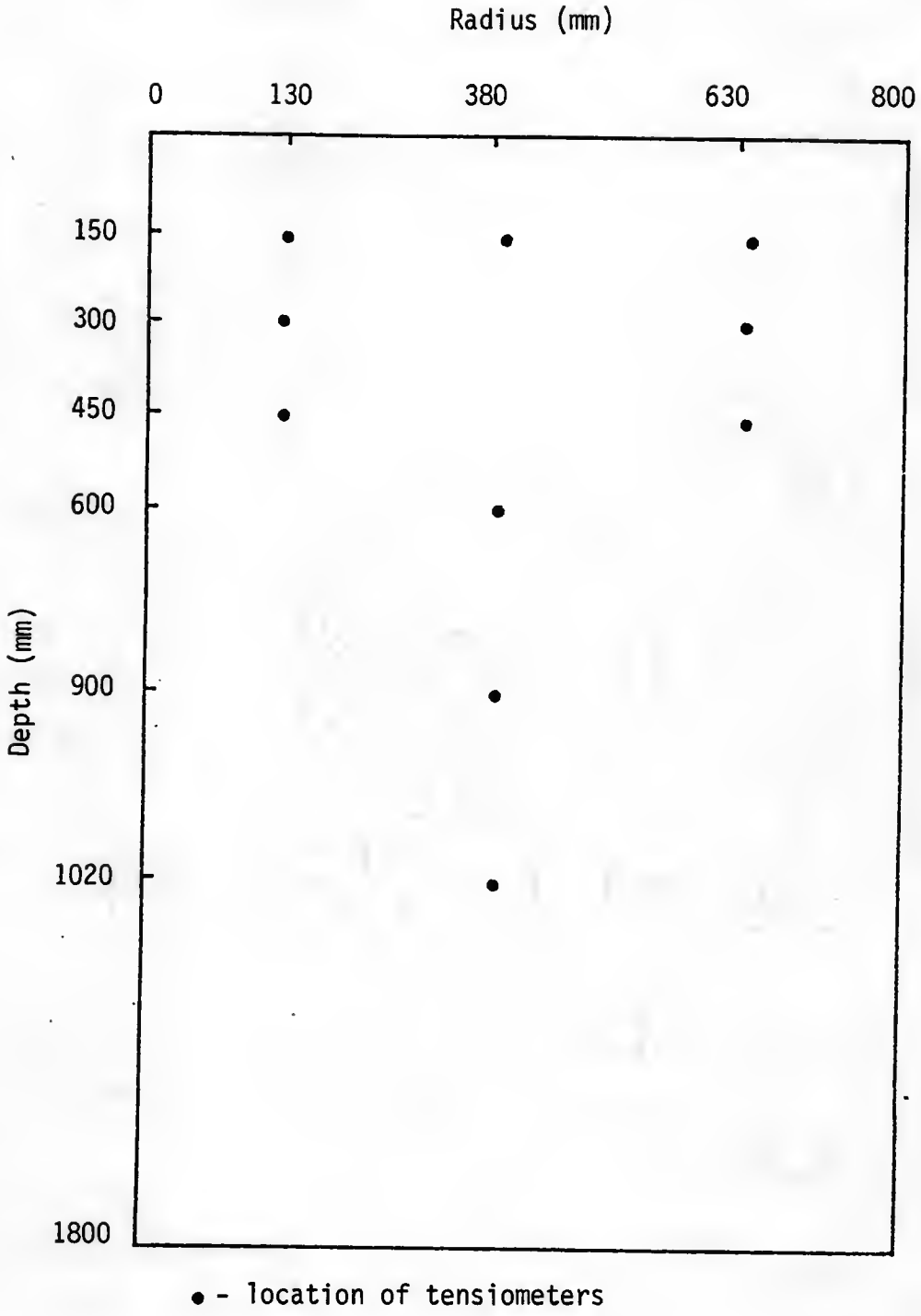

Figure 3-4. Location of tensiometers in 1986 field experiment for young citrus trees in grassed and bare soil lysimeters.

assumptions were: (1) The physical properties of the soil are homogeneous and isotropic; (2) The physical and chemical properties of the soil are constant in time; and (3) The hydraulic conductivity and soil pressure potential are single-valued functions of water content.

One-Dimensional Model

Equation (6) was used to describe the one-dimensional movement and extraction of water. Finite difference methods were used to solve the water potential based flow equation. The model used an implicit finite difference technique with explicit linearization of the soil parameters. The finite difference form of equation (3) was written as

$$C_i^k \frac{(h_i^{k+1} - h_i^k)}{\Delta t} = \frac{K_{i+1/2}^k (h_{i+1}^{k+1} - h_i^{k+1}) - K_{i-1/2}^k (h_i^{k+1} - h_{i-1}^{k+1})}{\Delta z^2} + \frac{K_{i-1/2}^k - K_{i+1/2}^k}{\Delta z} - S_i^k \qquad (16)$$

where

$$K_{i-1/2}^k = \frac{K_i^k + K_{i-1}^k}{2} \qquad (17)$$

and

$$K_{i+1/2}^k = \frac{K_{i+1}^k + K_i^k}{2} \qquad (18)$$

The subscript i refers to distance and the superscript k refers to time. To apply this equation to soil profiles, the soil was divided into a

finite number of layers or grids as shown in Figure 3-5. Equation (16) was rearranged so that unknowns were on the left side of the equation and the knowns were on the right side such that

$$-\left(\frac{\Delta t \; K^{k}_{i-1/2}}{2\,\Delta z\; C^{k}_{i}}\right) h^{k+1}_{i-1} + \left(1 + \frac{\Delta t \; K^{k}_{i-1/2}}{2\,\Delta z\; C^{k}_{i}} + \frac{\Delta t \; K^{k}_{i+1/2}}{2\,\Delta z\; C^{k}_{i}}\right) h^{k+1}_{i}$$

$$-\left(\frac{\Delta t \; K^{k}_{i+1/2}}{2\,\Delta z\; C^{k}_{i}}\right) h^{k+1}_{i+1} = h^{k}_{i} + \frac{\Delta t}{\Delta z}\left(\frac{K^{k}_{i-1/2} - K^{k}_{i+1/2}}{C^{k}_{i}}\right) - \frac{\Delta t}{C^{k}_{i}} S_{i} \qquad (19)$$

Equation (19) was written for each of the interior grids in the soil profile. The top and bottom grids of the system required equation (19) to be modified so that the equation would describe the boundary conditions. The system of equations which are formed by applying equation (19) to each grid produces a tridiagonal matrix which is implicit in terms of h, water potential. The tridiagonal matrix was solved using Gauss elimination. From explicit linearization, the coefficients of the unknown h terms were known at each time step. Thus equation (19) was reduced to

$$A_i\, h^{k+1}_{i-1} + B_i\, h^{k+1}_{i} + C_i\, h^{k+1}_{i+1} = D_i \qquad (20)$$

where

$$A_i = -\left(\frac{\Delta t \; K^{k}_{i-1/2}}{2\,\Delta z\; C^{k}_{i}}\right) \qquad (21)$$

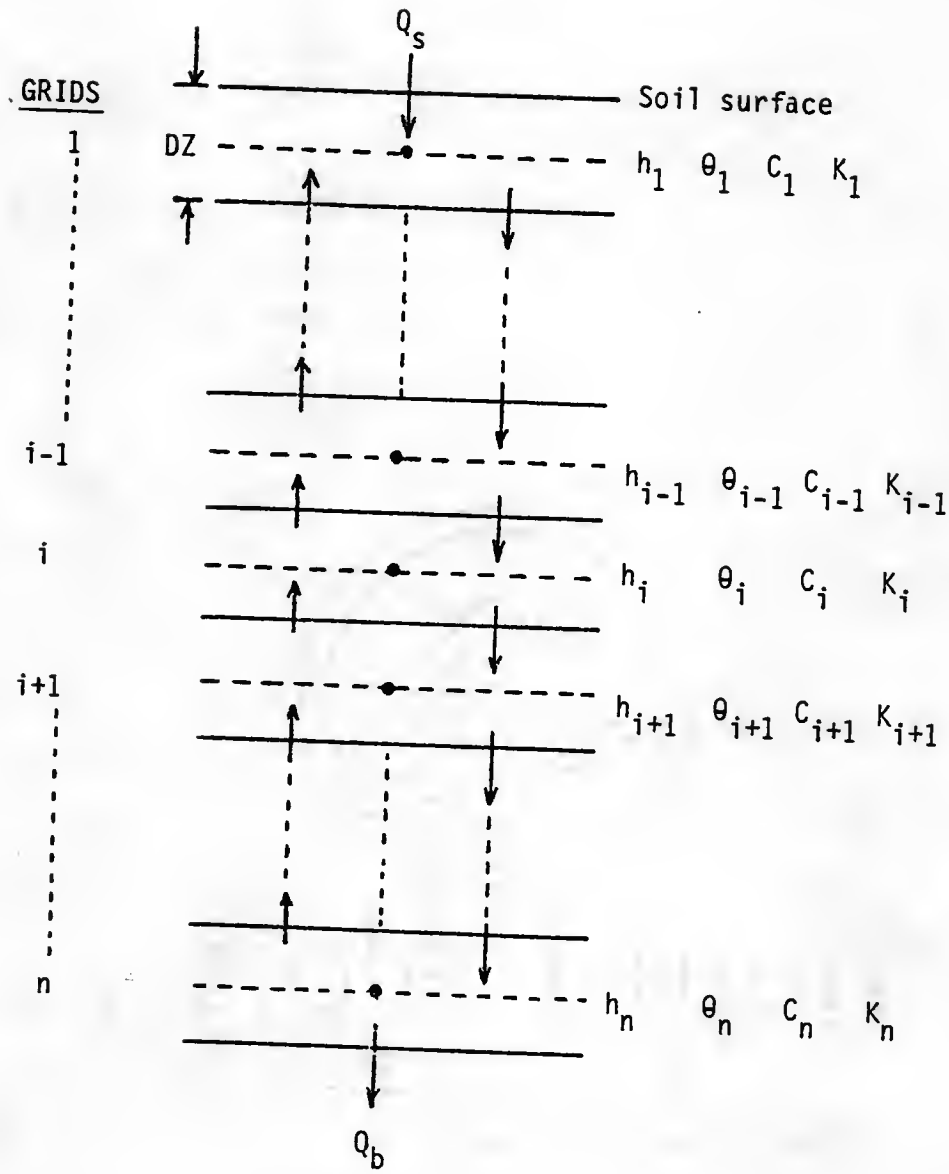

Figure 3-5. Schematic diagram of the finite-difference grid system for the one-dimensional model of water movement and extraction.

$$C_i = -\left(\frac{\Delta t \; K^{k}_{i+1/2}}{\Delta z^2 \; C^{k}_{i}}\right) \tag{22}$$

$$B_i = 1 - A_i - C_i \tag{23}$$

$$D_i^k = h_i^k + \frac{\Delta t}{\Delta z}\left(\frac{K^{k}_{i-1/2} - K^{k}_{i+1/2}}{C^{k}_{i}}\right) - \frac{\Delta t}{C^{k}_{i}} S_i \tag{24}$$

Boundary Conditions. The boundary condition for the surface grid was variable. A flux boundary condition was used to simulate infiltration during irrigation, and a no flux boundary condition was used for redistribution. Evaporation from the soil surface was included in the water extraction term. Equation (20) was modified for the surface boundary condition such that

$$B_1 h_1^{k+1} + C_1 h_2^{k+1} = D_1 \tag{25}$$

where

$$B_1 = 1 - C_1 \tag{26}$$

and

$$D_1^k = h_1^k + \frac{\Delta t}{\Delta z}\left(\frac{Qs - K^{k}_{1+1/2}}{C^{k}_{1}}\right) - \frac{\Delta t}{C^{k}_{1}} S_1 \tag{27}$$

The lower boundary was also a flux boundary and was written as

$$A_n h_{n-1}^{k+1} + B_n h_n^{k+1} = D_n \quad (28)$$

where

$$B_n = 1 - A_n \quad (29)$$

and

$$D_n = h_n^k + \frac{\Delta t}{\Delta z}\left(\frac{K_{n-1/2}^k - Qb}{C_n^k}\right) - \frac{\Delta t}{C_n^k} S_n \quad (30)$$

The variables Qs and Qb were, respectively, the surface and bottom fluxes imposed on the grid system. The bottom flux was set to either a no flow or a gravity flow boundary condition.

Surface infiltration. The infiltration rate during irrigation was set equal to the water application rate until the irrigation event was completed. The total depth of water infiltrated at any time was calculated as the summation of the incremental infiltration volumes at all previous time steps.

Time steps. The time steps for implicit numerical techniques can generally be much larger than those for explicit numerical techniques, and still maintain stability. Haverkamp et al. (1977) stated that stability conditions must be determined by trial and error because they depend on the degree of nonlinearity of the equations.

The time step was estimated by a method given by Feddes et al. (1978) and used by Clark (1982):

$$\Delta t < \frac{x \ \Delta z}{| \ Qmax \ |} \qquad (31)$$

where Qmax was the maximum net flux occuring across any grid boundary and x is a factor where $0.015<x<0.035$. The lower value of x was used to accommodate the rapid movement of water during infiltration and early stages of redistribution. The value of x may be assumed to be the maximum permissible change in water content for any grid in the soil profile.

Updating of soil parameters. The updating of the soil parameters was achieved by use of a tabulated search to determine the corresponding values of hydraulic conductivity, specific water capacity and water content for the new values of soil water potential at each time step. A logarithmic interpolation method was used to reduce computer time. The table was set up with linearly increasing multiples of the logarithmic values of soil water potentials.

Mass balance. A mass balance was calculated at each time step to check the stability of the simulation model. The method used the initial volume of water in the profile plus the infiltration and minus the extraction by the plant. Evaporation from the soil surface was included in the water extraction term as extraction from the surface grids.

Because the grid system approximates a continuous system with discrete points, some error will result from the numerical calculations of the simulation model. The error decreases as the grid size decreased.

Two-Dimensional Model

Water movement and extraction under young citrus trees was simulated using a two-dimensional soil water extraction model. A radial

flow model may be used to describe water movement and extraction in a soil profile which is nonuniformly irrigated as in water flow from trickle emitters and spray jets. The radial flow model may also describe the water extraction under widely spaced crops such as citrus.

With the assumption of radial symmetry, equation (8) was solved in the vertical and radial directions. This equation is a second order, nonlinear parabolic partial differential equation which expresses the water potential distribution as a function of time and space coordinates. No known analytical solution of equation (8) exist. Thus it was solved numerically using finite difference equations. The model developed in this research used an implicit finite difference technique with explicit linearization of the soil parameters. Two solution methods were used to solve the finite difference equations for the two-dimensional model. It was solved implicitly using a Gauss elimination method. Because of the time required to solve a large system of equations by Gauss elimination, an alternation direction implicit (ADI) method was also utilized to solve equation (8).

The finite difference equation for the solution of equation (8) utilizing the Gauss elimination method was

$$C^{k}_{i,j}\frac{(h^{k+1}_{i,j}-h^{k}_{i,j})}{\Delta t}=\frac{K^{k}_{i+1/2,j}(h^{k+1}_{i+1,j}-h^{k+1}_{i,j})-K^{k}_{i-1/2,j}(h^{k+1}_{i,j}-h^{k+1}_{i-1,j})}{\Delta z^{2}}+\frac{r_{i,j+1/2}K^{k}_{i,j+1/2}(h^{k+1}_{i,j+1}-h^{k+1}_{i,j})-r_{i,j-1/2}K^{k}_{i,j-1/2}(h^{k+1}_{i,j}-h^{k+1}_{i,j-1})}{r_{i,j}\Delta r^{2}}$$

$$+ \frac{K^{k}_{i-1/2,j} - K^{k}_{i+1/2,j}}{\Delta z} - S^{k}_{i,j} \qquad (32)$$

To apply this equation to the soil profiles, the soil was divided into a finite number grids as shown in Figure 3-6. Equation (32) was arranged such that the unknowns were on the left side of the equation and the knowns were on the right side as follows

$$- \left(\frac{\Delta t \; K^{k}_{i-1/2,j}}{2 \; \Delta z \; C^{k}_{i,j}}\right) h^{k+1}_{i-1,j} - \left(\frac{\Delta t \; r_{i,j-1/2}}{2 \; \Delta r \; r_{i,j}} \frac{K^{k}_{i-1/2,j}}{C^{k}_{i,j}}\right) h^{k+1}_{i,j-1}$$

$$+ \left(1 + \frac{\Delta t \left(K^{k}_{i-1/2,j} + K^{k}_{i+1/2,j} \right)}{2 \; \Delta z \; C^{k}_{i,j}} + \right.$$

$$\left. \frac{\Delta t \left(r_{i,j+1/2} K^{k}_{i,j+1/2} + r_{i,j-1/2} K^{k}_{i,j-1/2} \right)}{2 \; \Delta r \; r_{i,j} \; C^{k}_{i,j}} \right) h^{k}_{i,j}$$

$$- \left(\frac{\Delta t \; K^{k}_{i+1/2,j}}{2 \; \Delta z \; C^{k}_{i,j}}\right) h^{k+1}_{i+1,j} - \left(\frac{\Delta t \; r_{i,j+1/2}}{2 \; \Delta r \; r_{i,j}} \frac{K^{k}_{i+1/2,j}}{C^{k}_{i,j}}\right) h^{k+1}_{i,j+1}$$

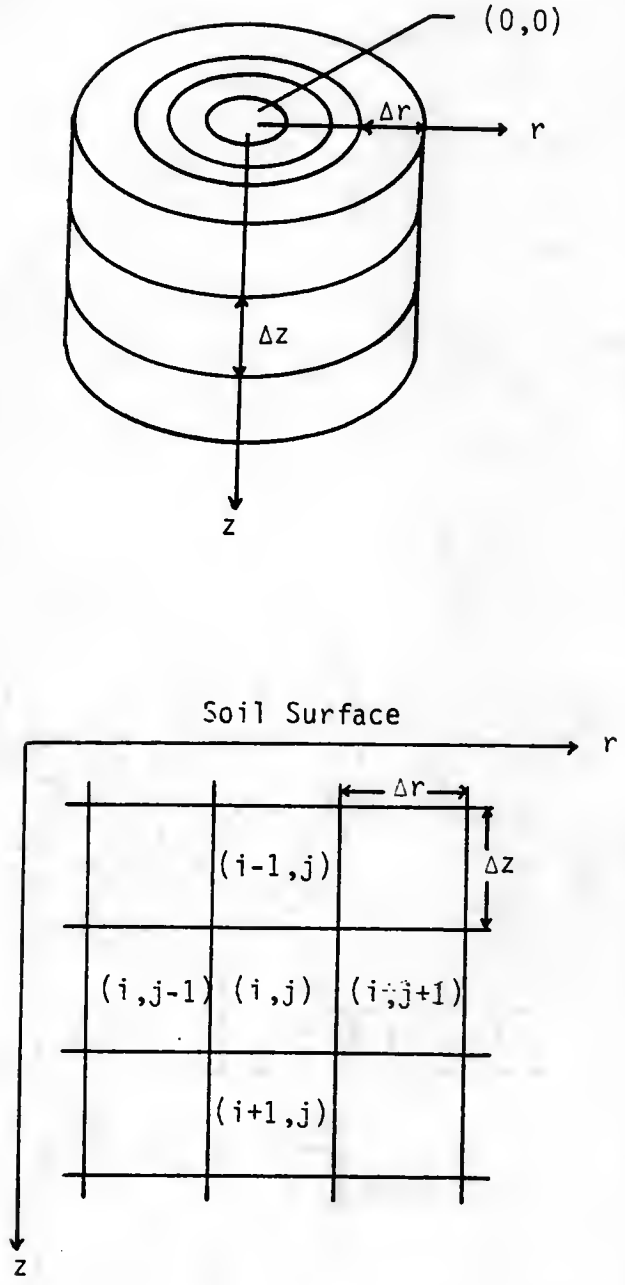

Figure 3-6. Schematic diagram of the finite-difference grid system for the two-dimensional model of water movement and extraction.

$$= h^{k}_{i,j} + \frac{\Delta t}{\Delta z}\left(\frac{K^{k}_{i-1/2,j} - K^{k}_{i+1/2,j}}{C^{k}_{i,j}}\right) - \frac{\Delta t}{C^{k}_{i,j}} S^{k}_{i,j} \qquad (33)$$

Equation (33) was reduced to

$$A_{i,j} h^{k+1}_{i-1,j} + B_{i,j} h^{k+1}_{i,j-1} + C_{i,j} h^{k+1}_{i,j} + D_{i,j} h^{k+1}_{i+1,j}$$

$$+ E_{i,j} h^{k+1}_{i,j+1} = F_{i,j} \qquad (34)$$

where

$$A_{i,j} = -\left(\frac{\Delta t}{\Delta z^{2}} \frac{K^{k}_{i-1/2,j}}{C^{k}_{i,j}}\right) \qquad (35)$$

$$B_{i,j} = -\left(\frac{\Delta t}{\Delta r^{2}} \frac{r_{i,j-1/2}}{r_{i,j}} \frac{K^{k}_{i-1/2,j}}{C^{k}_{i,j}}\right) \qquad (36)$$

$$D_{i,j} = -\left(\frac{\Delta t}{\Delta z^{2}} \frac{K^{k}_{i+1/2,j}}{C^{k}_{i,j}}\right) \qquad (37)$$

$$E_{i,j} = -\left(\frac{\Delta t}{\Delta r^{2}} \frac{r_{i,j+1/2}}{r_{i,j}} \frac{K^{k}_{i+1/2,j}}{C^{k}_{i,j}}\right) \qquad (38)$$

$$C_{i,j} = 1 - A_{i,j} - B_{i,j} - D_{i,j} - E_{i,j} \tag{39}$$

$$F_{i,j} = h^{k}_{i,j} + \frac{\Delta t}{\Delta z}\left(\frac{K^{k}_{i-1/2,j} - K^{k}_{i+1/2,j}}{C^{k}_{i,j}}\right) - \frac{\Delta t}{C^{k}_{i,j}} S^{k}_{i,j} \tag{40}$$

Boundary Conditions. The boundary condition for the surface grids was a flux boundary condition which accounted for irrigation and rainfall at the soil surface. At times when no irrigation occured the surface boundary was a no flux boundary. Evaporation from the soil surface was included in the water extraction term. The modification of equation (34) to describe the surface boundary condition was

$$B_{1,j}\, h^{k+1}_{1,j-1} + C_{1,j}\, h^{k+1}_{1,j} + D_{1,j}\, h^{k+1}_{2,j} + E_{1,j}\, h^{k+1}_{1,j+1} = F_{1,j} \tag{41}$$

where

$$C_{1,j} = 1 - B_{1,j} - D_{1,j} - E_{1,j} \tag{42}$$

$$F_{1,j} = h^{k}_{1,j} + \frac{\Delta t}{\Delta z}\left(\frac{Qs_{j} - K^{k}_{1+1/2,j}}{C^{k}_{1,j}}\right) - \frac{\Delta t}{C^{k}_{1,j}} S^{k}_{1,j} \tag{43}$$

The lower boundary condition was also represented as a flux boundary. The lower boundary in this research was an impermeable boundary which represented the bottom of the lysimeter. The modification of equation (34) to describe the lower no flux boundary was

$$A_{n,j}\,h^{k+1}_{n-1,j} + B_{n,j}\,h^{k+1}_{n,j-1} + C_{n,j}\,h^{k+1}_{n,j} + E_{n,j}\,h^{k+1}_{n,j+1} = F_{n,j} \tag{44}$$

where

$$C_{n,j} = 1 - A_{n,j} - B_{n,j} - E_{n,j} \tag{45}$$

$$F^{k}_{n,j} = h^{k}_{n,j} + \frac{\Delta t}{\Delta z}\left(\frac{K^{k}_{n-1/2,j} - Qb_{j}}{C^{k}_{n,j}}\right) - \frac{\Delta t}{C^{k}_{n,j}}\,S^{k}_{n,j} \tag{46}$$

The boundary conditions for the radial boundaries were both no flux boundaries. The no flux boundary condition for the outer radius (j=m) represented the outer wall of the lysimeter and was written as

$$A_{i,m}\,h^{k+1}_{i-1,m} + B_{i,m}\,h^{k+1}_{i,m-1} + C_{i,m}\,h^{k+1}_{i,m} + D_{i,m}\,h^{k+1}_{i+1,m} = F_{i,m} \tag{47}$$

where

$$C_{i,m} = 1 - A_{i,m} - B_{i,m} - D_{i,m} \tag{48}$$

$$F^{k}_{i,m} = h^{k}_{i,m} + \frac{\Delta t}{\Delta z}\left(\frac{K^{k}_{i-1/2,m} - K^{k}_{i+1/2,m}}{C^{k}_{n,m}}\right) - \frac{\Delta t}{C^{k}_{n,m}}\,S^{k}_{i,m} \tag{49}$$

The boundary condition for the inner radius was also represented as a no flux boundary. For the inner radius r(i,j) = 0, and its inclusion into equation (8) would result in a division by zero. Therefore the second term in equation (8) was rewritten as

$$\frac{1}{r}\frac{\partial}{\partial r}\left(r\,K(h)\frac{\partial h}{\partial r}\right) = \frac{K}{r}\frac{\partial h}{\partial r} + \frac{\partial}{\partial r}\left(K(h)\frac{\partial h}{\partial r}\right) \tag{50}$$

a no flux boundary at r = 0 implies that $\frac{dh}{dr} = 0$. Then if $\frac{dh}{dr} = 0$, the $\lim \frac{1}{r}\frac{dh}{dr} = 0$. We rewrite equation (8) as

$$C\frac{\partial h}{\partial t} = \frac{\partial}{\partial z}\left(K(h)\frac{\partial h}{\partial z}\right) + \frac{\partial}{\partial r}\left(K(h)\frac{\partial h}{\partial r}\right) - \frac{\partial K(h)}{\partial z} - S(z,r,t) \qquad (51)$$

The finite difference equation for equation (51) at the inner radius may be written as

$$-\left(\frac{\Delta t\, K^{k}_{i-1/2,1}}{2\,\Delta z\, C^{k}_{i,1}}\right)h^{k+1}_{i-1,1} + \left(1 + \frac{\Delta t\,(K^{k}_{i-1/2,1} + K^{k}_{i+1/2,1})}{2\,\Delta z\, C^{k}_{i,1}}\right)$$

$$+\left(\frac{\Delta t\, K^{k}_{i,1+1/2}}{2\,\Delta r\, C^{k}_{i,1}}\right)h^{k+1}_{i,1} - \left(\frac{\Delta t\, K^{k}_{i+1/2,1}}{2\,\Delta z\, C^{k}_{i,1}}\right)h^{k+1}_{i+1,1}$$

$$-\left(\frac{\Delta t}{2\,\Delta r}\,\frac{K^{k}_{i,1+1/2}}{C^{k}_{i,1}}\right)h^{k+1}_{i,2} = h^{k}_{i,1}$$

$$+\frac{\Delta t}{\Delta z}\left(\frac{K^{k}_{i-1/2,1} - K^{k}_{i+1/2,1}}{C^{k}_{i,1}}\right) - \frac{\Delta t}{C^{k}_{i,1}}\,S^{k}_{i,1} \qquad (52)$$

or as

$$A_{i,1}\,h^{k+1}_{i-1,1} + C_{i,1}\,h^{k+1}_{i,1} + D_{i,1}\,h^{k+1}_{i+1,1} + E_{i,1}\,h^{k+1}_{i,2} = F_{i,1} \qquad (53)$$

where

$$A_{i,l} = -\left(\frac{\Delta t \; K^{k}_{i-1/2,l}}{\Delta z^{2} \; C^{k}_{i,l}}\right) \tag{54}$$

$$D_{i,l} = -\left(\frac{\Delta t \; K^{k}_{i+1/2,l}}{\Delta z^{2} \; C^{k}_{i,l}}\right) \tag{55}$$

$$E_{i,l} = -\left(\frac{\Delta t}{\Delta r^{2}} \; \frac{K^{k}_{i,l+1/2}}{C^{k}_{i,l}}\right) \tag{56}$$

$$C_{i,l} = 1 - A_{i,l} - D_{i,l} - E_{i,l} \tag{57}$$

$$F^{k}_{i,l} = h^{k}_{i,l} + \frac{\Delta t}{\Delta z}\left(\frac{K^{k}_{i-1/2,l} - K^{k}_{i+1/2,l}}{C^{k}_{i,l}}\right) - \frac{\Delta t}{C^{k}_{i,l}} S^{k}_{i,l} \tag{58}$$

Updating of the soil parameters, surface infiltration, mass balance and time steps were implimented as described for the one-dimensional soil water flow model.

The system of equations for the two dimensional model produces a banded matrix. The matrix is a five banded matrix with the form of

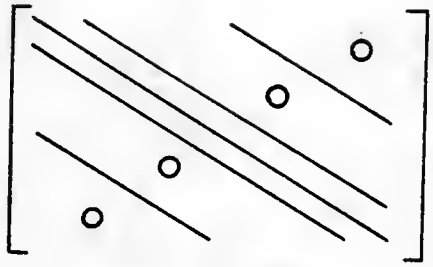

Reddel and Sunada (1970) utilized a Gauss elimination method for the solution of a two-dimensional groundwater model. They used an algorithm developed by Thurnau (1963) which operates only on the banded part of the solution matrix. Computer storage is not required for the matrix elements above or below the band. A minimum band width is desirable and an appropriate choice of the grid numbering pattern can reduce the total width of the band.

In this model of two-dimensional soil water movement and extraction, a subroutine was written which used the BANDSOLVE algorithm developed by Thurnau (1963) to solve the system of equations. A subroutine was also written which solves equation (8) using an alternating direction implicit method. The finite difference equations for the ADI solution are presented in Appendix A.

Soil Water Extraction

A macroscopic soil water extraction term was used in this research. The model used was based on actual field measurements reported in the literature. Denmead and Shaw (1962) conducted experiments which compared actual ET to potential ET of corn as a function of the available soil water. Their study showed that under high potential ET demands, the actual ET was considerably less than the potential rate even though the available soil water was considered adequate. They also observed that under low potential ET demands, the actual ET was equal to

the potential ET down to very low soil water contents. Ritchie (1973) observed similar results in separate experiments.

Saxton et al. (1974) used these observed relationships in modeling soil water movement and extraction under a corn and under a grass crop. Smajstrla (1982) used these relationships to model the soil water status under a grass cover crop in Florida.

The soil water extraction function used in this research was modeled after that used by Smajstrla (1982). The soil water extraction rate was calculated as a function of the actual evapotranspiration rate and the current soil water status. The water extraction term was defined as

$$S_i = ET \ RDF_i \ R_i^{(ET / R_i)} \tag{59}$$

where S_i = the soil water extraction rate per soil zone,

ET = the actual evapotranspiration rate,

RDF_i = the relative water extraction per soil zone at field capacity, and

R_i = the relative available soil water per soil zone defined as

$$R_i = \frac{(\theta - \theta_{wp})}{(\theta_{fc} - \theta_{wp})} \tag{60}$$

where θ = the soil water content of the soil zone,

θ_{wp} = the soil water content at wilting point, and

θ_{fc} = the soil water content at field capacity.

The relative water extraction per soil zone (RDF) was defined as the percentage of water extraction for the ith soil zone when soil water is not limiting. It may also be considered to be a rooting activity term which indicates the percentage of active roots in the ith soil zone.

Figure 3-7 shows the form of equation (59). Equation (59) permits a rapid rate of soil water extraction when soil water is readily available. As soil water is depleted, the water extraction function produces a logarithmic rate of decline of soil water extraction. It allows recovery of near potential rates of extraction during periods of low potential ET and it rapidly limits extraction during periods of high potential ET. It prevents the soil permanent wilting point from being reached by limiting ET to very low rates as the permanent wilting point is approached.

In this research equation (59) was used to limit water extraction from a given soil zone as the water in that zone became less available. Equation (59) was not used to limit the ET from the profile, only to repartition the extraction within the soil profile.

Equation (59) was applied to calculate a water extraction rate from each grid for each time step during model operation. The soil water extraction rate per soil grid was then multiplied by the grid volume to calculate the total water extraction at that time step. If the calculated total water extraction rate was not equal to the actual ET, the soil water extraction rates were linearly adjusted so that the calculated and actual ET rates were equal.

The adjusted soil water extraction rates (S_i) were computed as

$$S_i = S_i \frac{ET}{\Sigma S_i \Delta v} \qquad (61)$$

where Δv is the volume of the ith soil grid.

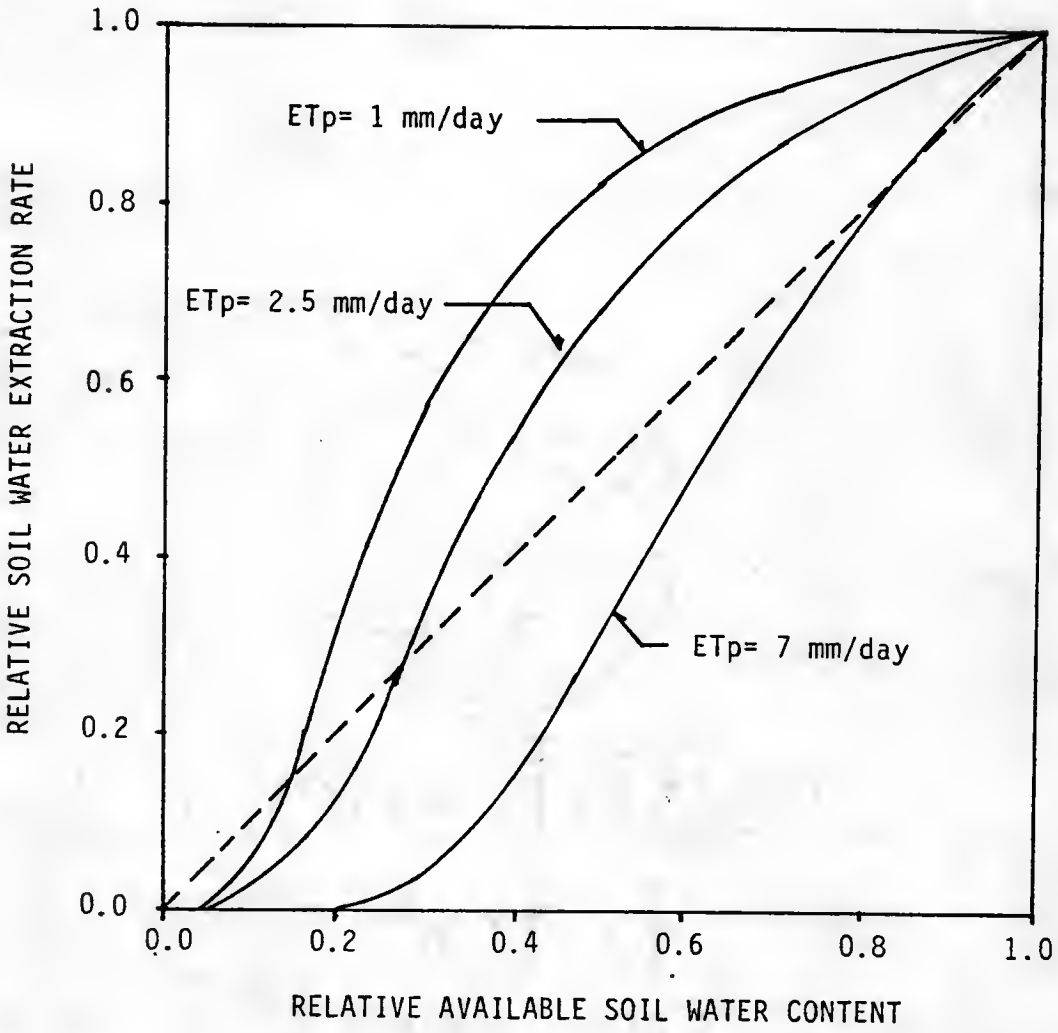

Figure 3-7. Relationship of the relative available soil water and potential soil water extraction rate on the soil water extraction rate.

CHAPTER IV
RESULTS AND DISCUSSION

Instrumentation Performance

Three pressure transducers were individually calibrated to analyze their response characteristics. A typical calibration curve (for pressure transducer No. 1) is shown in Figure 4-1. The three calibration equations are

$$\text{Volts} = 0.04812\ (\text{kPa}) + 0.9861 \qquad R^2 = 0.999 \tag{62}$$

$$\text{Volts} = 0.04781\ (\text{kPa}) + 0.9867 \qquad R^2 = 0.999 \tag{63}$$

$$\text{Volts} = 0.04804\ (\text{kPa}) + 0.9819 \qquad R^2 = 0.999 \tag{64}$$

The coefficients for these equations were not significantly different ($\alpha = 0.05$), so that for many applications one equation could be used for all 3 pressure transducers without significant error. For the above 3 transducers, combined equations resulted in a maximum expected error of 0.06 kPa at 1 volt (-0.3 kPa potential) and 0.27 kPa at 5 volts (-83.67 kPa potential). Equations could therefore be combined for many field applications. For this research, individual transducer calibration curves were used in order to obtain the maximum accuracies possible with the instrumentation, and because the microcomputer memory was adequate to permit storage of the individual calibration curves.

In the calibration procedure, hysteresis effects were studied by measuring transducer outputs at decreasing water potentials from 0 to -80 kPa, followed by increasing potentials from -80 to 0 kPa. For these transducers there were no measurable hysteresis effects.

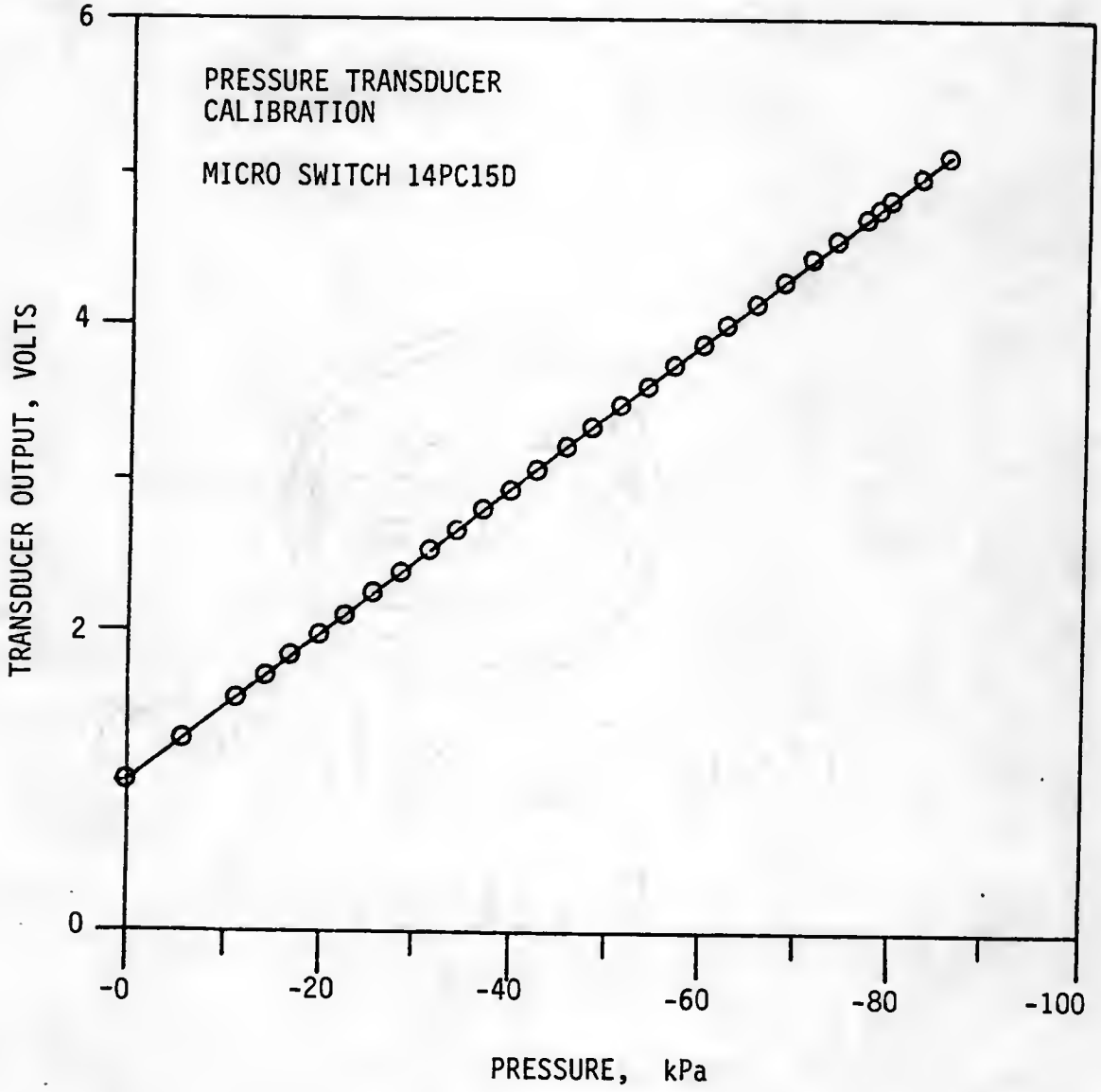

Figure 4-1. Calibration curve of output voltage versus pressure applied for pressure transducer no. 1.

The A/D board was found to have a linear relationship between voltage input and digital output as shown in Figure 4-2. The equation which related the voltage to digital output was

$$\text{Digital Units} = 49.98\ (\text{Volts}) \qquad R^2 = 0.999 \tag{65}$$

Equation (65) was combined with the individual transducer calibration equations (62-64) to obtain relationships between transducer-measured water potentials and the digital inputs to the microcomputer. Equation (65) is only valid in the range of 0-5 volts and 0-255 units for the 8-bit A/D board used. The 8-bit board, therefore, allowed a resolution of only the nearest 0.02 volts. Greater resolution could be achieved by the use of a 12-bit, 16-bit or other higher resolution A/D board. A resolution of 0.02 volts is a resolution of approximately 0.4 kPa (from equations 62-64). For this work this degree of resolution was judged to be acceptable.

Tests of the assembled tensiometer-pressure transducer systems were conducted in the laboratory by manually and automatically recording tensiometer water potentials as water was allowed to evaporate from the tensiometer ceramic cups. Figure 4-3 shows the changes in water potential with time for 2 tensiometers. The continuous automatic readings by the microcomputer are shown as solid lines. Open circles show mercury manometer data that were manually read. Excellent agreement between the automatic and manual readings was obtained. In all cases, agreement was within 1.0 kPa.

Figure 4-4 shows a comparison of the manual and automatic readings for the 3 tensiometers and pressure transducers tested. Agreement was excellent, with all data points located within 1 kPa of the 100% accuracy line.

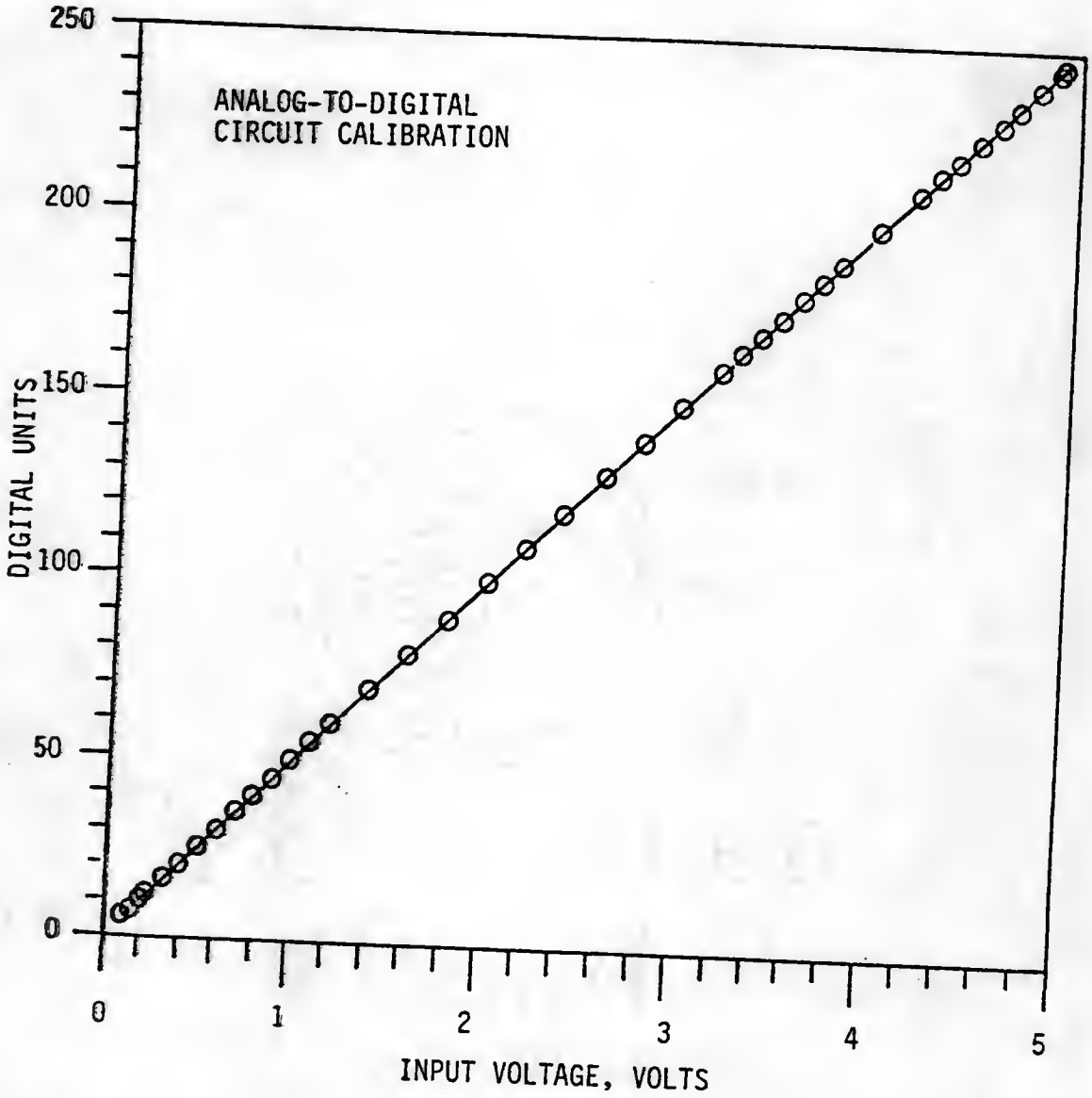

Figure 4-2. Calibration curve of digital units versus voltage applied for the analog-to-digital circuit used.

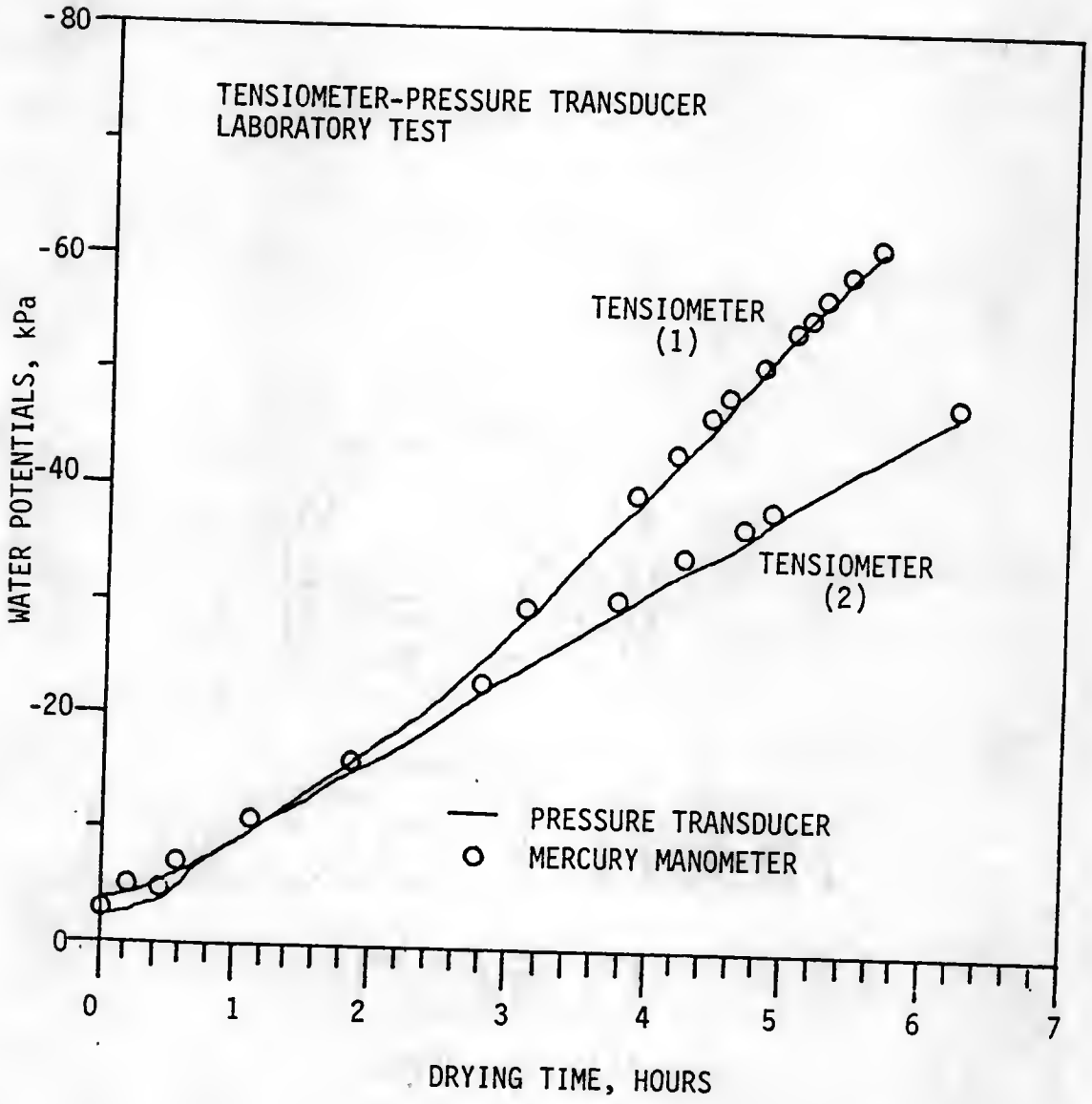

Figure 4-3. Comparisons of mercury manometer manually-read and pressure transducer automatically-read tensiometer water potentials during drying cycles for two tensiometers in the laboratory.

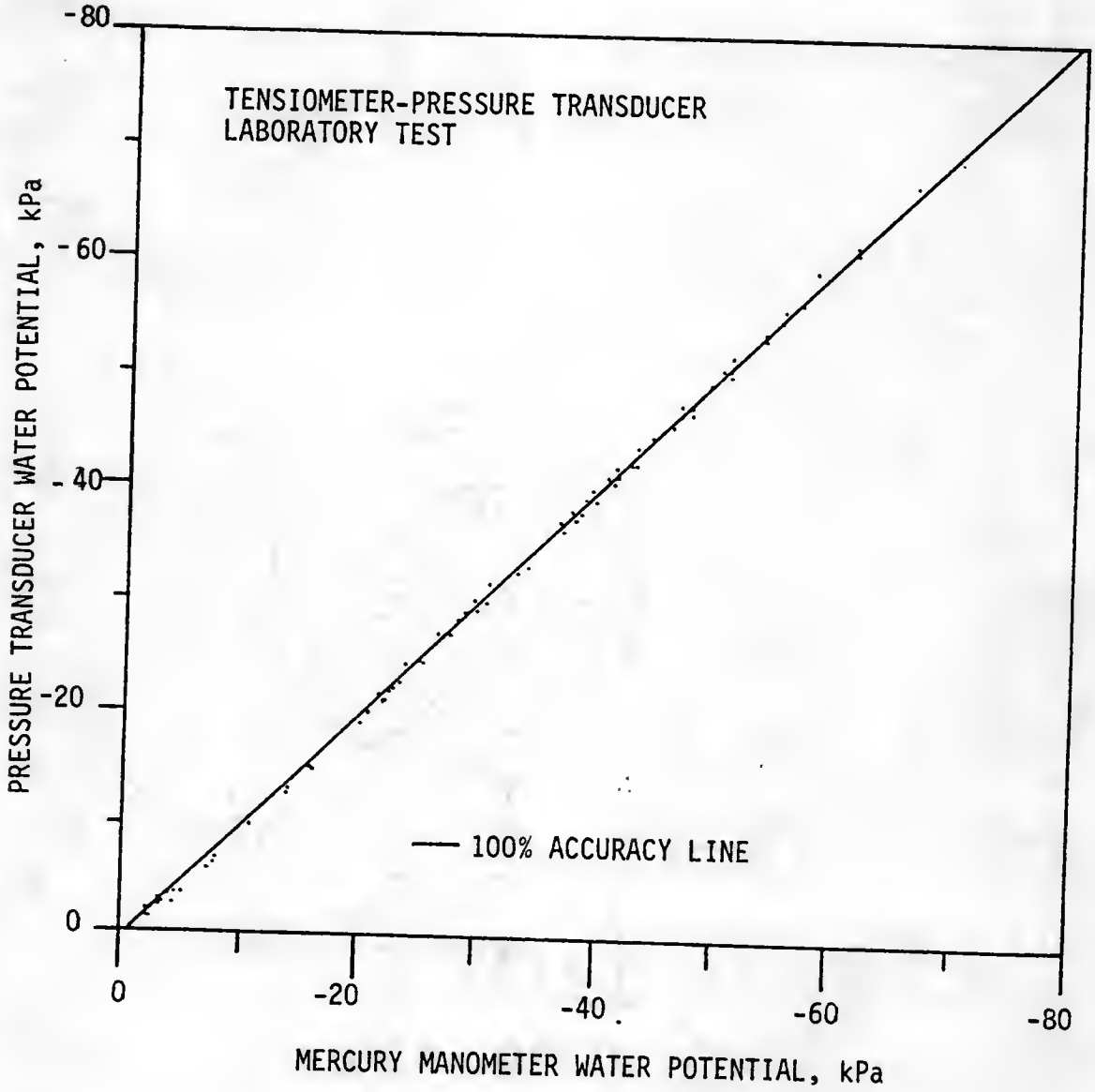

Figure 4-4. Comparisons of mercury manometer manually-read and pressure transducer automatically-read tensiometer water potentials for all laboratory data.

To evaluate the performance of the microcomputer-based soil water potential monitoring system under field environmental conditions, 3 1-week studies were conducted at the IFAS Irrigation Research and Education Park. Typical results for 1 week are shown in Figure 4-5 to 4-7 for 3 pressure transducers and tensiometers. Microcomputer data were recorded hourly and are shown as the solid line in each figure. These lines show diurnal cycles in soil water potential and a gradually decreasing average daily water potential as the soil dried. Water potential changes were slow because of the low evaporative demand and relatively inactive grass cover during the February 25 - March 1 period during which these data were collected.

The open circles in Figure 4-5 to 4-7 show manually read mercury manometer data. Agreement between these and the automatically read data were excellent under field conditions. The average variation between manually and automatically read data was 0.47 kPa. This was approximately the 0.4 kPa resolution of the instrumentation. The maximum deviation observed was 1.76 kPa. These data demonstrated that an accurate, effective microcomputer-based data acquisition system was developed for automatically recording soil water potential measurements. Because it was microcomputer-based, the system was inexpensive and consisted of components that were readily available from local electronics companies.

Field Data Collection

Field data were collected at the Irrigation Research and Education Park as previously described. The data were collected for input and verification of the numerical models developed in this research.

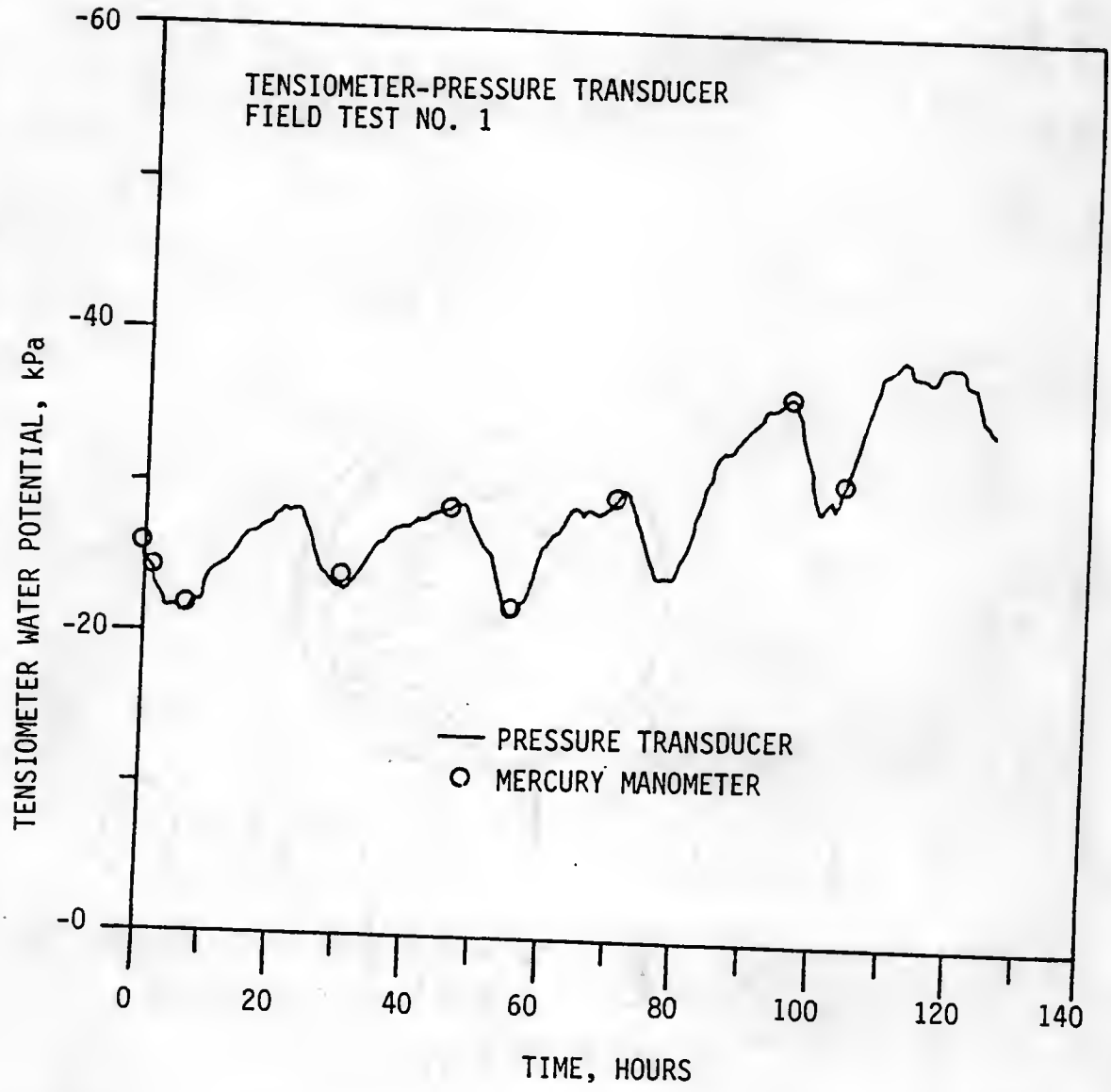

Figure 4-5. Evaluation of pressure transducer-tensiometer no. 1 by comparison of mercury manometer manually-read and pressure transducer automatically-read water potentials in the field.

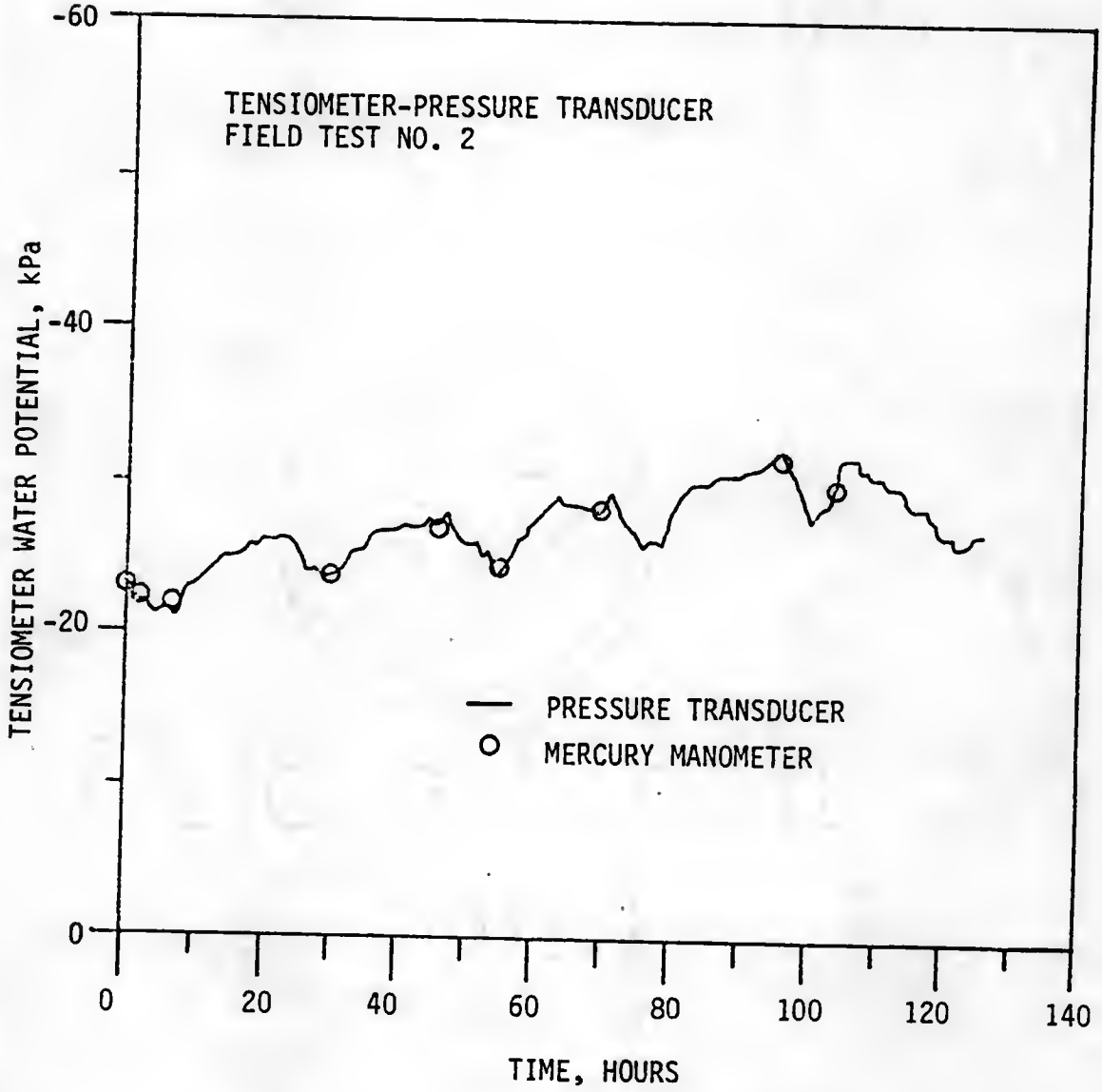

Figure 4-6. Evaluation of pressure transducer-tensiometer no. 2 by comparison of mercury manometer manually-read and pressure transducer automatically-read water potentials in the field.

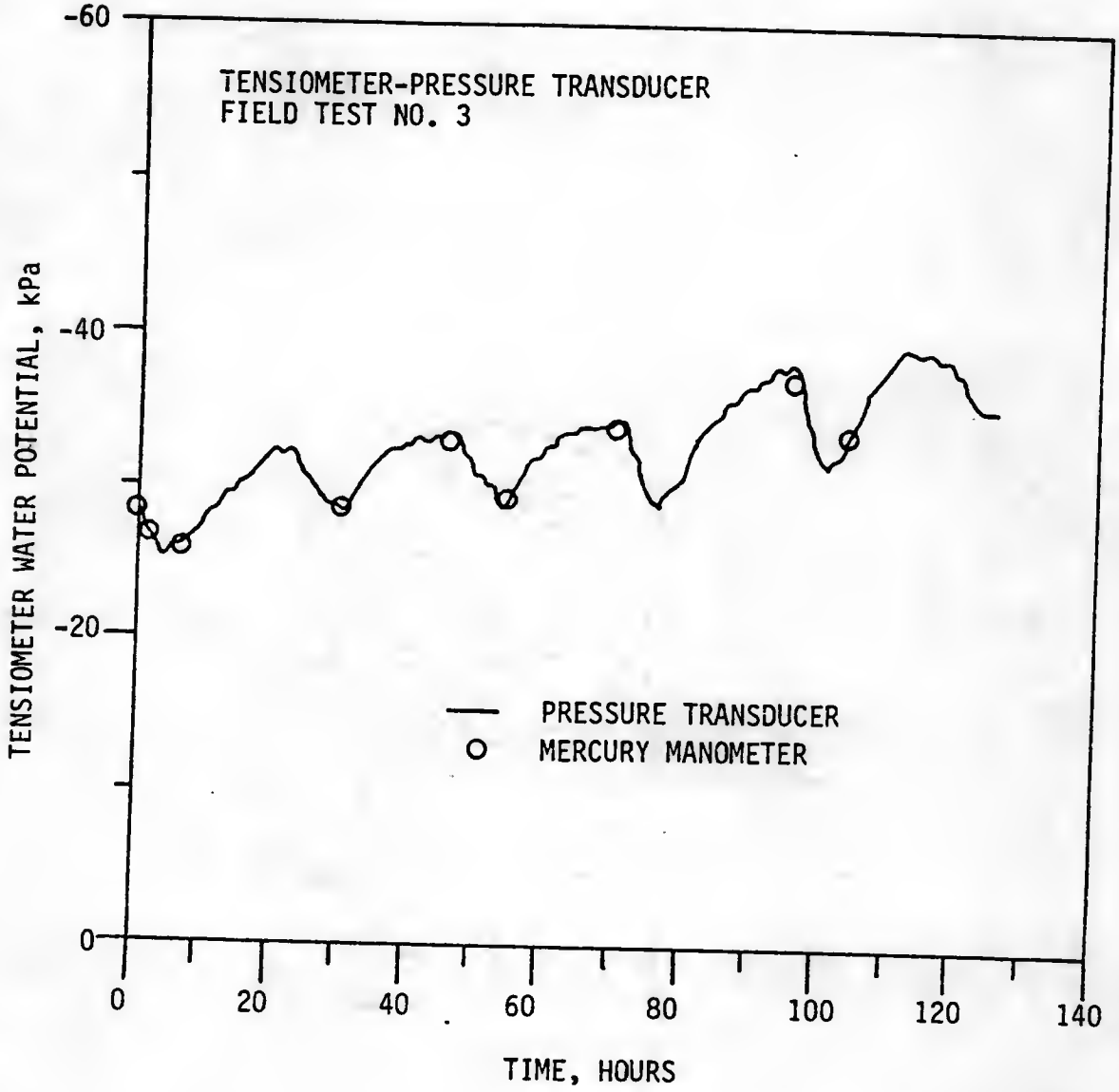

Figure 4-7. Evaluation of pressure transducer-tensiometer no. 3 by comparison of mercury manometer manually-read and pressure transducer automatically-read water potentials in the field.

The tensiometer data were used to calculate the soil water extraction from the lysimeters. A method described by van Bavel et al. (1968) was used to calculate the soil water extraction. Van Bavel's method used an integrated form of equation (1) to calculate the soil water extraction for a one-dimensional soil profile which was described as

$$R_z = \int_0^z \frac{\partial \theta}{\partial t} dz - q_z \qquad (66)$$

where R_z = the total soil water extraction rate for the soil profile to a depth of z. The total soil water extraction rate calculated for the entire profile depth z is then the ET rate.

A direct measurement of the surface evaporation was not made. Evaporation was included in the soil water extraction from the surface grid. The tensiometer nearest the surface was located at 150 mm. Water extraction from this surface grid included surface evaporation and ET for that zone. Gravity flow drainage from the lower grid was assumed. The hydraulic conductivity for the lower grid was assigned as the flux out of the soil profile. This was justified because observed changes in soil water potentials for the lower tensiometer were small.

1985 Field Data. The ET rates for selected drying cycles from the 1985 field experiments are shown in Figures 4-8 and 4-9. The observed drying cycles occured from August 20 to September 6. Figure 4-8 is the ET rate from the 20 kPa young citrus tree with grass cover. Figure 4-9 is the ET rate for the 20 kPa young citrus tree on bare soil. Several data points for the tree with no grass were missed throughout the experiment due to equipment failure. Due to these problems the tree with no grass cover was treated as a one-dimensional profile for analysis.

Differences between the ET rates in Figures 4-8 and 4-9 show that the ET rates for the tree with grass cover were greater than those of the tree with no grass cover. The higher ET rates for the tree with grass cover were expected and were also observed by Smajstrla et al. (1986).

The distribution of water extraction for the two citrus tree treatments are shown in Table 4-1. The water extraction rates are shown as percentages of the total soil water extraction and soil water extraction per soil zone. These values were computed for input into the water extraction models. Table 4-1 shows the differences between the soil water extractions for the two treatments. Approximately 97% of the water from the tree with no grass cover was extracted from the top 750 mm of the soil profile. The water extraction for the tree with grass cover shows that approximately 73% of the water was extracted from the top 750 mm of the soil profile. The water extraction rates from Table 4-1 also suggest that, for the tree with grass cover, water was extracted below the 1050 mm depth observed with the data collection system.

A two-dimensional distribution of soil water extraction is shown in Table 4-2 for the tree with grass cover. Table 4-2 shows that water was extracted almost uniformly throughout the profile. Greater percentages of water were extracted from the inner radii of the lysimeter.

1986 Field Data. The ET rates for a selected drying cycle from 1986 field experiments are shown in Figures 4-10 and 4-11. Figure 4-10 is the ET rate from the 20 kPa young citrus tree with grass cover. Figure 4-11 shows the ET rate for the 20 kPa young citrus tree with no grass cover. The observed drying cycles occurred from June 16 to June

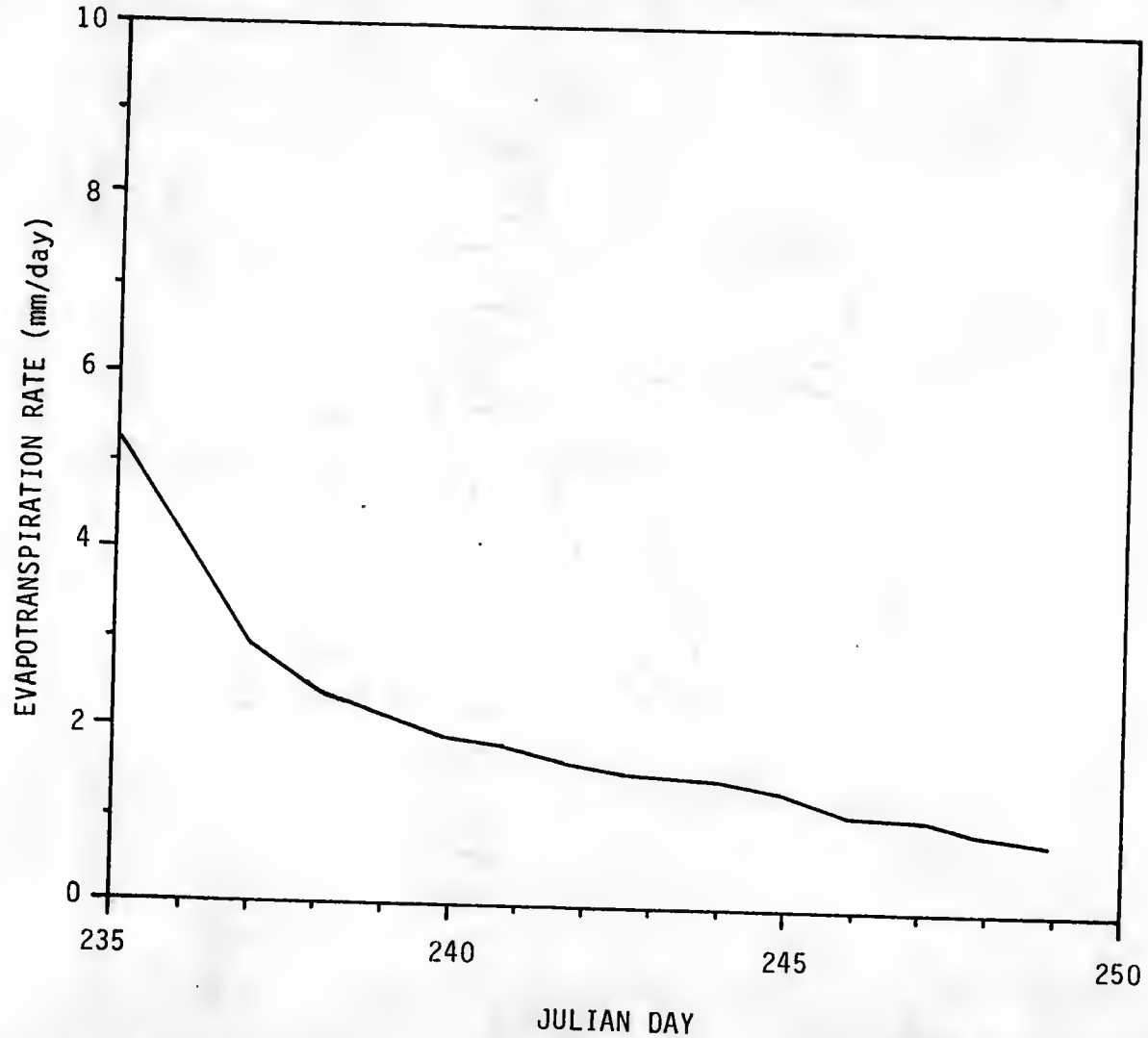

Figure 4-8. Evapotranspiration rate from the 1985 field experiments with a 20 kPa soil water potential treatment young citrus tree with grass cover.

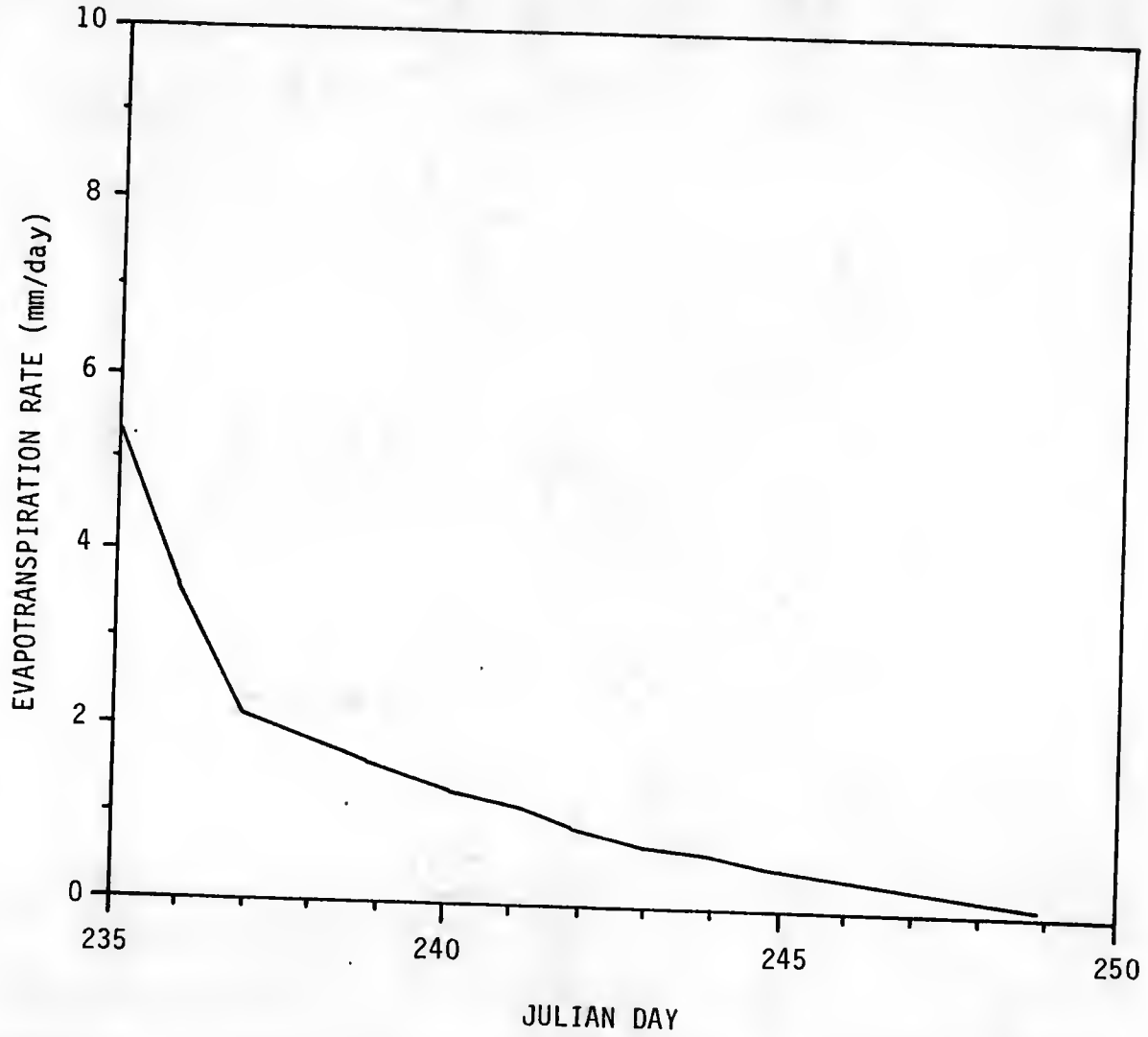

Figure 4-9. Evapotranspiration rate from the 1985 field experiment with a 20 kPa soil water potential treatment young citrus tree with bare soil.

Table 4-1. One-dimensional distribution of water extraction for a 15 day drying cycle for Young Citrus trees with and without grass cover.

Depth (mm)	Depth Increment (mm)	Water Extraction (mm)	Water Extraction (mm/mm)	Relative Water Extraction (%)
		Tree with Grass Cover		
0-375	375	9.8	0.026	32.3
375-750	375	7.3	0.019	23.8
750-1050	300	8.7	0.029	28.6
below 1050		4.7	0.016	15.2
		Tree with No Grass Cover		
0-375	375	5.9	0.016	27.9
375-750	375	7.4	0.020	35.3
750-1050	300	7.0	0.024	33.5
below 1050		0.7	0.0023	3.3

Table 4-2. Two-dimensional distribution of water extraction for a 15 day drying cycle for young Citrus with grass cover.

Depth (mm)	Depth Increment (mm)	Radius (mm) 100	300	500	700
		Relative Water Extraction (%)			
0-375	375	8.59	10.46	6.92	7.66
375-750	375	5.65	5.79	5.46	5.65
750-1050	300	8.03	8.26	3.94	4.07
below 1050		4.21	3.45	6.33	6.04
		Water Extraction (mm)			
0-375	375	2.6	3.2	2.1	2.3
375-750	375	1.7	1.8	1.7	1.7
750-1050	300	2.4	2.5	1.2	1.2
below 1050		1.3	1.1	1.9	1.8
		Water Extraction (mm/mm)			
0-375	375	0.0070	0.0085	0.0056	0.0062
375-750	375	0.0046	0.0047	0.0044	0.0046
750-1050	300	0.0082	0.0084	0.0040	0.0041
below 1050		0.0043	0.0035	0.0064	0.0061

24. Differences between the two treatments showed that ET of the tree with grass cover was greater than that of the tree with no cover, especially early in the drying cycle. The 1220 mm depth tensiometer for the tree with no grass did not function properly so these data were not included in the data anaylysis, but this did not introduce a large error, from Table 4-1.

The water extraction distributions are shown in Table 4-3. The percentage of water extracted from the top layer was greater for the tree with grass cover.

Evapotranspiration data for the two grass cover treatments are shown in Figures 4-12 and 4-13. Figure 4-12 shows ET rates of the 20 kPa grass covered lysimeter and Figure 4-13 shows ET rates of the 40 kPa grass covered lysimeter. Comparison of Figure 4-12 and 4-13 shows that the ET of the 20 kPa treatment was higher than that of the 40 kPa treatment. The grass had more water available for ET in the 20 kPa treatment.

Table 4-4 shows the water extraction distributions for the two grass treatments. Both distributions were similar with both having approximately the same soil water extraction percentages for each layer.

Model Verification

The accuracy of the numerical models in simulating the infiltration and redistribution of soil water was determined by comparison with other computer simulations from previous works in the literature.

The one-dimensional computer model was compared to the simulations of Rubin and Steinhardt (1963) and Hiler and Bhuiyan (1971). Their work provided data from soils with widly different hydraulic properties and also provided simulation results which were used for model verification.

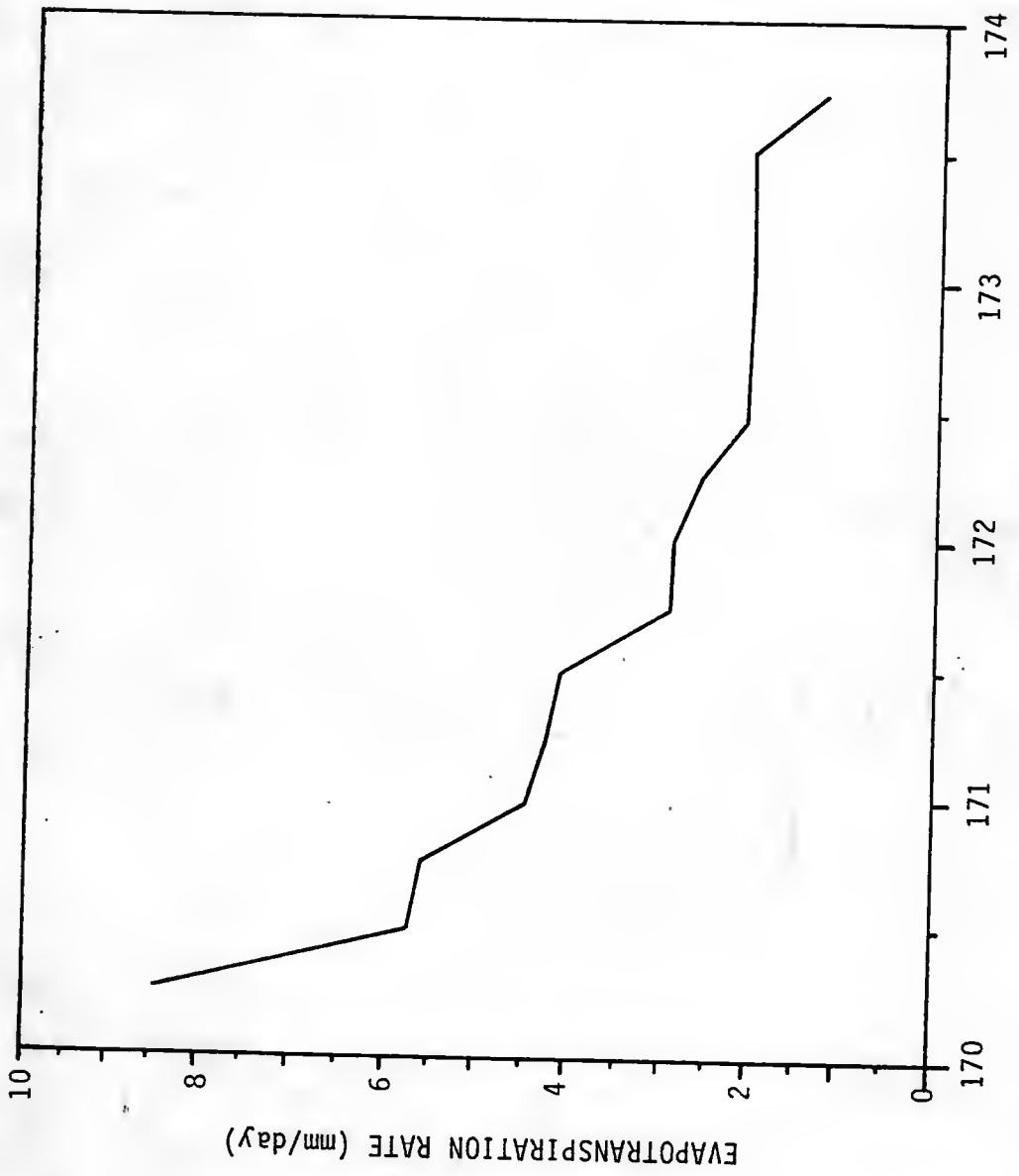

Figure 4-10. Evapotranspiration rate from the 1986 field experiment with a 20 kPa soil water potential treatment young citrus tree with grass cover.

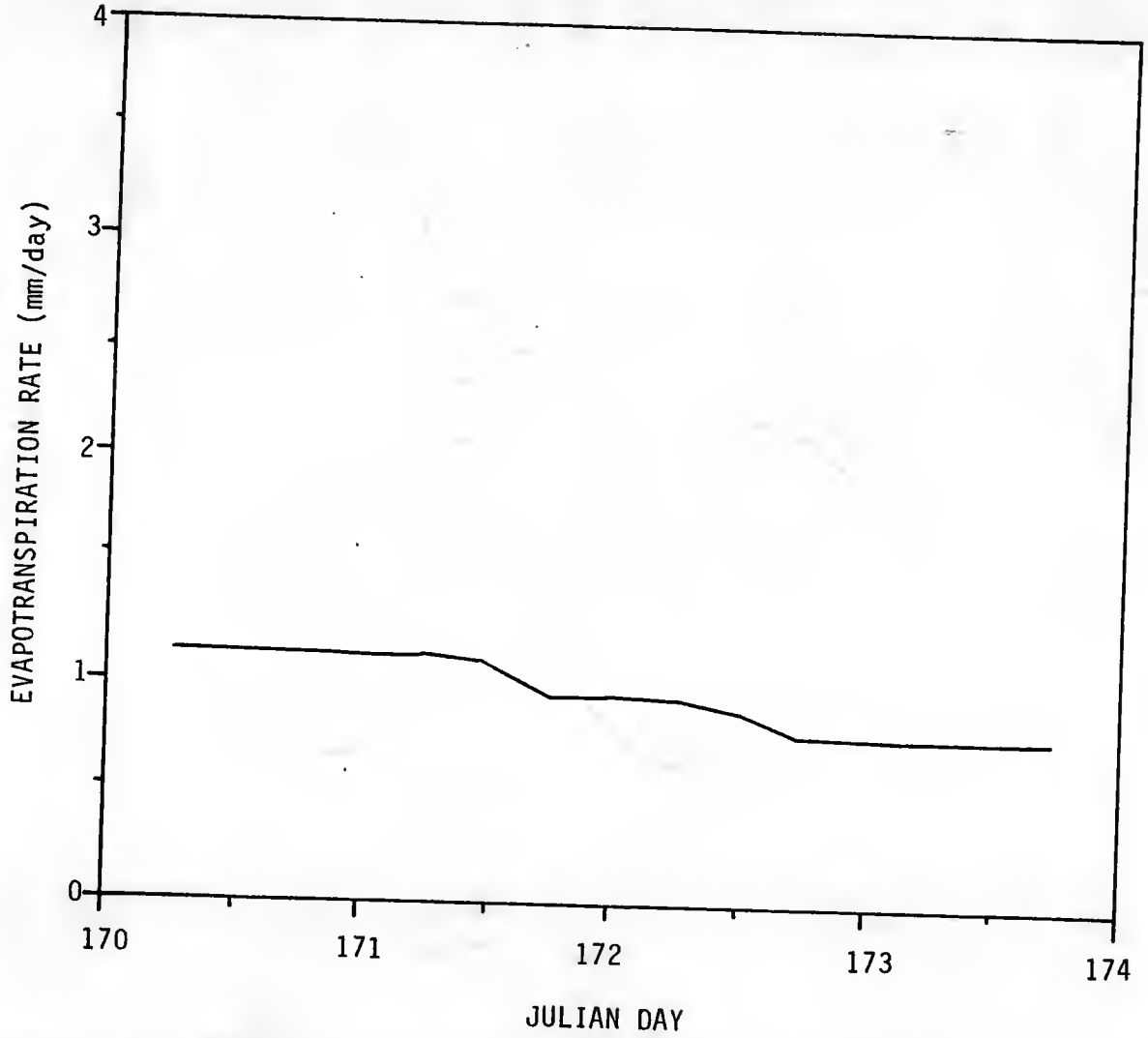

Figure 4-11. Evapotranspiration rate from the 1986 field experiment with a 20 kPa soil water potential treatment young citrus tree with bare soil.

Table 4-3. Two-dimensional distribution of water extraction for a 4 day drying cycle for young citrus trees with and without grass cover.

Depth (mm)	Depth Increment (mm)	Radius (mm)			
		200	600	200	600
		Tree with Grass Cover		Tree with No Grass Cover	
		Relative Water Extraction (%)			
0-225	225	28.2	31.2	19.9	16.95
225-375	150	12.2	15.2	12.3	17.9
375-525	150	4.45	1.2	6.85	3.75
525-750	225	4.4	1.2	8.4	8.7
750-1050	300	0.75	1.2	2.6	2.65
		Water Extraction (mm)			
0-225	225	1.6	1.8	0.9	0.8
225-375	150	0.7	0.9	0.6	0.8
375-525	150	0.3	0.07	0.3	0.2
525-750	225	0.3	0.07	0.4	0.4
750-1050	300	0.04	0.07	0.1	0.1
		Water Extraction (mm/mm)			
0-225	225	0.0073	0.0081	0.0041	0.0035
225-375	150	0.0048	0.0059	0.0038	0.0057
375-525	150	0.0017	0.00046	0.0021	0.0011
525-750	225	0.0011	0.00031	0.0017	0.0018
750-1050	300	0.0001	0.00023	0.0004	0.0004

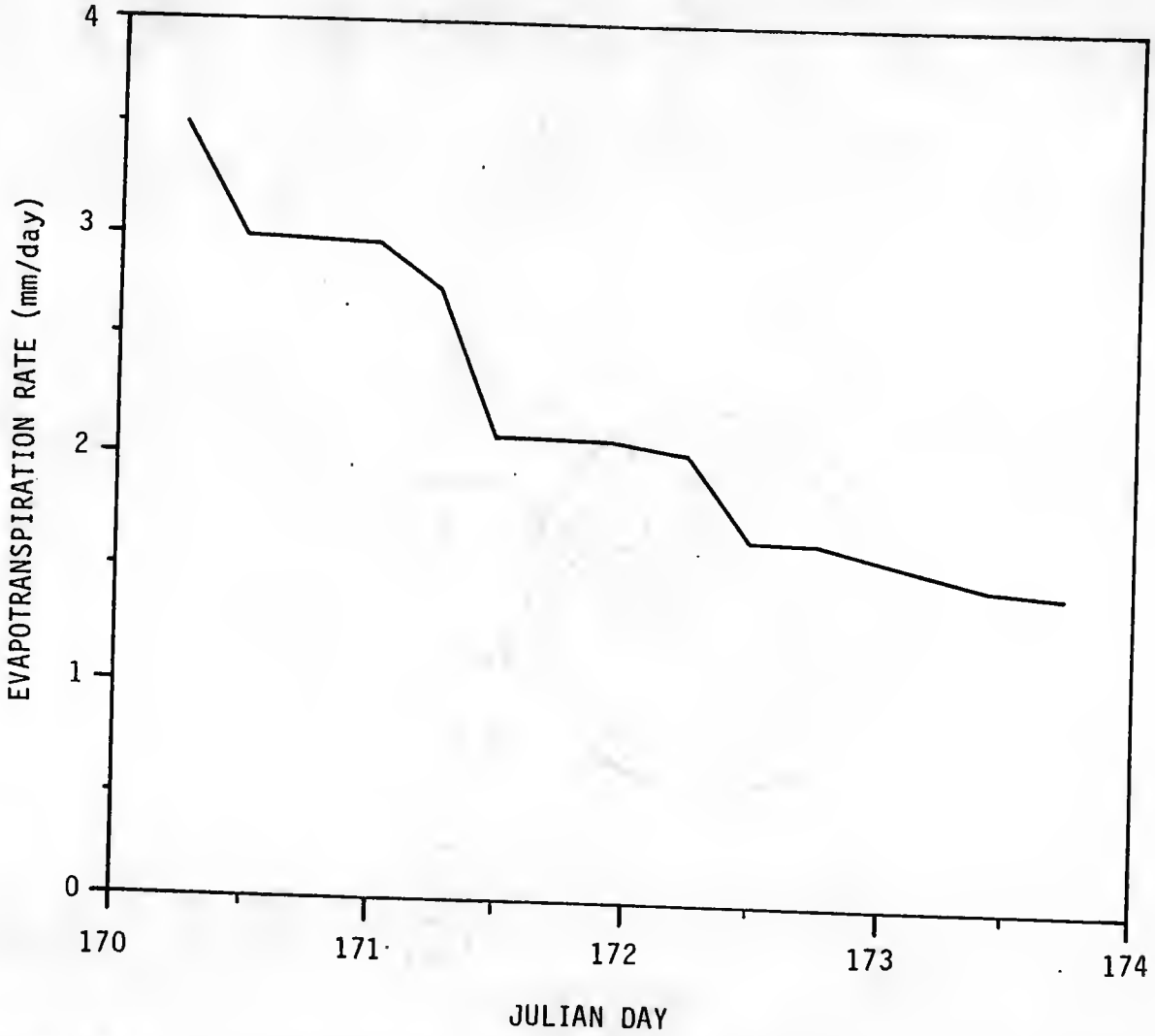

Figure 4-12. Evapotranspiration rate from the 1986 field experiment with a 20 kPa soil water potential treatment with a grass cover.

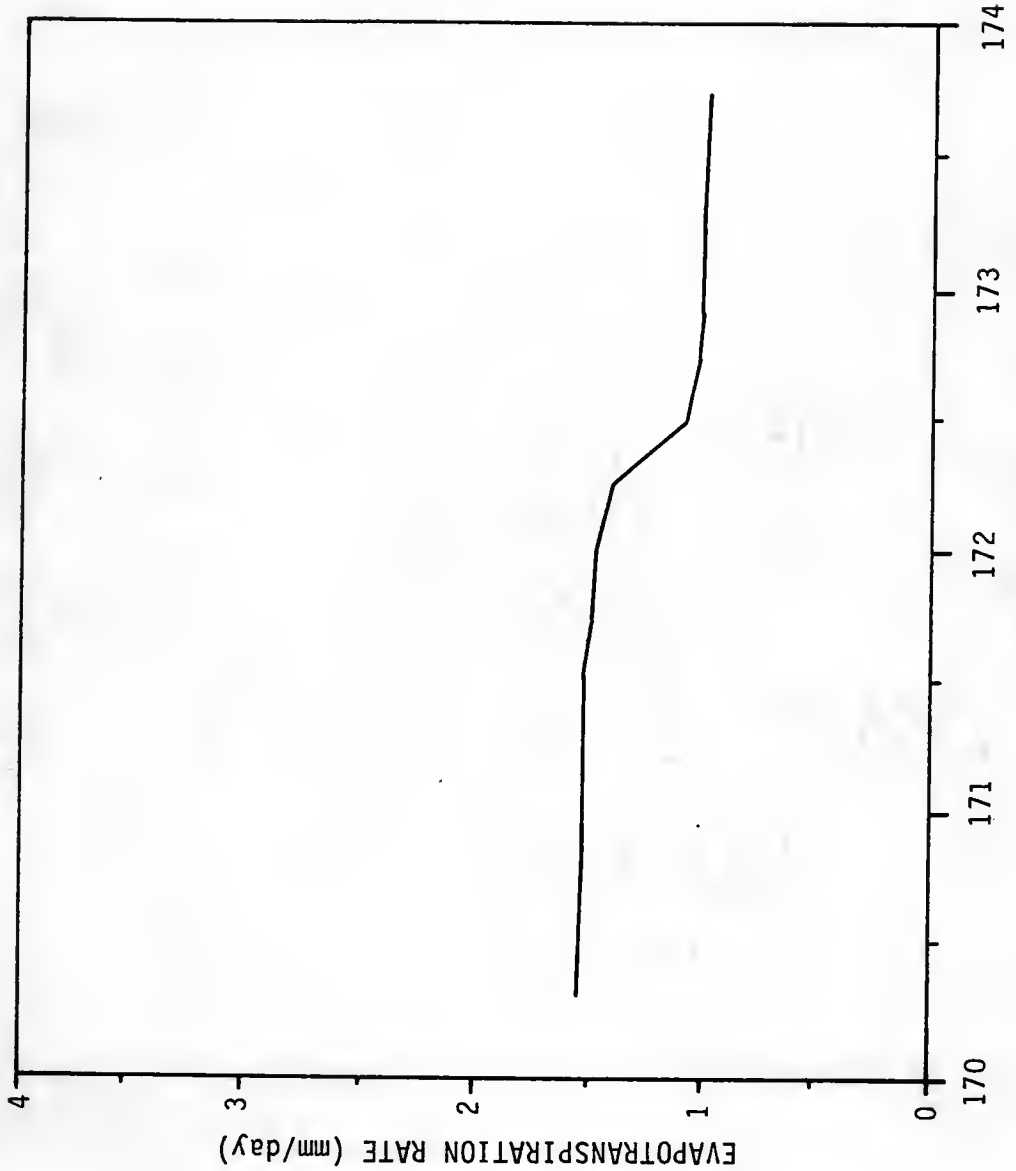

Figure 4-13. Evapotranspiration rate from the 1986 field experment with a 40 kPa soil water potential treatment with a grass cover.

Table 4-4. One-dimensional distribution of water extraction for a 4 dry drying cycle for a grass cover crop at water depletion levels of 20 kPa and 40 kPa.

Depth (mm)	Depth Increment (mm)	Water Extraction (mm)	Water Extraction (mm/mm)	Relative Water Extraction (%)
		20 kPa Treatment Tree with Grass Cover		
0-225	225	6.3	0.028	57.9
225-375	150	2.0	0.014	18.6
375-525	150	0.9	0.006	8.3
525-750	225	1.1	0.005	9.9
750-1050	300	0.6	0.002	5.3
		40 kPa Treatment Tree with Grass Cover		
0-225	225	3.9	0.0170	63.1
225-375	150	0.8	0.0055	13.5
375-525	150	0.5	0.0036	8.7
525-750	225	0.4	0.0019	6.9
750-1050	300	0.5	0.0016	7.8

Rubin and Steinhardt (1963) used an implicit solution of the Richards equation in terms of water content. Their model was used to study constant intensity rainfall infiltration on a Rehovot sand. The soil data were presented as analytic functions which were tabulated for use in this work. The soil hydraulic characteristics are shown in Figures 4-14 and 4-15.

The simulated soil profile had a uniform initial soil water content of 0.005. A uniform grid size of 10 mm was used. Figures 4-16 and 4-17 contain plots of soil water content profiles for infiltration into the Rehovot sand. The figures show both the results from Rubin and Steinhardt (1963) and this work. Figure 4-16 contains the soil water content profiles for a constant infiltration rate of 12.7 mm/hr. Figure 4-17 contains the soil water content profiles for a constant infiltration rate of 47 mm/hr. Results of this work are in excellent agreement with those of Rubin and Steinhardt (1963).

The work of Hiler and Bhuiyan (1971) was also used to verify the accuracy of the model developed in this work. They used a computer model written in CMSP to solve the Richards equation. Surface infiltration was simulated for two soils, Yolo light clay, and Adelanto loam. The hydraulic characteristics of these soils are presented in Figures 4-18 through 4-21.

The simulation results for these soils are presented in Figures 4-22 through 4-24. Figures 4-22 and 4-23 show water content profiles with time for the Yolo light clay at different initial conditions. Figure 4-24 shows the soil water content profiles with time for the Adelanto loam.

Comparison of results for the two soils showed excellent agreement between Hiler and Bhuiyan's CMSP model and this work. The minor differences between the results of the models could have resulted from the interpolation of the soil properties.

The two-dimensional model was tested by simulating infiltration for a Nahal Sinai sand (Bresler et al. 1971). Results were compared with a steady-state analytical solution developed by Wooding (1968) and with an ADI-Newton numerical simulation method presented by Brandt et al. (1971).

These models simulated the infiltration of water into the soil from a point source. The boundary condition used for the simulations was a constant flux for the innermost surface grid ($r = 0$). The flux was set equal to the saturated hydraulic conductivity of the soil. No flow boundaries were used for the lower and radial boundaries. The simulated soil profile had a uniform initial soil water content of 0.037. Figures 4-25 and 4-26 show the soil characteristics for the Nahal Sinai sand.

Figures 4-27 and 4-28 show a comparison between this work and that of Wooding (1968) and Brandt et al. (1971). The data are presented in dimensionless form with the relative water content defined as $S(\theta)/S(\theta_{sat})$ where $S(\theta)$ was defined by Philip (1968) as

$$S(\theta) = \int_{\theta_n}^{\theta} D \, d\theta \qquad (67)$$

where D = the hydraulic diffusivity and θ_n = the residual soil water content. The total infiltration time was 57 min in Figure 4-27 and 297 min in Figure 4-28.

Figures 4-27 and 4-28 demonstrate that this model accurately simulates the results of Brandt et al. (1971). Differences between the

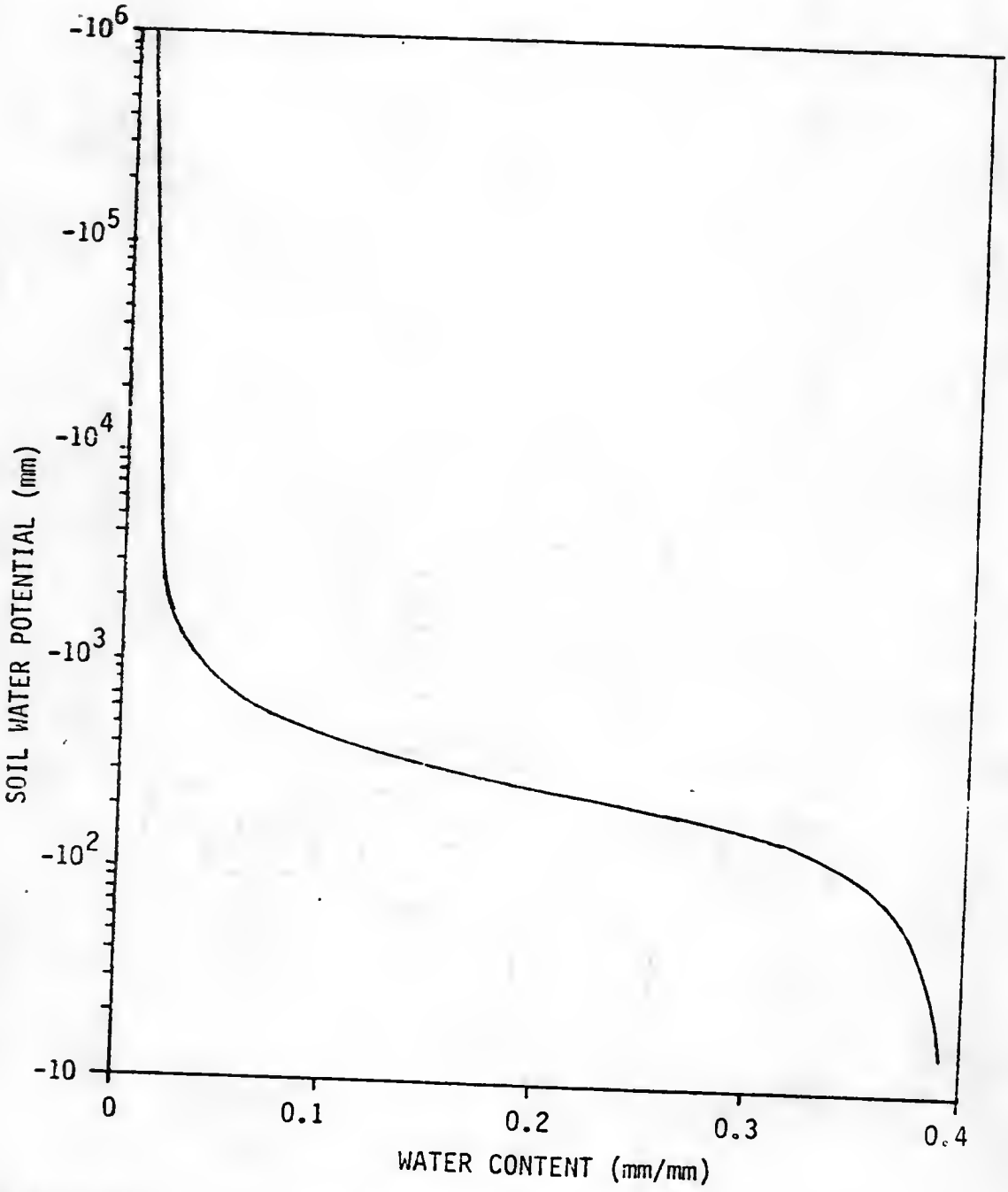

Figure 4-14. Soil water potential-soil water content relationship for Rehovot sand.

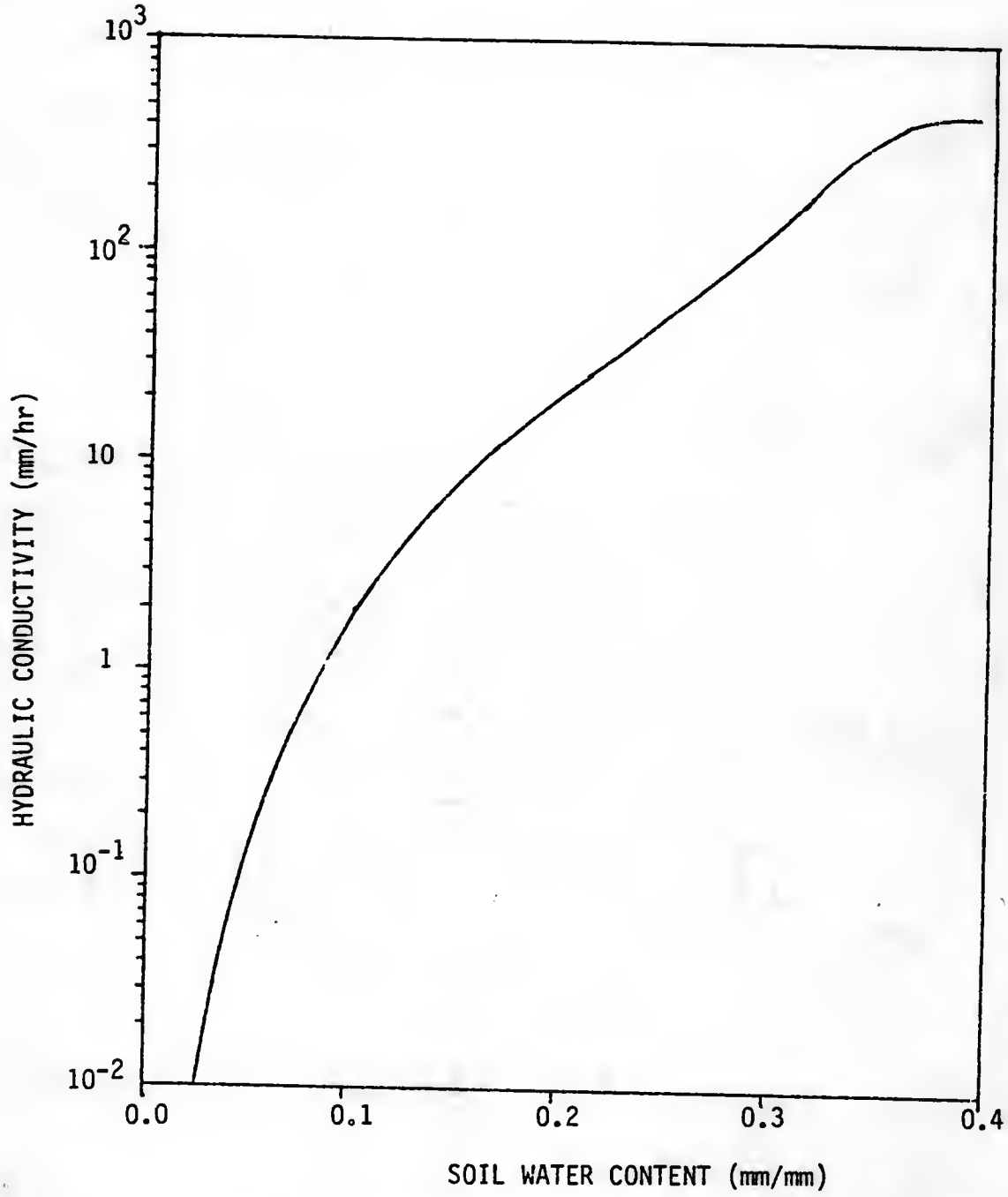

Figure 4-15. Hydraulic conductivity-soil water content relationship for Rehovot sand.

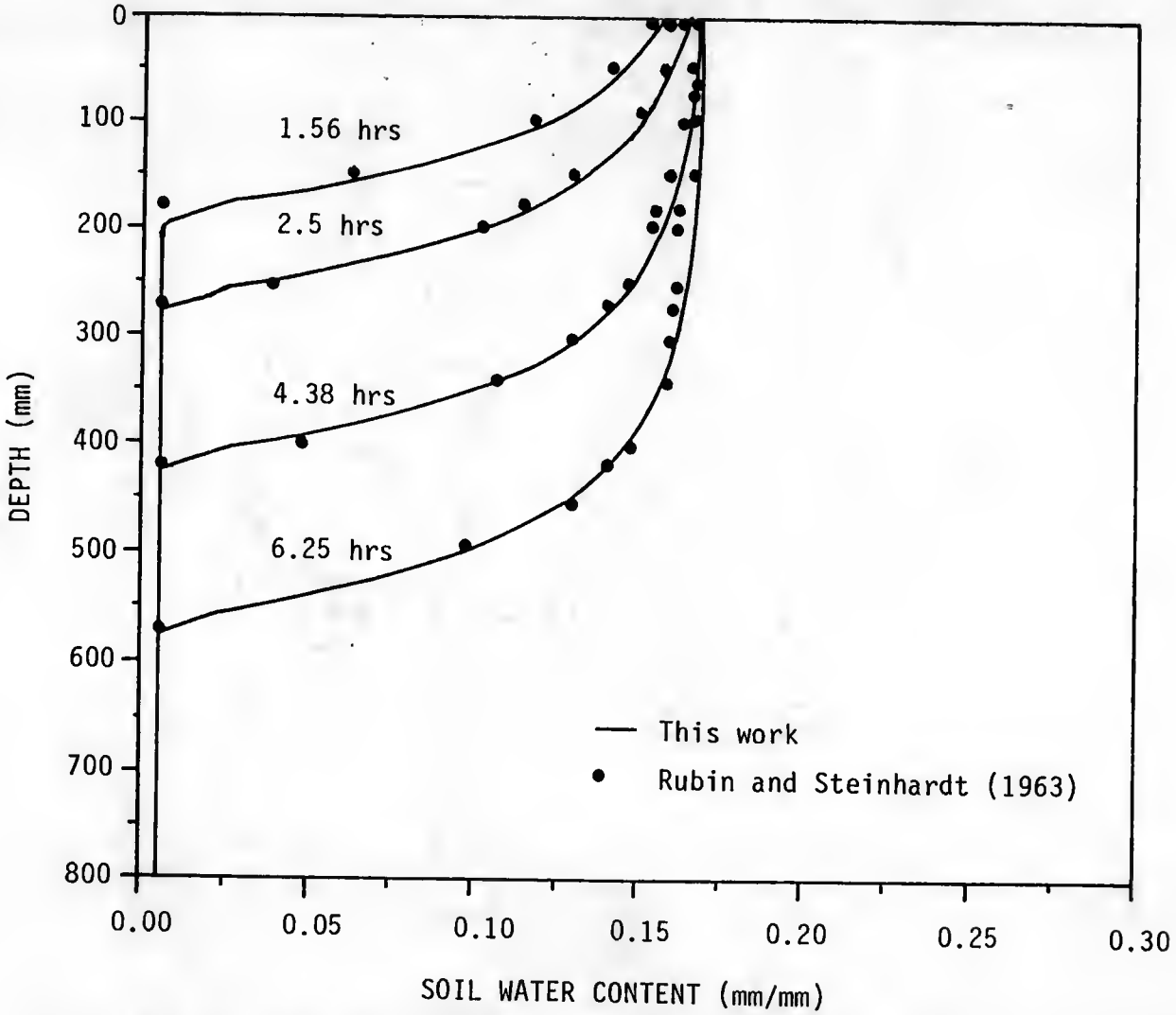

Figure 4-16. Simulated results of soil water content profiles for infiltration into a Rehovot sand under constant rain intensity of 12.7 mm/hr.

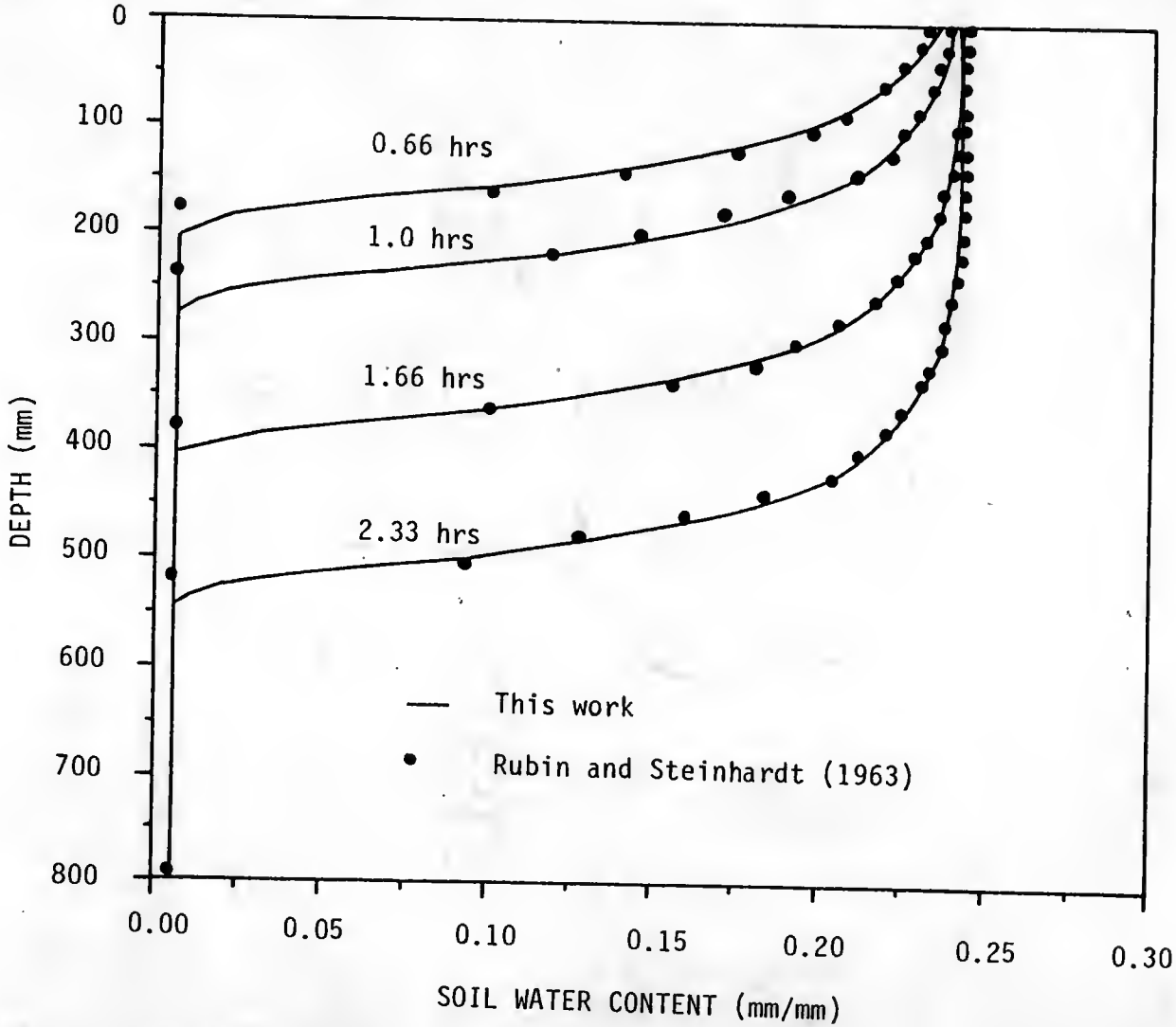

Figure 4-17. Simulated results of soil water content profiles for infiltration into a Rehovot sand under constant rain intensity of 47 mm/hr.

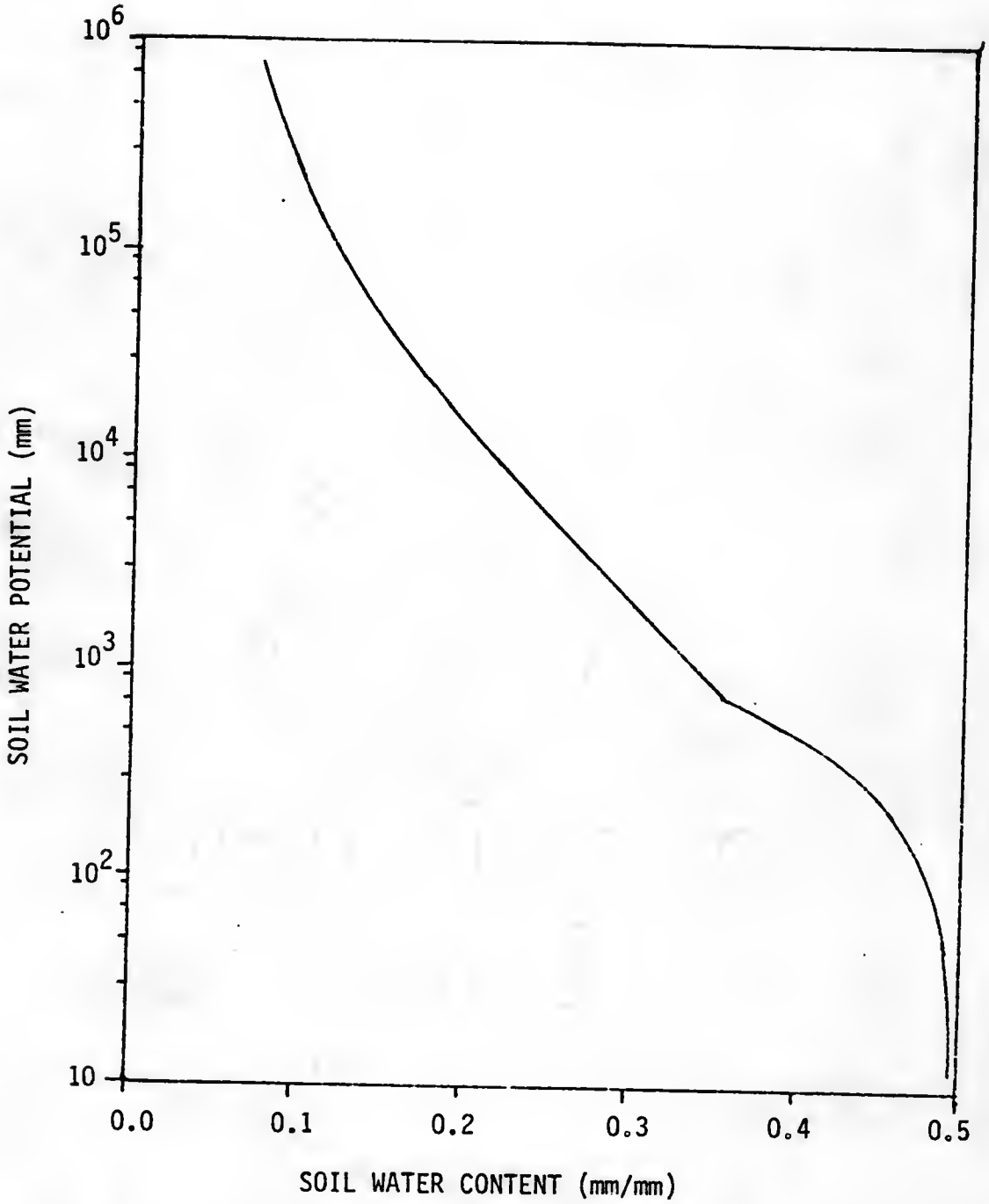

Figure 4-18. Soil water potential-soil water content relationship for Yolo light clay.

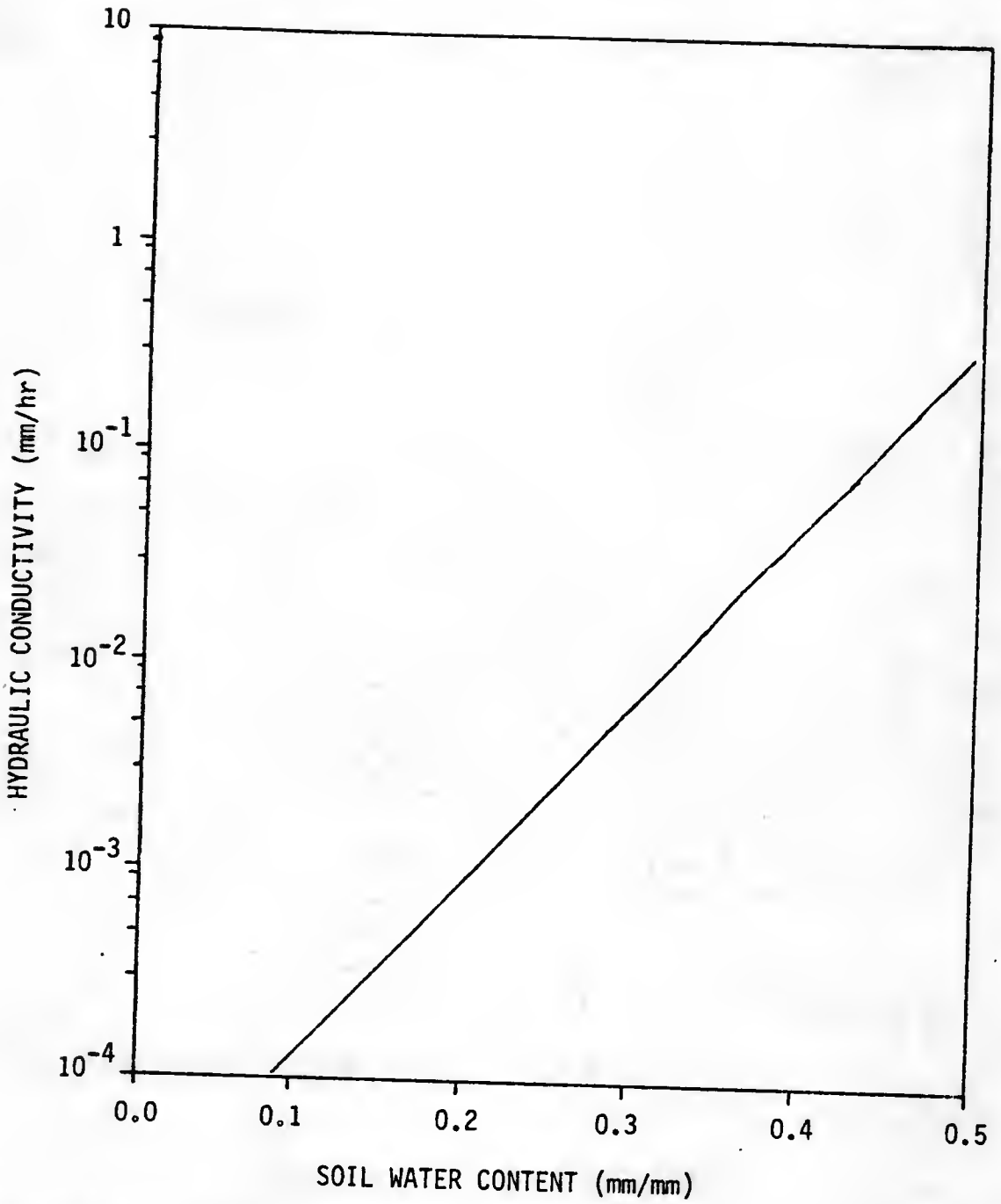

Figure 4-19. Hydraulic conductivity-soil water content relationship for Yolo light clay.

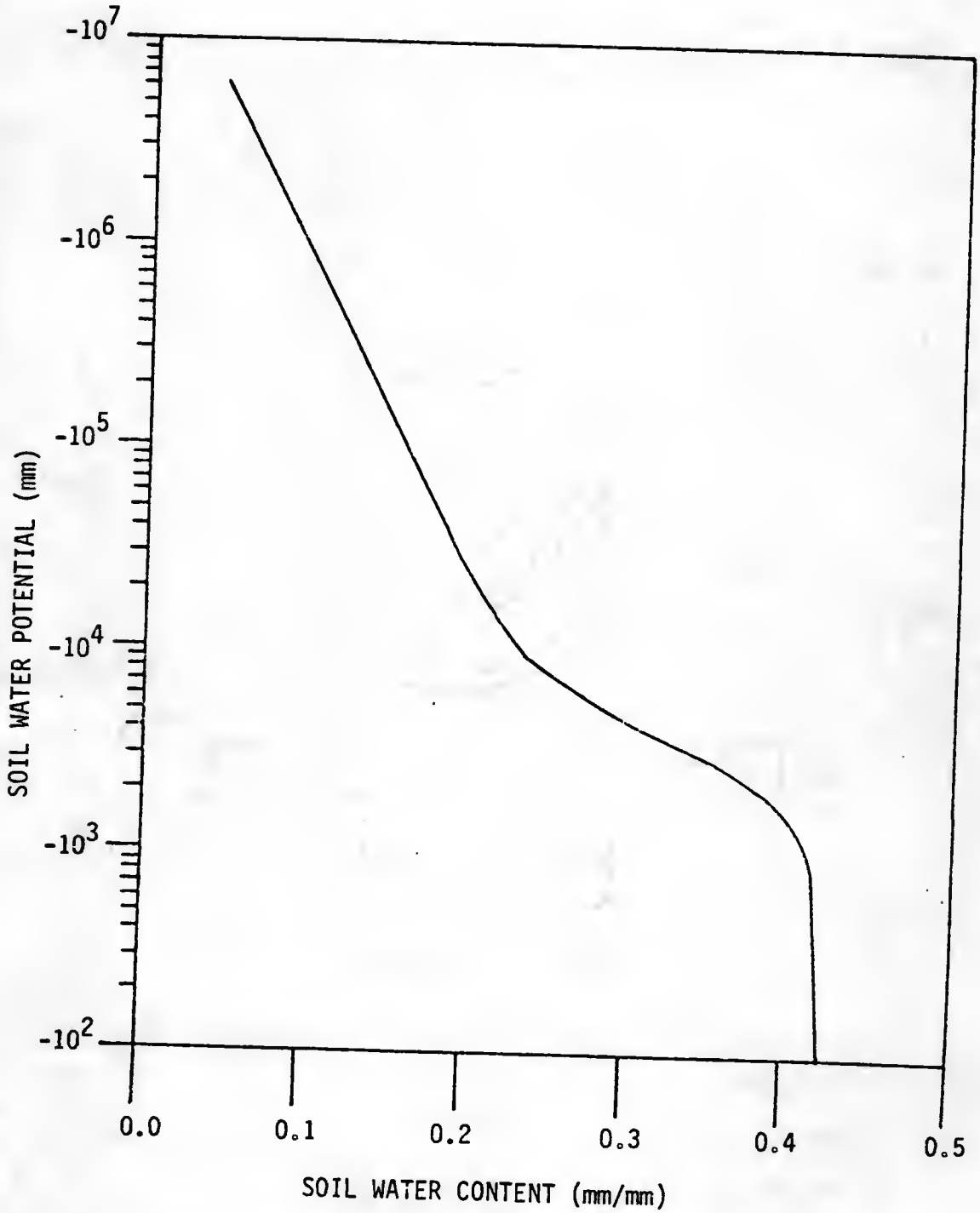

Figure 4-20. Soil water potential-soil water content relationship for Adelanto loam.

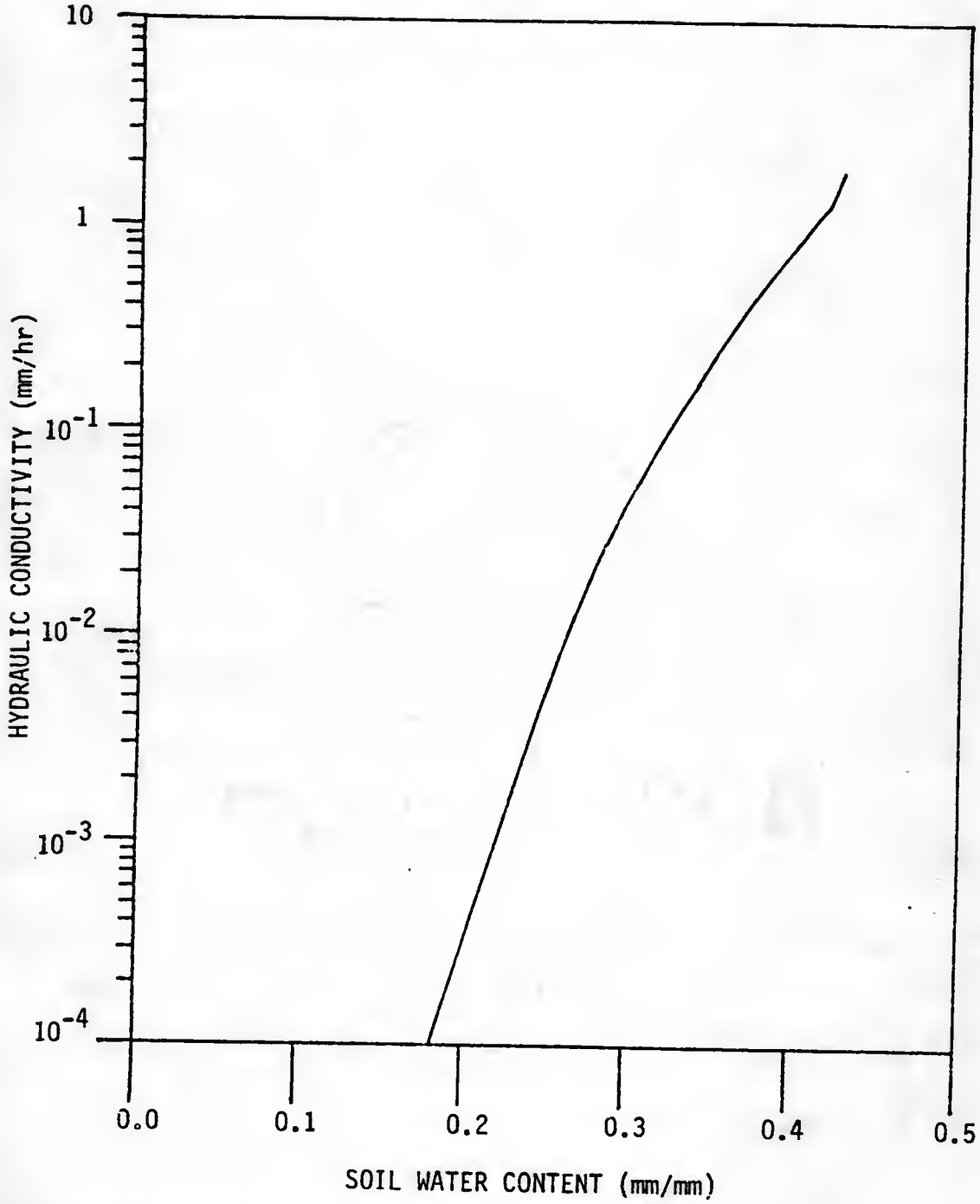

Figure 4-21. Hydraulic conductivity-soil water content relationship for Adelanto loam.

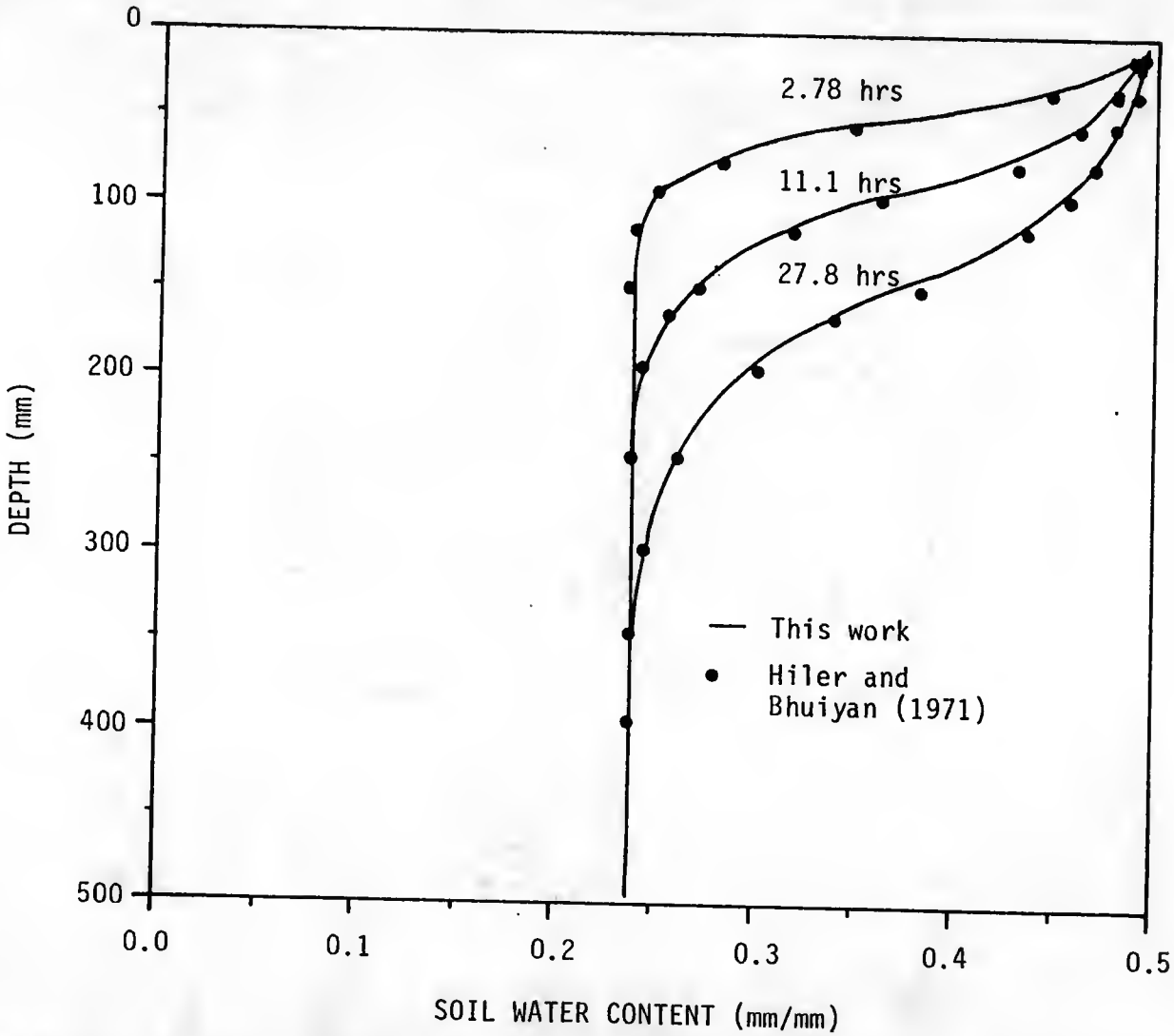

Figure 4-22. Simulated results of soil water content profiles for infiltration into a Yolo light clay with initial pressure potential at -66 kPa.

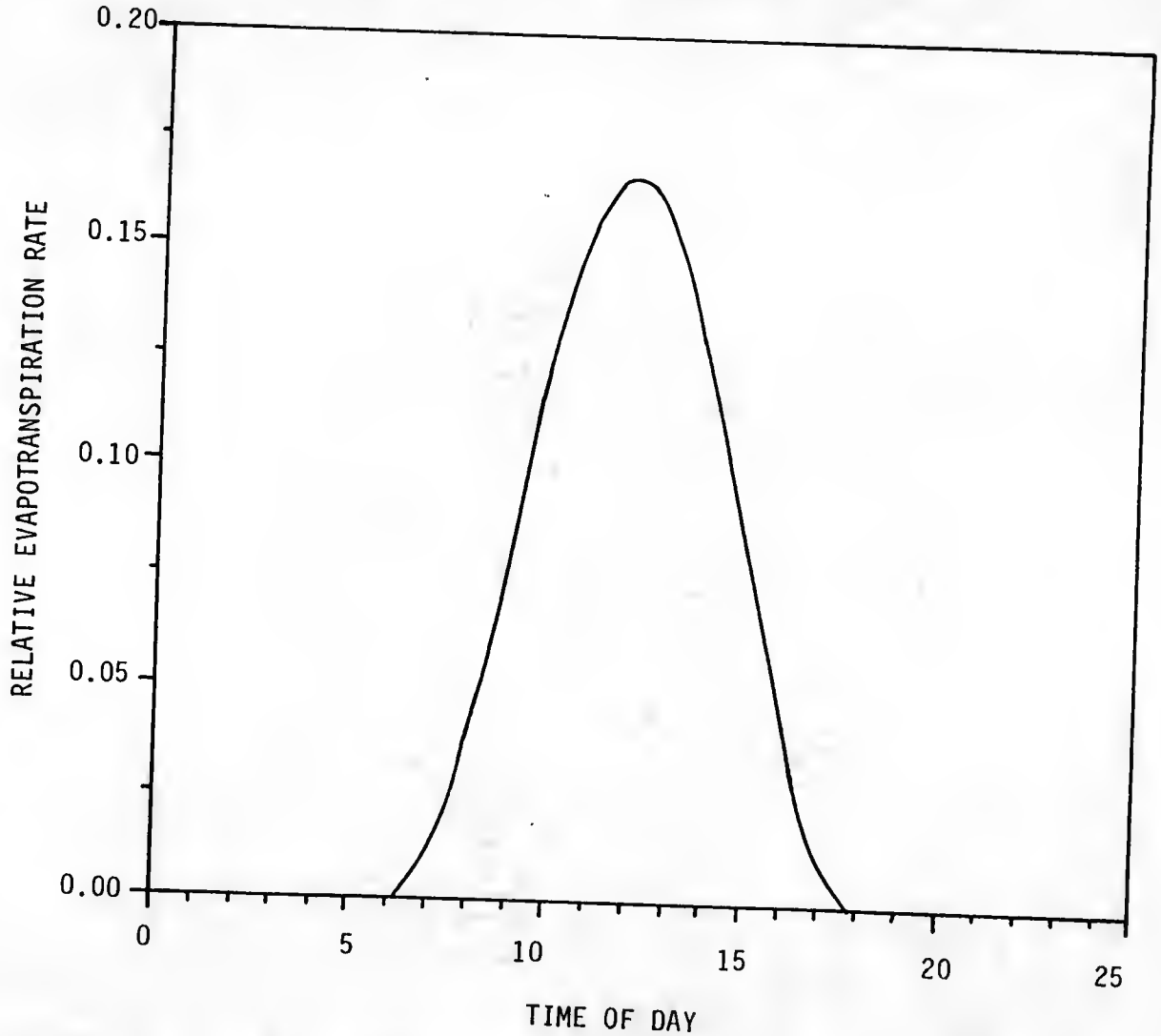

Figure 4-32. Distribution of evapotranspiration through the daylight hours.

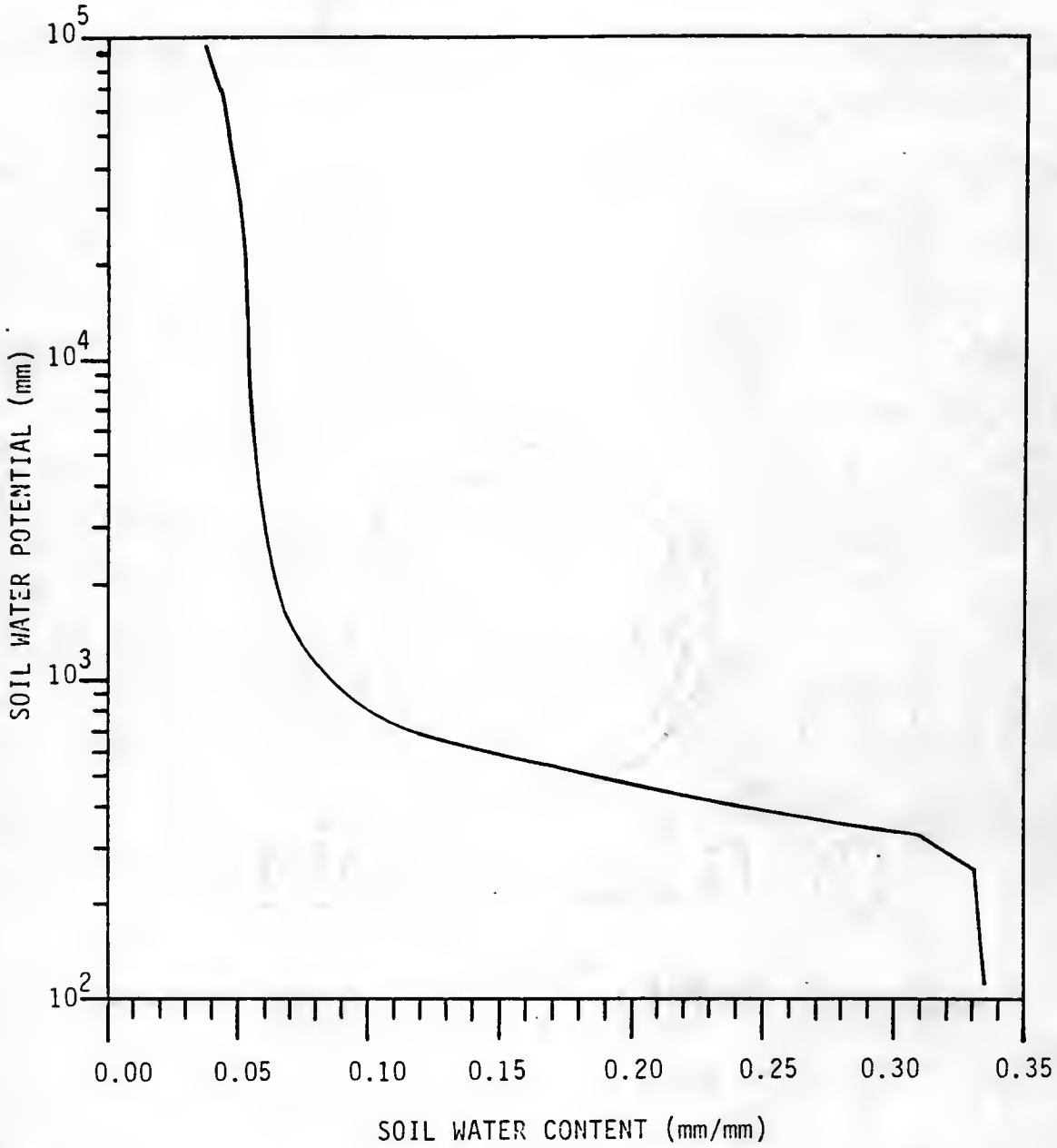

Figure 4-33. Soil water potential-soil water content relationship for Arredondo fine sand.

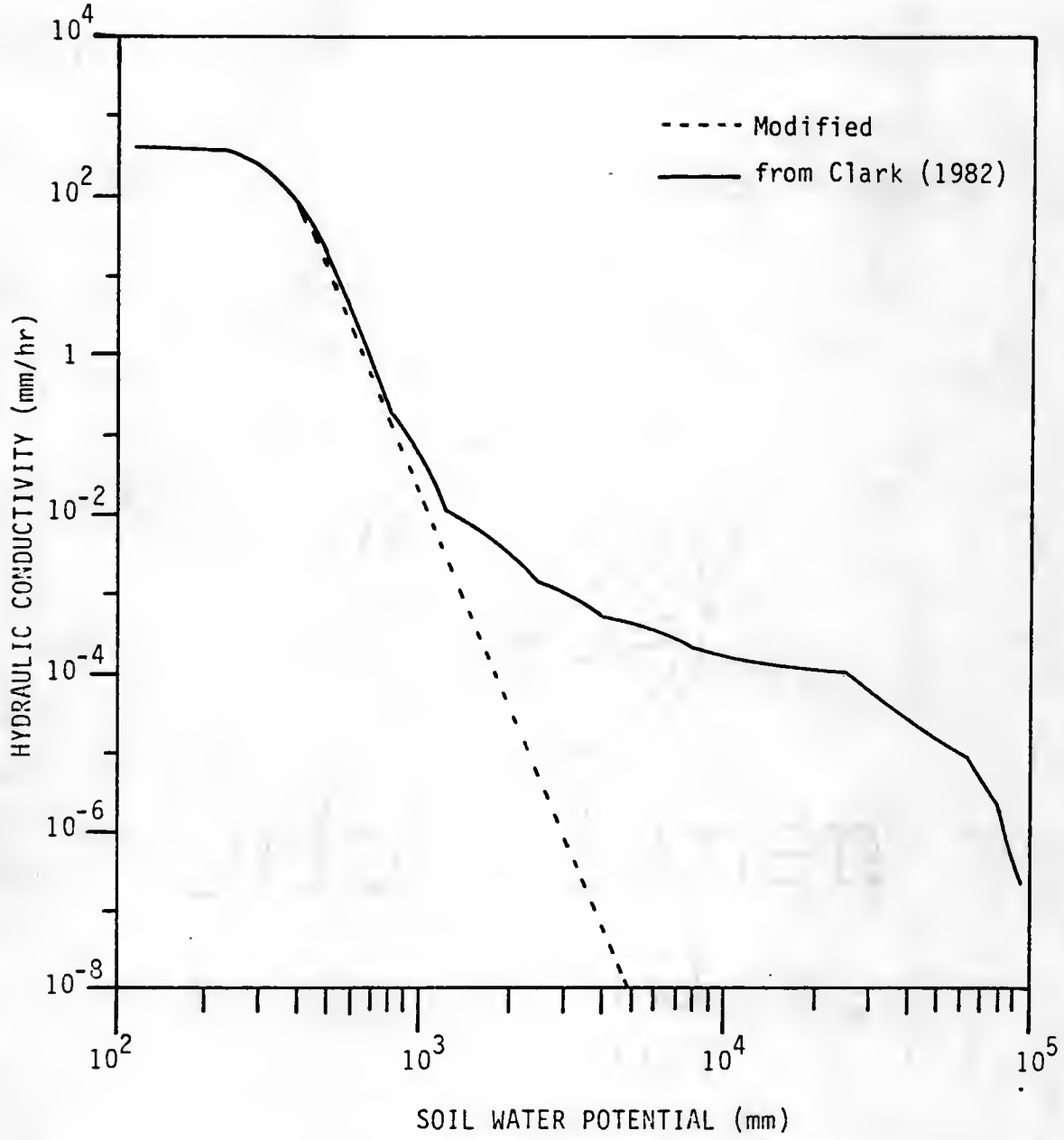

Figure 4-34. Hydraulic conductivity-soil water potential relationship for Arredondo fine sand.

conductivity function produced results with the numerical model which were in agreement with those from the observed field data.

One-dimensional Model

Time Steps. A sensitivity analysis was conducted to evaluate optimum grid sizes and timesteps. The time step used was variable, and the criteria for determining the variable time step were presented in equation (31). Operation of the model provided data from which limits for maximum and minimum time steps were determined. The maximum time step for model operation was determined to be 1 hour. Operation of the model with greater maximum time step produced varing results while operation with smaller maximum time steps gave results in agreement with the 1 hour timestep. The maximum time step was a upper limit for the calculated time step. The maximum time step was used when water movement in the soil profile was small. When water movements in the soil profile were large, as during infiltration, a minimum time step was determined. The minimum time step for the range of infiltration used in the model was determined to be 0.0001 hours. The use of a smaller time step slowed the model execution while not improving the mass balance. Larger time steps caused the mass balance to increase, thus indicating a reduction in model accuracy.

Grid Size. The optimum grid sizes were also determined by sensitivity analysis. A grid size of 30 mm was determined to be adequate to describe water movement in the soil profile for the one-dimensional model. Larger grid sizes decreased model execution time, but the soil water distribution was not adequately described. Smaller grid sizes increased the execution time while not improving the model accuracy.

Model Operation. The accuracy of the one-dimensional model was verified by simulating 35 days of observed water extraction, infiltration and redistribution under a young citrus tree with grass cover in a field lysimeter system. Initial conditions for the model were obtained directly from the observed soil water potentials and calculated root activity distributions. Observed average daily ET values were input to the numerical model. A no flux boundary condition was specified for the lower boundary. The surface boundary was set to a constant flux during irrigation and no flux at the end of the irrigation. Evapotranspiration from the top grid in the model was accounted for in the soil water extraction term.

Simulations of the observed field data were in good agreement with the experimental data. The simulated water contents were compared to field data in Figures 4-35 to 4-39. These data represent the five soil depths monitored with the data acquisition system. The simulated water contents for the first drying cycle were in excellent agreement with the field data.

An irrigation of 28 mm of water was applied to the lysimeter. The model simulated this irrigation, redistribution and extraction for a second drying cycle. The simulation results were in excellent agreement with the field data for the second drying cycle also. The water contents for the 450, 600 and 900 mm depths were in excellent agreement with the observed field water contents throughout the drying cycle. The water contents for the 150 mm depth was in good agreement throughout most of the second drying cycle. The simulated water contents for the 300 mm depth were greater than the observed field data.

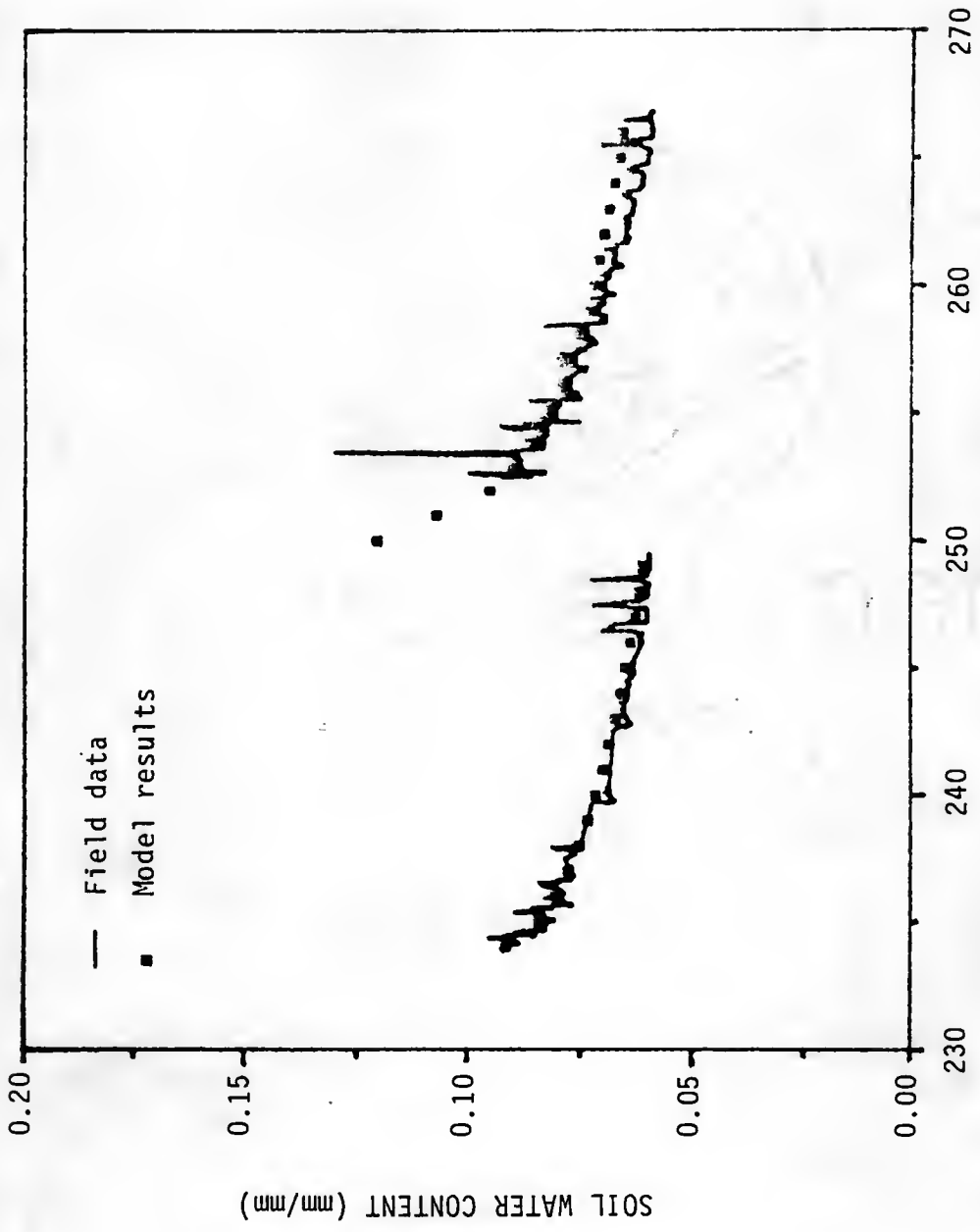

Figure 4-35. Simulation results for the one-dimensional model with field data for the 150 mm depth.

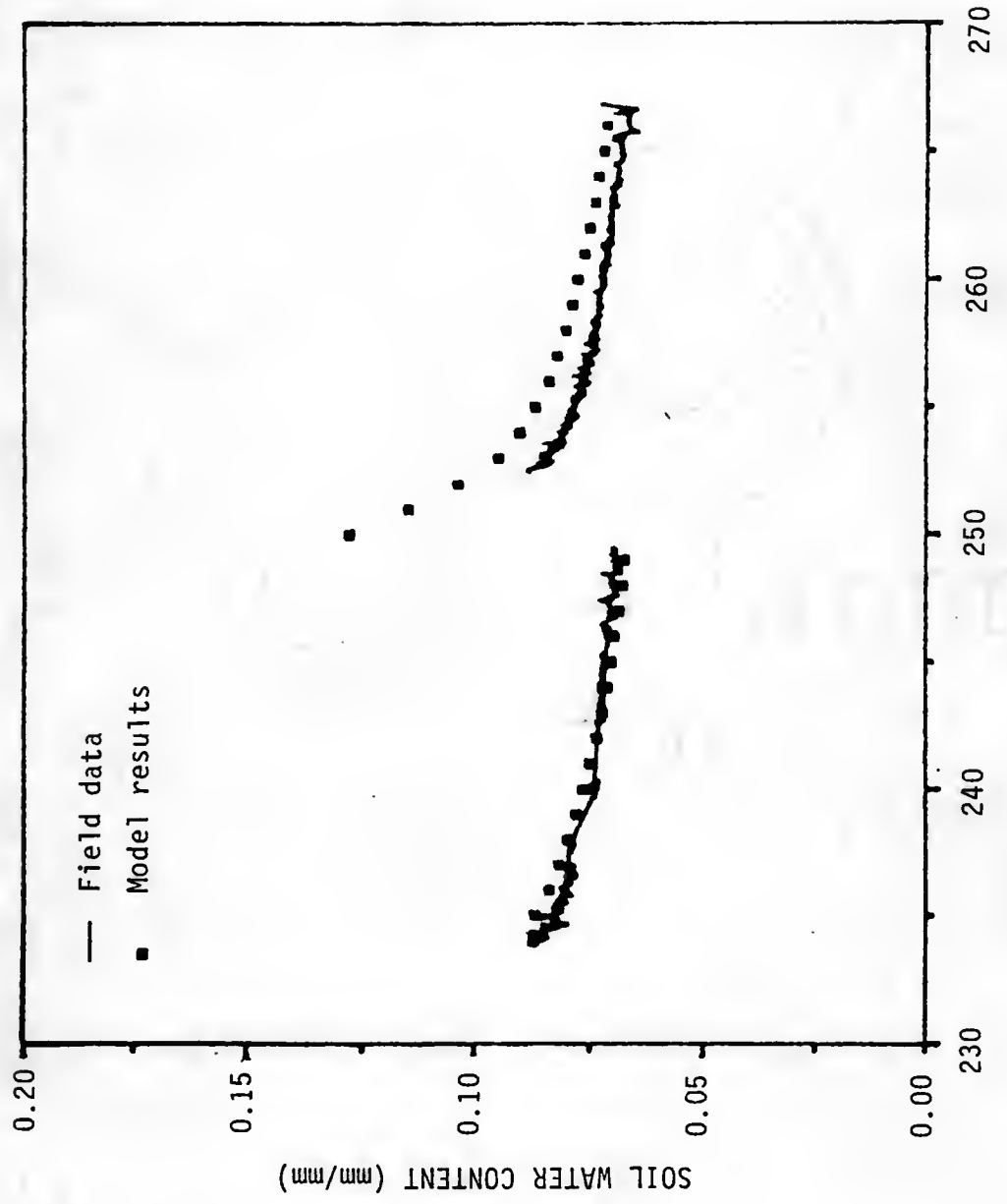

Figure 4-36. Simulation results for the one-dimensional model with field data for the 300 mm depth.

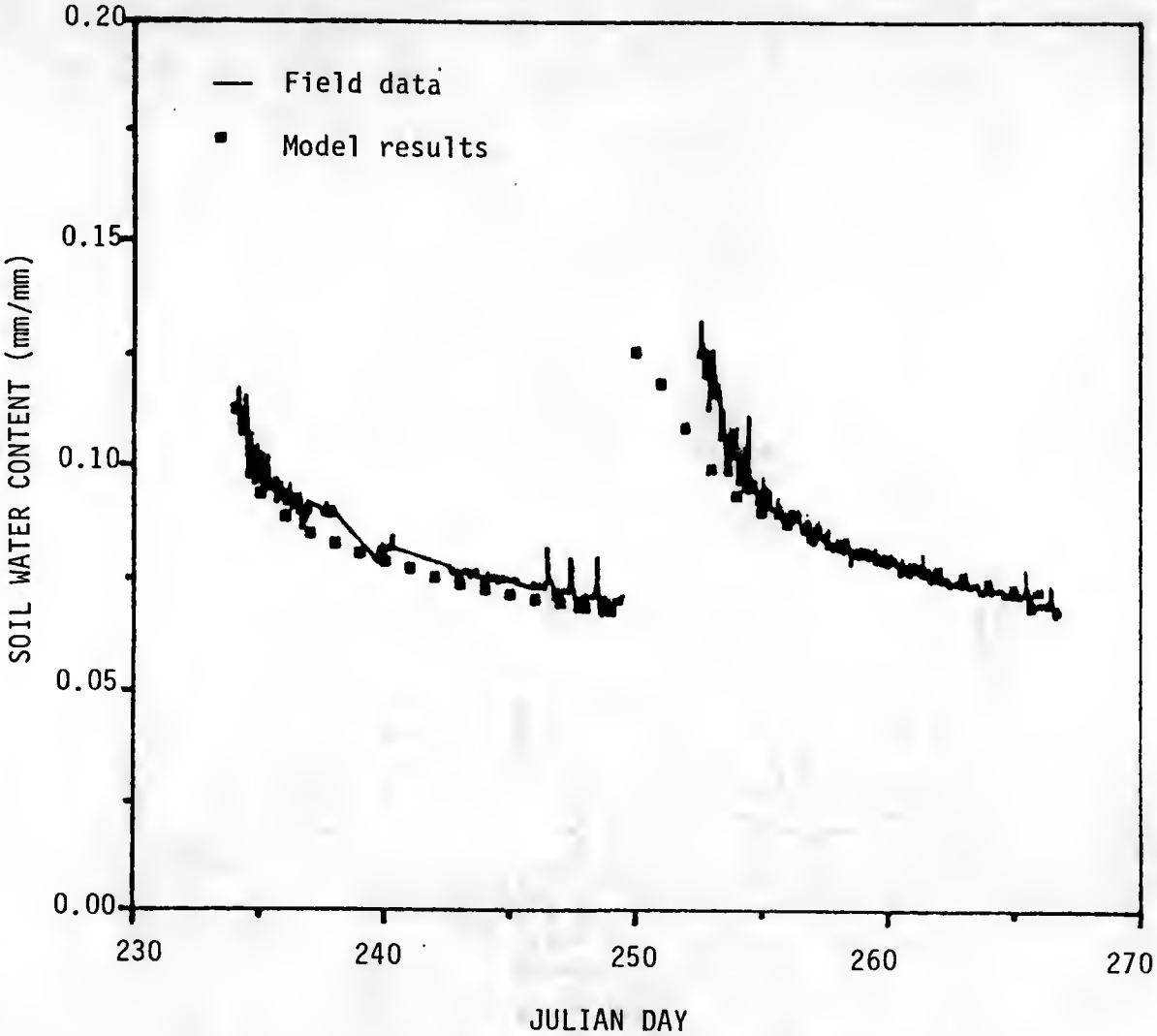

Figure 4-37. Simulation results for the one-dimensional model with field data for the 450 mm depth.

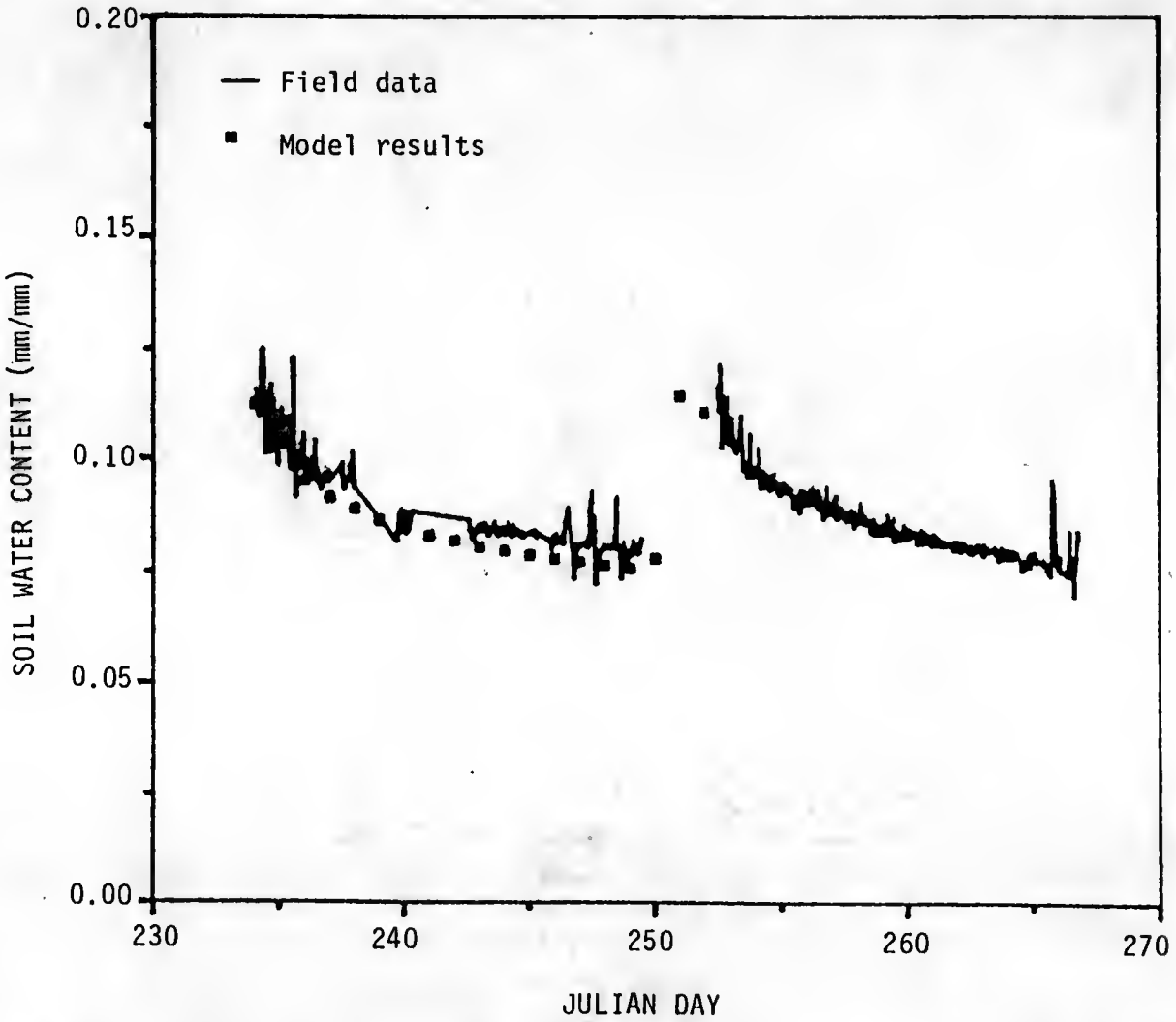

Figure 4-38. Simulation results for the one-dimensional model with field data for the 600 mm depth.

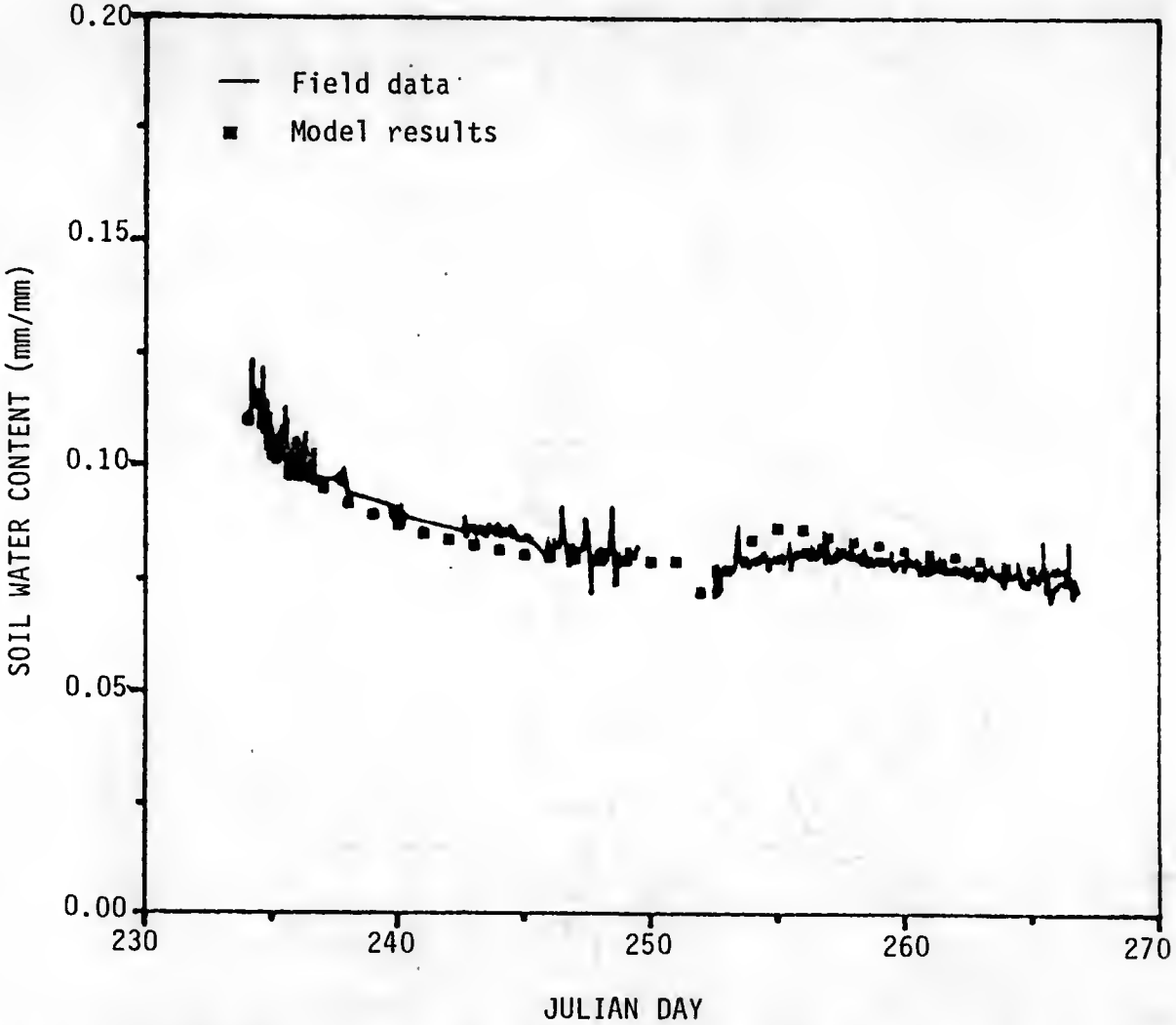

Figure 4-39. Simulation results for the one-dimensional model with field data for the 900 mm depth.

The differences between the simulated and observed water contents may have been due to the variations in the soil properties under field conditions. The model assumed homogeneous and isotropic soil conditions. This cause is supported by the random variations between observed and simulated water contents. Overall the model simulated changes in soil water movement and extraction with excellent agreement.

Two-dimensional Model

Time Steps. A sensitivity analysis was conducted to evaluate optimum grid sizes and time steps for the two-dimensional model. The time step used was variable, and the criteria for determining the variable time step were presented in equation (31). Operation of the model provided data from which limits for maximum and minimum time steps were determined. These maximum and minimum time steps were determined to be the same as used with the one-dimensional model. The maximum allowable time step for model operation was determined to be 1 hour. The minimum allowable time step for the range of infiltration used in the model was determined to be 0.0001 hours.

Grid Size. The grid sizes for the two-dimensional model were also determined by sensitivity analysis. A grid size of 30 mm was determined to be adequate to accurately describe water movement in the vertical direction. The radial grid size of 50 mm was determined to be adequate to accurately describe water movement in the radial direction.

Model Operation. The two-dimensional model was used to simulate 35 days of water extraction, infiltration and redistribution under a young citrus tree with grass cover in a field lysimeter. The initial conditions for the model were determined directly from the observed soil water potentials and root distributions. Observed daily ET amounts were

input to the model. Boundary conditions for the two-dimensional model were all no flow boundaries when there was no infiltration. During infiltration, a surface flux equal to the irrigation application rate was used. When irrigation was completed, the surface boundary condition was reset to a no flow condition.

Simulations of the observed field data were in excellent agreement with the experimental data for the first drying cycle. The simulated water contents were compared to the field data in Figures 4-40 to 4-44. These data represent the 15 sites in the soil profile which were monitored with the data acquisiton system. The observed and simulated water contents for the drying cycle are presented for each of the four radii measured. Simulated water contents were in excellent agreement with the observed field water contents for almost all of the observed sites during the first drying cycle. The 450 mm depth water contents did not agree as well at the 100 mm radius for the later part of the drying cycle.

Simulated soil water movement and extraction for the second drying cycle were in good agreement with the observed field data. Simulated water contents for the 100 and 300 mm radii were in excellent agreement with field water contents for all five observed depths. The simulated water contents for the outer radii were different than observed water contents for several locations. These differences may be attributed to variations in the soil properties or nonuniform application of irrigation water at the surface. The soil properties were assumed to be homogenous and isotropic. The model assumed that the irrigation application was uniform. Overall the model results were in good agreement with the observed field data.

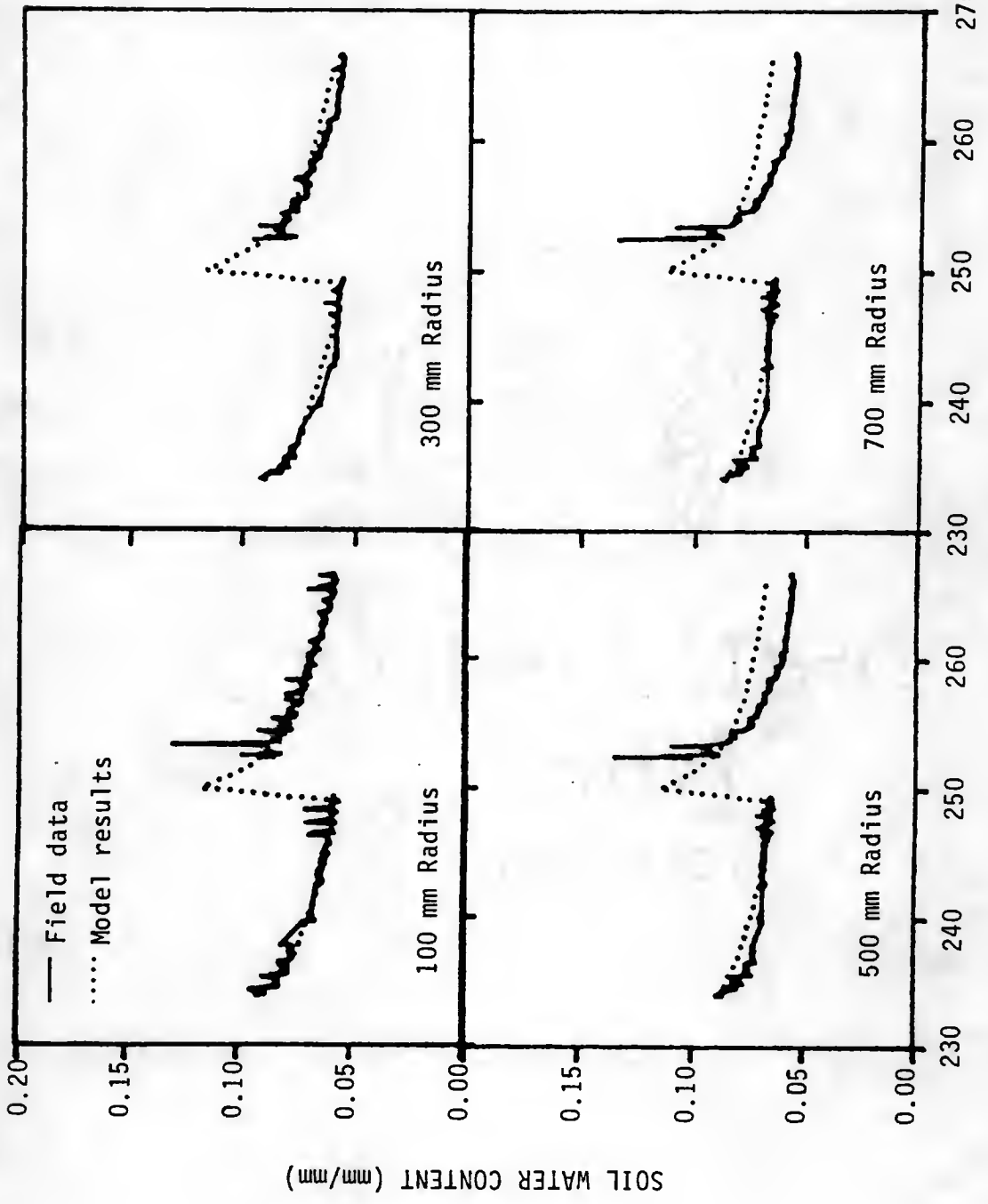

Figure 4-40. Simulation results for the two-dimensional model with field data for the 150 mm depth.

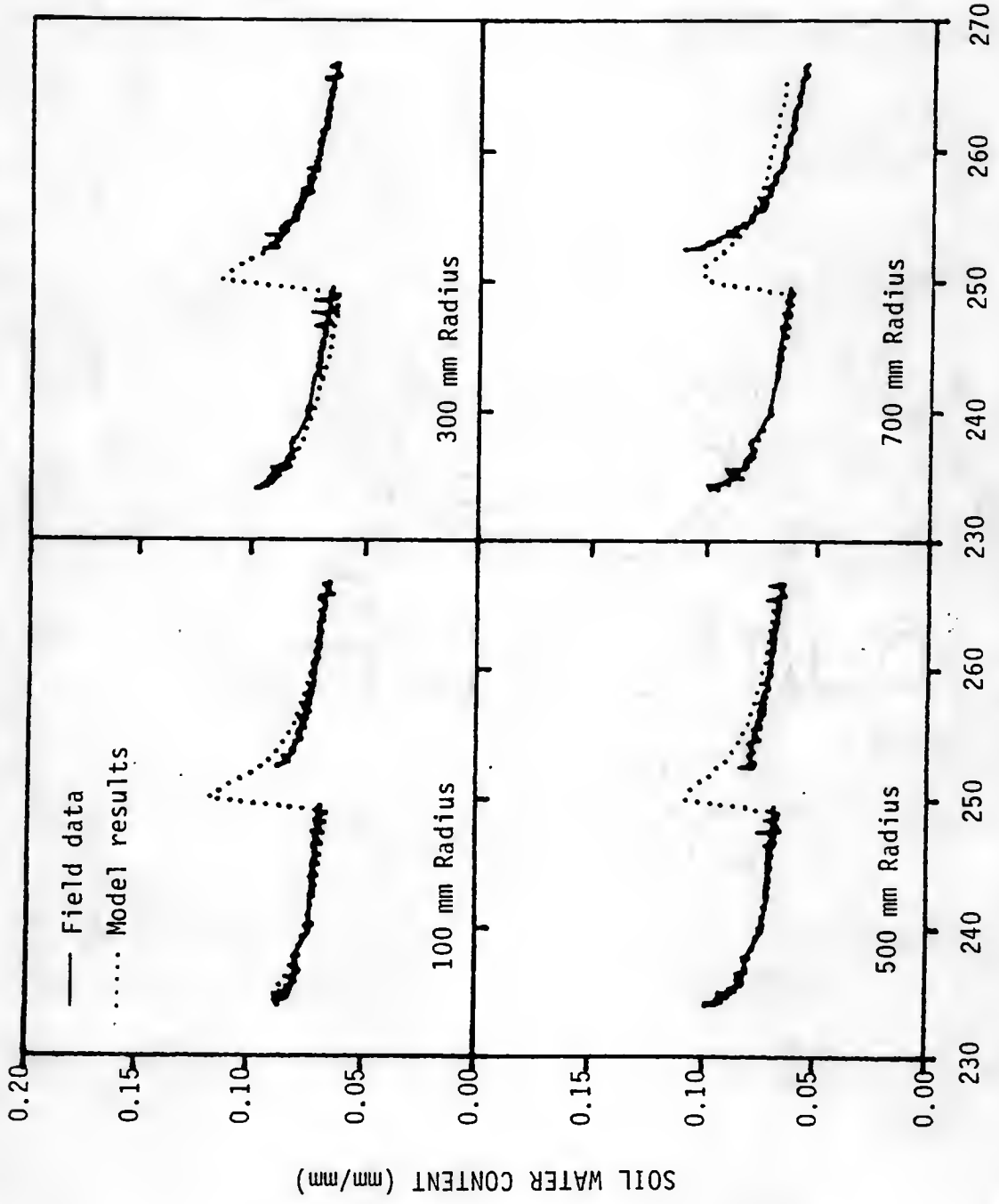

Figure 4-41. Simulation results for the two-dimensional model with field data for the 300 mm depth.

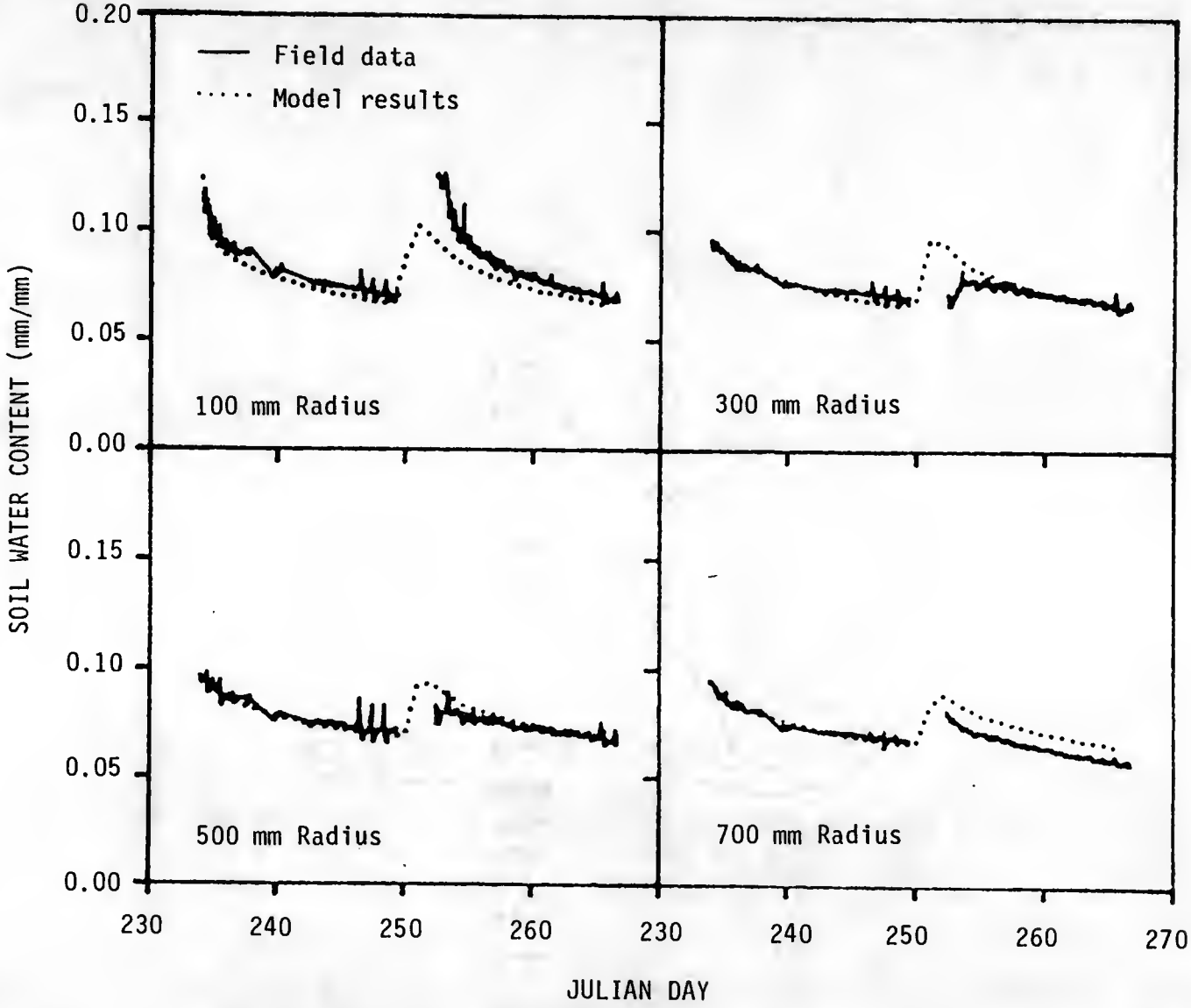

Figure 4-42. Simulation results for the two-dimensional model with field data for the 450 mm depth.

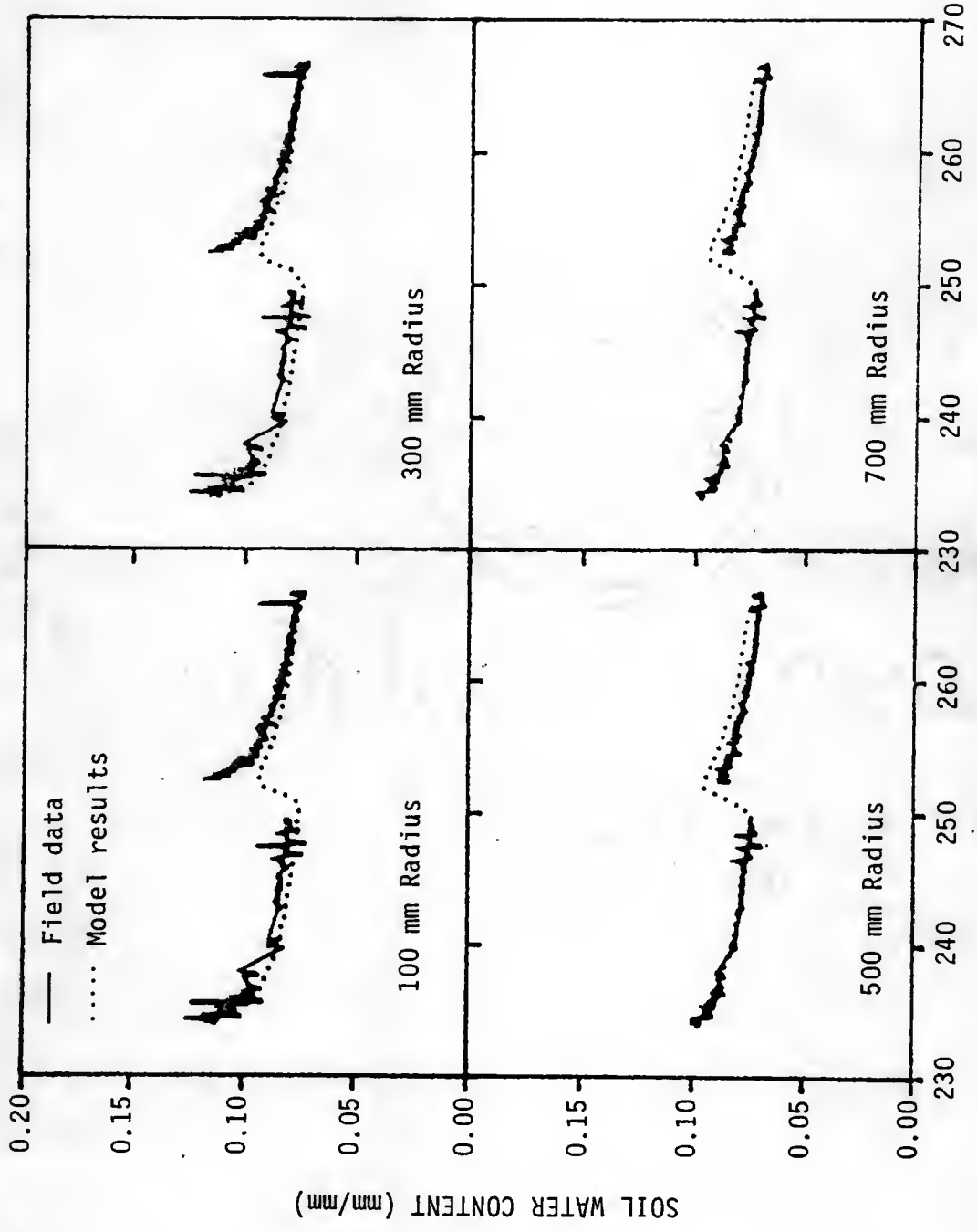

Figure 4-43. Simulation results for the two-dimensional model with field data for the 600 mm depth.

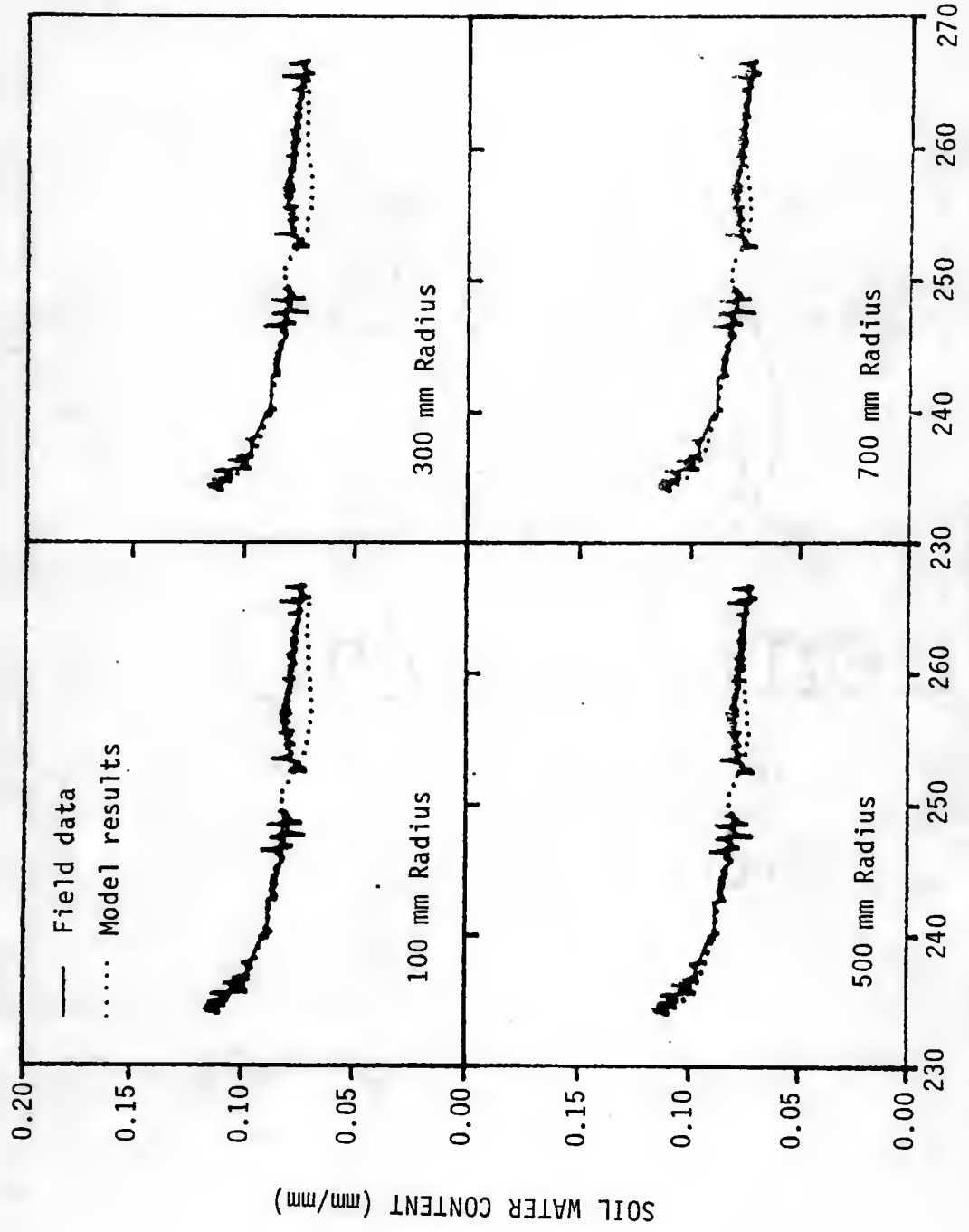

Figure 4-44. Simulation results for the two-dimensional model with field data for the 900 mm depth.

Model Applications

The numerical models developed in this research can provide researchers with numerical models of soil water movement to study infiltration, water extraction and solute movement. The models may be used to determine optimum irrigation scheduling for a wide variety of soils and atmospheric conditions. The numerical models allow the input of historic rainfall and ET data.

To demonstrate potential applications of the numerical models developed, the one-dimensional numerical model was used to compare three irrigation strategies. The first strategy studied was to schedule irrigations to occur when the water potential in the soil profile dropped below -10 kPa at a specified depth in the soil profile. The second was to schedule irrigations to occur when the water potential in the soil profile dropped below -20 kPa and the third when the water potential dropped below -30 kPa. The numerical model was modified to monitor specific depths in the soil profile to represent tensiometer (or other soil water status monitoring equipment) locations as in field operations. Depths of 300 and 900 mm were monitored in this study. An irrigation depth of 25 mm was applied when the soil water potential at any monitoring depth dropped below the set water potential. Rainfall interactions were not considered in these simulations but could be taken into account with the numerical model by inputting historical data.

The inputs to the model were the initial soil water potentials which were assumed to be at field capacity. Evapotranspiration was input on a daily interval, and for these simulations was assumed to be a constant 4 mm/day. The surface boundary condition for the one-dimensional model was a no flux when irrigation was not occurring.

During irrigation the surface boundary condition was a flux boundary with the flux equal to the irrigation application rate. The lower boundary condition for the model was a gravity flow condition to simulate deep percolation from the soil profile.

Simulation results for the three irrigation strategies were shown in Figures 4-45 to 4-49. Figure 4-45 and 4-46 show the soil water contents monitored at 300 and 900 mm. From the soil water contents, it appears that the irrigations for the -10 kPa treatment were controlled by the potentials at the 300 mm depth because of the frequent and small irrigations applications. The irrigations for the -20 and -30 kPa treatments appear to be controlled by the 900 mm depth because of the less frequent and larger irrigation applications. These demonstrate another use of the numerical model to determine the optimum depths to monitor for different soils and different allowable soil water depletions.

Figure 4-47 shows the soil water storage in the profile during the simulation period. The soil water storage for the -10 kPa treatment was consistantly more uniform, while the soil water storage for the -20 and -30 kPa treatments varied widely.

Figures 4-48 and 4-49 shows the irrigation applied and the drainage out of the profile. The same amount of irrigation was applied for all three treatments. Irrigation was applied more frequently for the -10 kPa treatment. Irrigations were less frequent for the -20 and -30 kPa treatments but they required several irrigations to bring the soil water potentials in the soil profile above the set limits. Figure 4-49 showed the drainage loss out of the bottom of the profile for the different

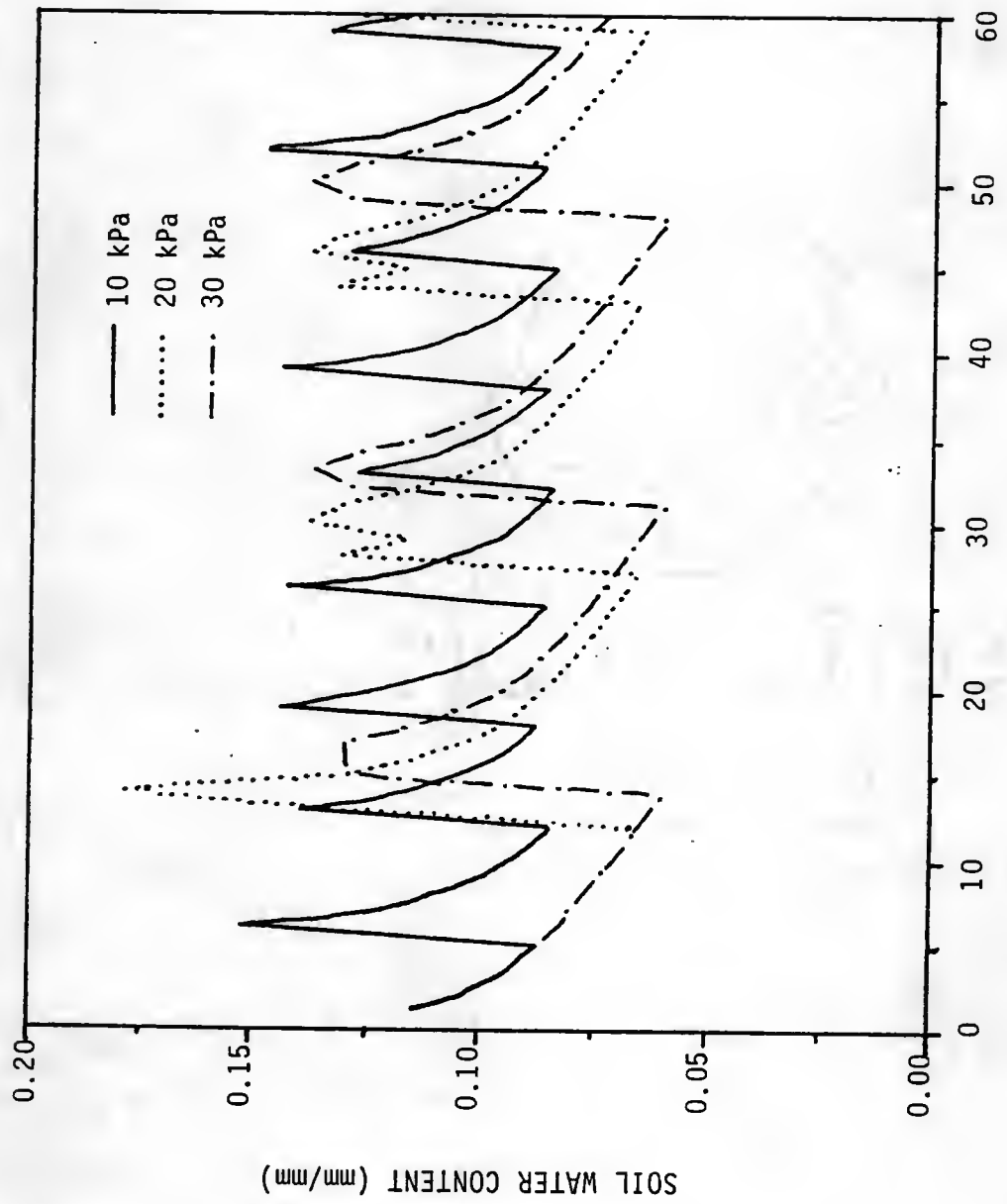

Figure 4-45. Soil water contents for the three irrigation treatments at the 300 mm depth.

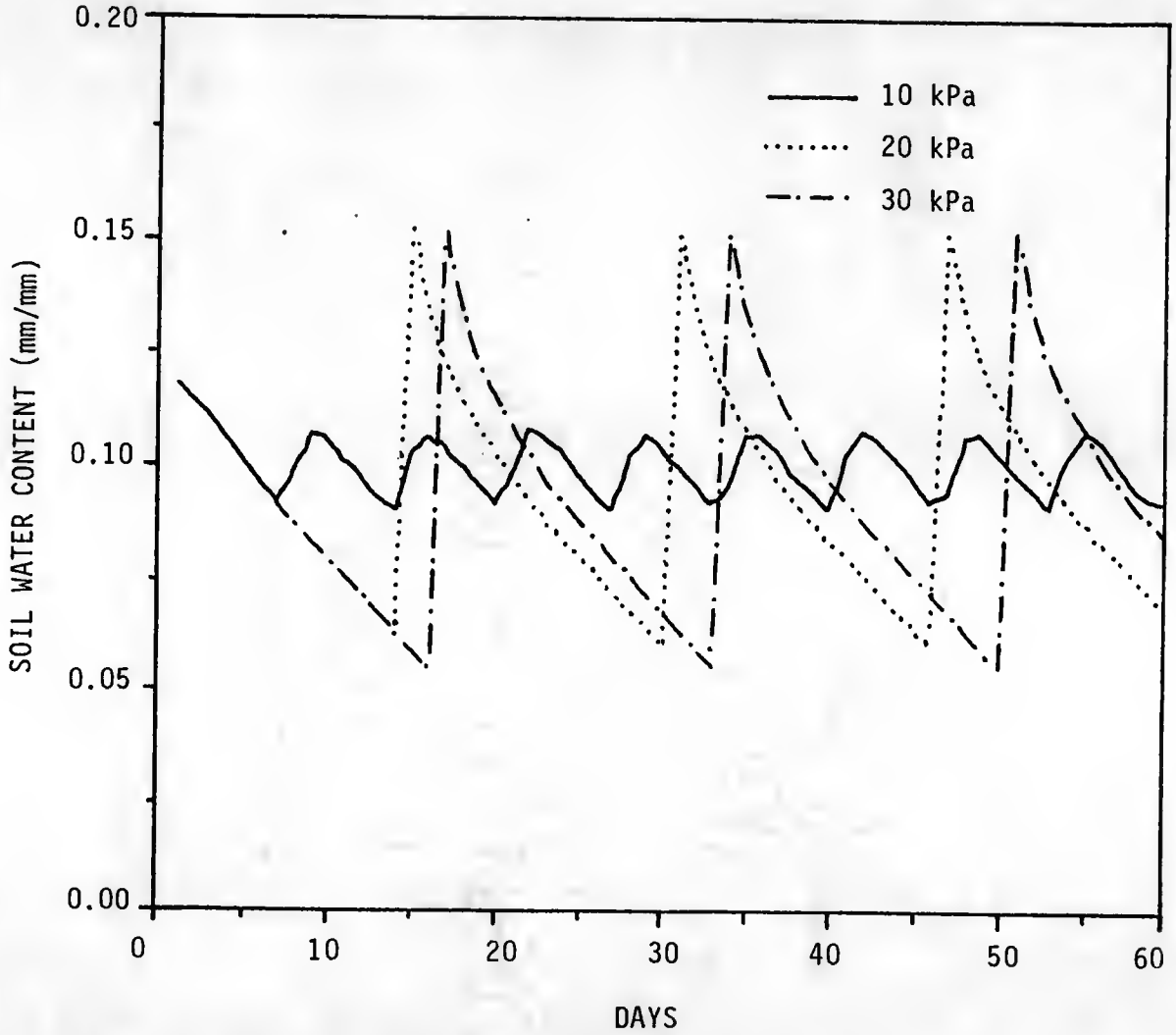

Figure 4-46. Soil water contents for the three irrigation treatments for the 900 mm depth.

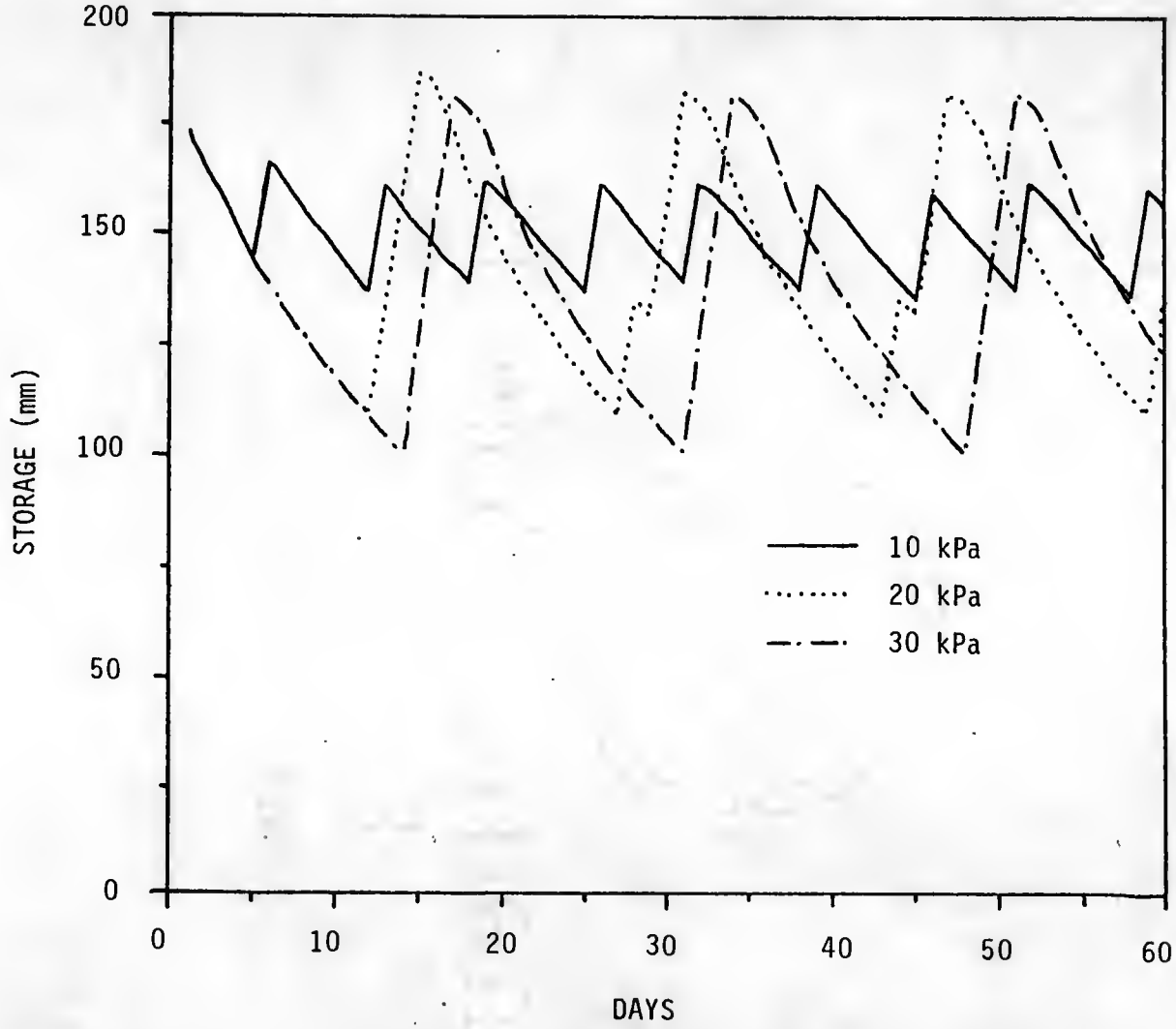

Figure 4-47. Soil water storage for the three irrigation treatments.

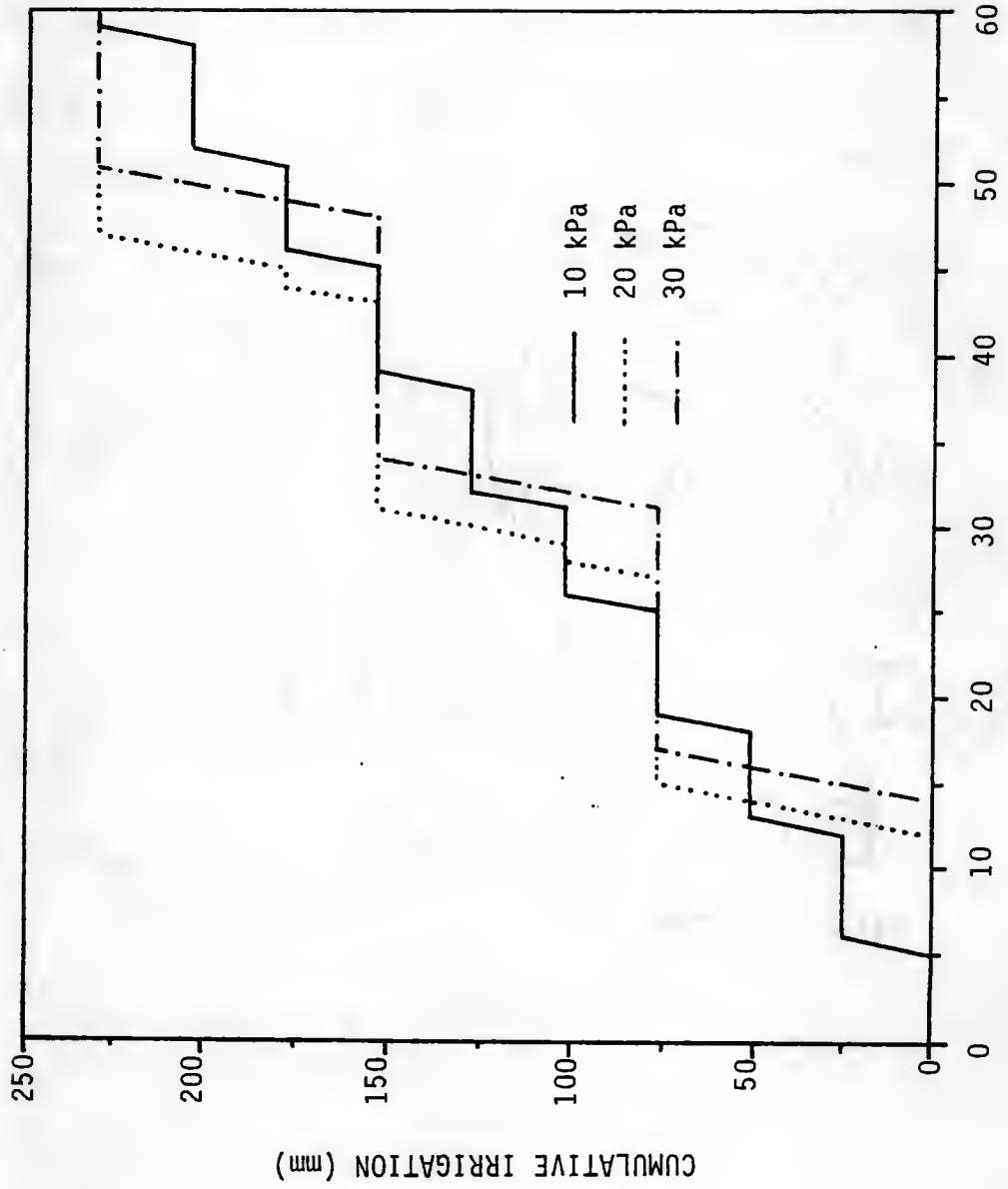

Figure 4-48. Cumulative irrigation for the three irrigation treatments.

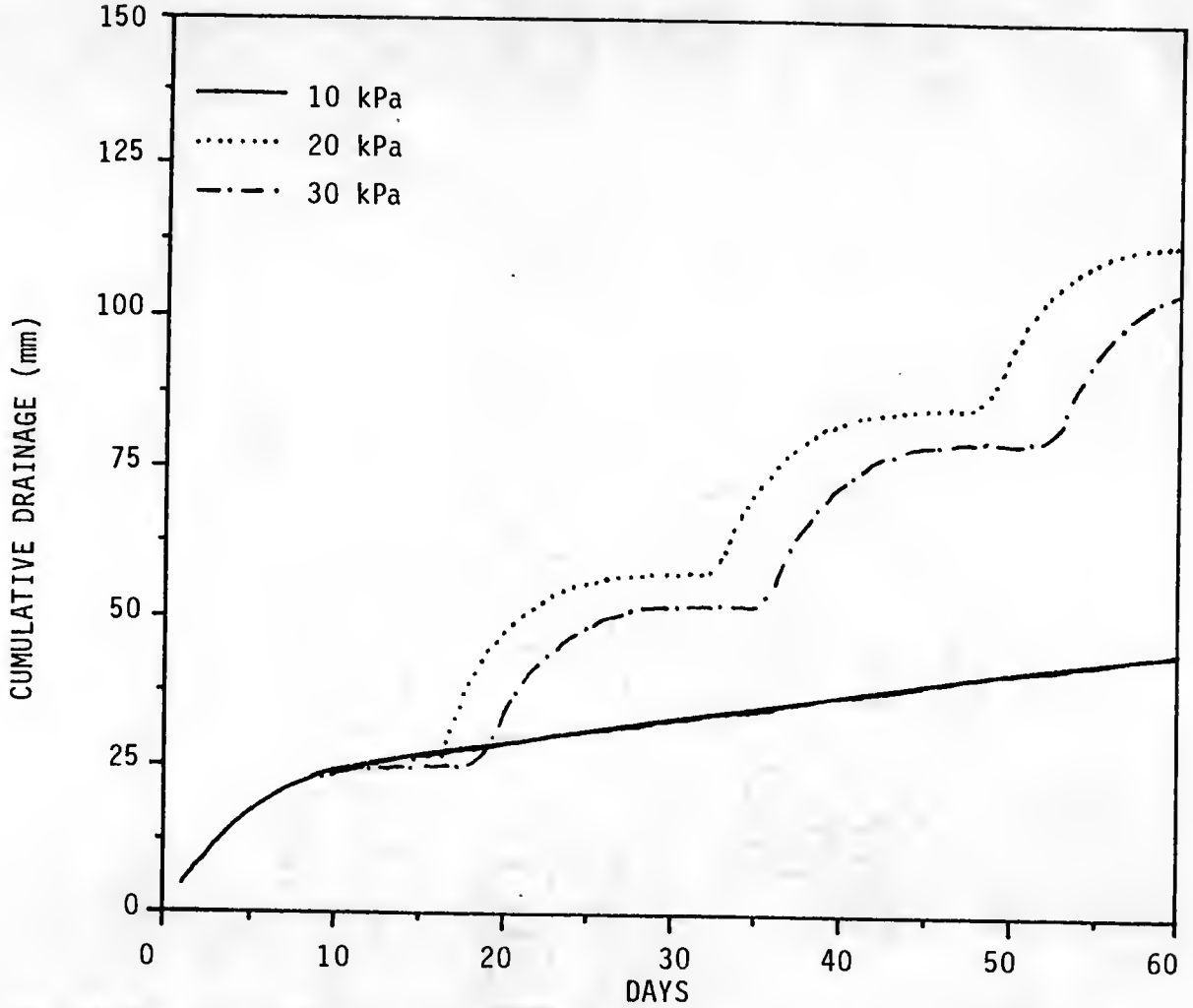

Figure 4-49. Cumulative drainage from the soil profile for the three irrigation treatments.

treatments. The drainage out of the all of the treatments was large at first because of the initial conditions. The drainage for the -10 kPa teatment was small for the duration of the simulation period. Drainage from the other treatments were higher because of the larger amounts of water applied at each irrigation.

CHAPTER V
SUMMARY AND CONCLUSIONS

A data collection system was developed which provides researchers with information needed for developing and validating models of soil water movement, crop water use and evapotranspiration. Two numerical models were developed to simulate soil water movement and extraction. These numerical models may be used to compare irrigation scheduling strategies.

Microcomputer-based Data Acquisition System

A low-cost microcomputer-based data acquisition system to continuously record soil water potentials was developed and tested. Excellent agreement was obtained between soil water potentials read with the data acquisition system and those read manually using mercury manometers. Typical agreement was within 0.47 kPa. The maximum deviation observed for all evaluations conducted was 1.76 kPa. The microcomputer based data acquisition system has the ability to monitor inputs and make decisions based upon the input data to control events in the field.

Field Data

The data acquisition system developed was used to measure soil water extraction patterns under young citrus trees and under a grass cover crop grown in field lysimeters. Observations were monitored during two drying cycles and one irrigation. The data collected were evaluated and parameters determined for input to the numerical simulation models. Evapotranspiration, soil water extraction rates and

relative soil water extractions were calculated from the soil water potential measurements.

Modeling Soil Water Movement and Extraction

A one-dimensional numerical model was developed to simulate soil water movement and extraction under a uniformly irrigated soil profile. The model was verified using data from the literature. It was then used to simulate the soil water movement and extraction from a young citrus tree in a field lysimeter. Two drying cycles and one irrigation were simulated. Simulated results were in excellent agreement with the data collected using the microcomputer based data acquisition system.

A two-dimensional numerical model was developed to simulate soil water movement and extraction under a nonuniformly irrigated soil profile. The model was compared to both one- and two-dimensional models of soil water movement from the literature. It was then used to simulate the two-dimensional movement and extraction of soil water in a field lysimeter with a young citrus tree. Two drying cycles and one irrigation were simulated. The model results were in good agreement with the data collected using the microcomputer based data acquisition system.

Model Applications

The numerical models may be used to study irrigation scheduling problems. A comparison of three different irrigation scheduling strategies was conducted to demonstrate one use of the models. These numerical models will also be useful in other applications such as the modeling of solute movement in soils, modeling of fertilizer movement under a trickle emitter, or as inputs to a larger crop modeling system.

APPENDIX A

Alternating Direction Implicit Finite Differencing

An alternating direction implicit solution method was developed to solve the two-dimensional radial flow model. The solution method divides the solution into two half cycles, thus two cycles are required to solve for one time step. Equation (8) was solved in the radial direction during the first half cycle and then solved in the vertical direction during the second half cycle. The ADI solution for equation (8) may be written as

$$C^{k+1/2}\frac{\partial h}{\partial t}^{k+1/2} = \frac{1}{r}\left(\frac{1}{2}\frac{\partial}{\partial r}\left(r K^{k+1/2}\frac{\partial h}{\partial r}\right)^{k+1/2} + \frac{1}{2}\frac{\partial}{\partial r}\left(r K^{k+1/2}\frac{\partial h}{\partial r}\right)^{k+1/2}\right)$$

$$+ \left(\frac{1}{2}\frac{\partial}{\partial z}\left(K^{k+1}\frac{\partial h}{\partial z}\right)^{k+1} + \frac{1}{2}\frac{\partial}{\partial z}\left(K^{k}\frac{\partial h}{\partial z}\right)^{k}\right)$$

$$+ \left(\frac{1}{2}\frac{\partial K}{\partial z}^{k+1/2} + \frac{1}{4}\left(\frac{\partial K}{\partial z}^{k+1} + \frac{\partial K}{\partial z}^{k}\right)\right) - S(z,r,t) \qquad (68)$$

The finite difference equations used for the solution of equation (8) were expressed as

$$C\frac{\partial h}{\partial t} = C_{i,j}\frac{(h_{i,j}^{k+1} - h_{i,j}^{k})}{\Delta t} \qquad (69)$$

$$\frac{\partial}{\partial z}\left(K \frac{\partial h}{\partial z}\right) = \frac{K_{i+1/2,j}(h_{i+1,j} - h_{i,j}) - K_{i-1/2,j}(h_{i,j} - h_{i-1,j})}{\Delta z^2} \quad (70)$$

$$\frac{1}{r}\left(\frac{\partial}{\partial r}\left(r K \frac{\partial h}{\partial r}\right)\right) = \frac{1}{r_{i,j}\,\Delta r^2}\left(r_{i,j+1/2} K_{i,j+1/2}(h_{i,j+1} - h_{i,j}) - r_{i,j-1/2} K_{i,j-1/2}(h_{i,j} - h_{i,j-1})\right) \quad (71)$$

$$\frac{\partial K}{\partial z} = \frac{K_{i-1/2,j} - K_{i+1/2,j}}{\Delta z} \quad (72)$$

Equation (68) was divided into two parts and arranged such that the unknowns are on the left side of the equations and the knowns are on the right side such that

$$-\left(\frac{1}{2}\,\frac{\Delta t}{\Delta r^2}\,\frac{r_{i,j-1/2}}{r_{i,j}}\,\frac{K^{k+1/2}_{i-1/2,j}}{C_{i,j}}\right) h^{k+1/2}_{i,j-1}$$

$$+\left(\frac{1}{2}\,\frac{\Delta t}{\Delta r^2}\,\frac{r_{i,j+1/2} K^{k+1/2}_{i,j+1/2} + r_{i,j-1/2} K^{k+1/2}_{i,j-1/2}}{r_{i,j} C_{i,j}} + 1\right) h^{k+1/2}_{i,j}$$

$$
- \left(-\frac{1}{2}\frac{\Delta t}{\Delta r}\frac{r_{i,j+1/2}}{r_{i,j}}\frac{K^{k+1/2}_{i,j+1/2}}{C_{i,j}} \right) h^{k+1/2}_{i,j+1}
$$

$$
= h^{k}_{i,j} + \frac{1}{2}\frac{\Delta t}{\Delta z}\left(\frac{K^{k}_{i-1/2,j} - K^{k}_{i+1/2,j}}{C_{i,j}} \right) + \frac{1}{4}\frac{\Delta t}{\Delta z}\left(\frac{K^{k+1/2}_{i-1/2,j} - K^{k+1/2}_{i+1/2,j}}{C_{i,j}} \right)
$$

$$
+ \left(-\frac{1}{2}\frac{\Delta t}{\Delta z}\frac{K^{k}_{i-1/2,j}}{C_{i,j}} \right) \left(h^{k}_{i-1,j} - h^{k}_{i,j} \right)
$$

$$
+ \left(-\frac{1}{2}\frac{\Delta t}{\Delta z}\frac{K^{k}_{i+1/2,j}}{C_{i,j}} \right) \left(h^{k}_{i+1,j} - h^{k}_{i,j} \right) - \frac{1}{2}\frac{\Delta t}{C_{i,j}} S^{k}_{i,j} \qquad (73)
$$

and

$$
- \left(-\frac{1}{2}\frac{\Delta t}{\Delta z}\frac{K^{k+1}_{i-1/2,j}}{C_{i,j}} \right) h^{k+1}_{i-1,j}
$$

$$
+ \left(-\frac{1}{2}\frac{\Delta t}{\Delta z}\frac{K^{k+1}_{i-1/2,j} + K^{k+1}_{i+1/2,j}}{C_{i,j}} + 1 \right) h^{k+1}_{i,j}
$$

$$- \left(-\frac{1}{2} \frac{\Delta t}{2 \Delta z} \frac{K^{k}_{i+1/2,j}}{C_{i,j}} \right) h^{k+1}_{i+1,j}$$

$$= h^{k}_{i,j} + \frac{1}{4} \frac{\Delta t}{\Delta z} \left(\frac{K^{k+1/2}_{i-1/2,j} - K^{k+1/2}_{i+1/2,j}}{C_{i,j}} \right) - \frac{1}{2} \frac{\Delta t}{C_{i,j}} S^{k}_{i,j}$$

$$+ \left(\frac{1}{2} \frac{\Delta t}{\Delta r^{2}} \frac{r_{i,j-1/2}}{r_{i,j}} \frac{K^{k+1/2}_{i,j-1/2}}{C_{i,j}} \right) \left(h^{k+1/2}_{i,j-1} - h^{k+1/2}_{i,j} \right)$$

$$+ \left(\frac{1}{2} \frac{\Delta t}{\Delta r^{2}} \frac{r_{i,j+1/2}}{r_{i,j}} \frac{K^{k+1/2}_{i,j+1/2}}{C_{i}} \right) \left(h^{k+1/2}_{i,j+1} - h^{k+1/2}_{i,j} \right) \qquad (74)$$

where i represents the vertical distance, j represents the radial distance and k represents the time increment.

The system of equations which are formed by applying equations (73) and (74) to each grid point produces a tridiagonal matrix at each half time step. The tridiagonal matrices were solved using a Gauss elimination method for tridiagonal matrices. Equations (73) and (74) may be simplified such that equation (73) may be written as

$$- AR\, h^{k+1/2}_{i,j-1} + BR\, h^{k+1/2}_{i,j} - CR\, h^{k+1/2}_{i,j+1} = DR_{i,j} \qquad (75)$$

where

$$AR = \left(\frac{1}{2}\,\frac{\Delta t}{\Delta r^2}\,\frac{r_{i,j-1/2}}{r_{i,j}}\,\frac{K^{k+1/2}_{i,j-1/2}}{C_{i,j}}\right) \tag{76}$$

$$CR = \left(\frac{1}{2}\,\frac{\Delta t}{\Delta r^2}\,\frac{r_{i,j+1/2}}{r_{i,j}}\,\frac{K^{k+1/2}_{i,j+1/2}}{C_{i,j}}\right) \tag{77}$$

$$BR = 1 + AR + CR \tag{78}$$

and

$$DR = h^{k}_{i,j} + \frac{1}{2}\frac{\Delta t}{\Delta z}\left(\frac{K^{k}_{i-1/2,j} - K^{k}_{i+1/2,j}}{C_{i,j}}\right) + \frac{1}{4}\frac{\Delta t}{\Delta z}\left(\frac{K^{k+1/2}_{i-1/2,j} - K^{k+1/2}_{i+1/2,j}}{C_{i,j}}\right)$$

$$+ \left(\frac{1}{2}\,\frac{\Delta t}{\Delta z^2}\,\frac{K^{k}_{i-1/2,j}}{C_{i,j}}\right)\left(h^{k}_{i-1,j} - h^{k}_{i,j}\right)$$

$$+ \left(\frac{1}{2}\,\frac{\Delta t}{\Delta z^2}\,\frac{K^{k}_{i+1/2,j}}{C_{i,j}}\right)\left(h^{k}_{i+1,j} - h^{k}_{i,j}\right) - \frac{1}{2}\frac{\Delta t}{C_{i,j}}\,S^{k}_{i,j} \tag{79}$$

and equation (74) may be written as

$$- AV\, h^{k+1}_{i-1,j} + BV\, h^{k+1}_{i,j} - CV\, h^{k+1}_{i+1,j} = DV_{i,j} \tag{80}$$

where

$$AV = \left(-\frac{1}{2}\,\frac{\Delta t}{2\,\Delta z^2}\,\frac{K^{k+1}_{i-1/2,j}}{C_{i,j}} \right) \tag{81}$$

$$CV = \left(-\frac{1}{2}\,\frac{\Delta t}{2\,\Delta z^2}\,\frac{K^{k}_{i+1/2,j}}{C_{i,j}} \right) \tag{82}$$

$$BV = 1 + AV + CV \tag{83}$$

and

$$DV = h^{k}_{i,j} + \frac{1}{4}\,\frac{\Delta t}{\Delta z}\left(\frac{K^{k+1/2}_{i-1/2,j} - K^{k+1/2}_{i+1/2,j}}{C_{i,j}} \right) - \frac{1}{2}\,\frac{\Delta t}{C_{i,j}}\, S^{k}_{i,j}$$

$$+ \left(\frac{1}{2}\,\frac{\Delta t}{2\,\Delta r^2}\,\frac{r_{i,j-1/2}}{r_{i,j}}\,\frac{K^{k+1/2}_{i,j-1/2}}{C_{i,j}} \right) \left(h^{k+1/2}_{i,j-1} - h^{k+1/2}_{i,j} \right)$$

$$+ \left(\frac{1}{2}\,\frac{\Delta t}{2\,\Delta r^2}\,\frac{r_{i,j+1/2}}{r_{i,j}}\,\frac{K^{k+1/2}_{i,j+1/2}}{C_{i,j}} \right) \left(h^{k+1/2}_{i,j+1} - h^{k+1/2}_{i,j} \right) \tag{84}$$

Boundary Conditions. The boundary condition for the surface layers was a flux boundary condition which accounted for irrigation and rainfall at the soil surface. At times when no irrigation occured the surface boundary was a no flux boundary. Evaporation from the soil surface was included in the water extraction term. The modification of equations (75) and (80) to describe the surface boundary condition was

$$- AR_{1,j-1}^{k+1/2} + BR_{1,j}^{k+1/2} - CR_{1,j+1}^{k+1/2} = DR_{1,j} \qquad (85)$$

where

$$DR = h_{1,j}^{k} + \frac{1}{2}\frac{\Delta t}{\Delta z}\left(\frac{Qs_j - K_{1+1/2,j}^{k}}{C_{1,j}}\right) + \frac{1}{4}\frac{\Delta t}{\Delta z}\left(\frac{Qs_j - K_{1+1/2,j}^{k+1/2}}{C_{1,j}}\right)$$

$$+ \left(\frac{1}{2}\frac{\Delta t}{\Delta z^2}\frac{K_{1+1/2,j}^{k}}{C_{1,j}}\right)\left(h_{1+1,j}^{k} - h_{1,j}^{k}\right) - \frac{1}{2}\frac{\Delta t}{C_{1,j}} S_{1,j}^{k} \qquad (86)$$

and

$$BV\, h_{1,j}^{k+1} - CV\, h_{2,j}^{k+1} = DV_{1,j} \qquad (87)$$

where

$$BV = 1 + CV \qquad (88)$$

and

$$DV = h^{k}_{1,j} + \frac{1}{2}\frac{\Delta t}{\Delta z}\left(\frac{Qs_j - K^{k+1/2}_{1+1/2,j}}{C_{1,j}}\right) - \frac{1}{2}\frac{\Delta t}{C_{1,j}} S^{k}_{1,j}$$

$$+ \left(\frac{1}{2}\frac{\Delta t}{\Delta r^2}\frac{r_{1,j-1/2}}{r_{1,j}}\frac{K^{k+1/2}_{1,j-1/2}}{C_{1,j}}\right)\left(h^{k+1/2}_{1,j-1} - h^{k+1/2}_{1,j}\right)$$

$$+ \left(\frac{1}{2}\frac{\Delta t}{\Delta r^2}\frac{r_{1,j+1/2}}{r_{1,j}}\frac{K^{k+1/2}_{1,j+1/2}}{C_{1,j}}\right)\left(h^{k+1/2}_{1,j+1} - h^{k+1/2}_{1,j}\right) \qquad (89)$$

The lower boundary condition was also represented as a flux boundary. The lower boundary in this research was an impermeable boundary which represented the bottom of the lysimeter. The modifications of equations (75) and (80) to describe the lower boundary condition were

$$-AR\, h^{k+1/2}_{n,j-1} + BR\, h^{k+1/2}_{n,j} - CR\, h^{k+1/2}_{n,j+1} = DR_{n,j} \qquad (90)$$

where AR, BR and DR are as previously described and

$$DR = h^{k}_{n,j} + \frac{1}{2}\frac{\Delta t}{\Delta z}\left(\frac{K^{k}_{n-1/2,j} - Qb_j}{C_{n,j}}\right) + \frac{1}{4}\frac{\Delta t}{\Delta z}\left(\frac{K^{k+1/2}_{n-1/2,j} - Qb_j}{C_{n,j}}\right)$$

$$+\left(\frac{1}{2}\frac{\Delta t}{\Delta z^2}\frac{K^{k}_{n-1/2,j}}{C^{k}_{n,j}}\right)\left(h^{k}_{n-1,j}-h^{k}_{n,j}\right)-\frac{1}{2}\frac{\Delta t}{C^{k}_{n,j}}S^{k}_{n,j} \tag{91}$$

and

$$-AV\,h^{k+1}_{n-1,j}+BV\,h^{k+1}_{n,j}=DV_{n,j} \tag{92}$$

where AV was previously described and

$$BV = 1 + AV \tag{93}$$

and

$$DV = h^{k}_{n,j}+\frac{1}{4}\frac{\Delta t}{\Delta z}\left(\frac{K^{k+1/2}_{n-1/2,j}}{C^{j}_{n,j}}-Qb_{j}\right)-\frac{1}{2}\frac{\Delta t}{C^{k}_{n,j}}S^{k}_{n,j}$$

$$+\left(\frac{1}{2}\frac{\Delta t}{\Delta r^2}\frac{r_{n,j-1/2}}{r_{n,j}}\frac{K^{k+1/2}_{n,j-1/2}}{C^{k+1/2}_{n,j}}\right)\left(h^{k+1/2}_{n,j-1}-h^{k+1/2}_{n,j}\right)$$

$$+\left(\frac{1}{2}\frac{\Delta t}{\Delta r^2}\frac{r_{n,j+1/2}}{r_{n,j}}\frac{K^{k+1/2}_{n,j+1/2}}{C^{k+1/2}_{n,j}}\right)\left(h^{k+1/2}_{n,j+1}-h^{k+1/2}_{n,j}\right) \tag{94}$$

The boundary conditions for the radial boundaries were both no flux boundaries. The no flux boundary condition for the outer radius (j=m)

represented the outer wall of the lysimeter and equations (75) and (80) were written as

$$- AR\ h^{k+1/2}_{i,m-1} + BR\ h^{k+1/2}_{i,m} = DR_{i,m} \tag{95}$$

where

$$BR = 1 + AR \tag{96}$$

and

$$- AV\ h^{k+1}_{i-1,m} + BV\ h^{k+1}_{i,m} - CV\ h^{k+1}_{i+1,m} = DV_{i,m} \tag{97}$$

where

$$DV = h^{k}_{i,m} + \frac{1}{4}\frac{\Delta t}{\Delta z}\left(\frac{K^{k+1/2}_{i-1/2,m} - K^{k+1/2}_{i+1/2,m}}{C_{i,m}}\right) - \frac{1}{2}\frac{\Delta t}{C_{i,m}} S^{k}_{i,m}$$

$$+ \left(\frac{1}{2}\frac{\Delta t}{\Delta r^{2}}\frac{r_{i,m-1/2}}{r_{i,m}}\frac{K^{k+1/2}_{i,m-1/2}}{C_{i,m}}\right)\left(h^{k+1/2}_{i,m-1} - h^{k+1/2}_{i,m}\right) \tag{98}$$

The boundary condition for the inner radius was also represented as a no flux boundary. For the inner radius r(i,j) = 0, therefore its inclusion into equation (8) would result in a division by zero. Therefore, the second term in equation (8) was rewritten as described in equations (50) and (51) such that the finite difference equations for the ADI solution of equation (51) were expressed as

$$BR\ h_{i,1}^{k+1/2} - CR\ h_{i,2}^{k+1/2} = DR_{i,1} \tag{99}$$

where

$$CR = \left(\frac{1}{2} \frac{\Delta t}{\Delta r^2} \frac{K_{i+1/2,1}^{k+1/2}}{C_{i,1}} \right) h_{i,2}^{k+1/2} \tag{100}$$

$$BR = 1 + CR \tag{101}$$

and

$$- AV\ h_{i-1,1}^{k+1} + BV\ h_{i,1}^{k+1} - CV\ h_{i+1,1}^{k+1} = DV_{i,1} \tag{102}$$

where

$$DV = h_{i,1}^{k} + \frac{1}{4} \frac{\Delta t}{\Delta z} \left(\frac{K_{i-1/2,1}^{k+1/2} - K_{i+1/2,1}^{k+1/2}}{C_{i,1}} \right) - \frac{1}{2} \frac{\Delta t}{C_{i,1}} S_{i,1}^{k}$$

$$+ \left(\frac{1}{2} \frac{\Delta t}{\Delta r^2} \frac{K_{i,1+1/2}^{k+1/2}}{C_{i,1}} \right) \left(h_{i,2}^{k+1/2} - h_{i,1}^{k+1/2} \right) \tag{103}$$

Updating of the soil parameters, surface infiltration, mass balance and time steps were implimented as described for the one-dimensional soil water flow model.

APPENDIX B

Listing of Soil Water Movement and Extraction Model

```
C-----------------------------------------------------------------
C
C   This program models the water movement and extraction in both a one-
C   and a two-dimensional soil profiles.  The model was designed to
C   study water movement and extraction and how they affect irrigation
C   scheduling.  The program used an input file to input the parameters
C   for the model.  The input file is interactively asked for during
C   program execution.
C
C   The soils used in this model are assumed to homogenous and isotropic
C   The surface boundry is a flux boundary which may be specified in the
C   input file.  The boundary is assumed to be a no flux unless an
C   irrigation is occuring.  The lower boundary may be either a no flux
C   boundary or a gravity flow.  The radial boundaries for the two-
C   dimensional model are both no flow boundaries.
C
C-----------------------------------------------------------------
C    CONT       = table of conductivities
C    COND       = the hydraulic conductivity
C    DTIRR      = the duration of the irrigation event
C    DZ         = the vertical grid increment
C    DEPTH      = the depth of the grids
C    DR         = the radial grid increment
C    DT         = the time step
C    DTMAX      = the maximum time step
C    DTMIN      = the minimum time step
C    ENDTIME    = the ending simulation time
C    HEAD       = the matric water potential
C    HEDT       = table of soil matric potentials
C    ILOW       = the status of the lower boundary condition
C    ICONST     = the status of the surface boundary condition
C    ISOIL      = the soil type
C    MBFILE     = the output masbalance file
C    NL         = the number of vertical grids
C    NR         = the number of radial increments
C    R          = the radius of the grids
C    QS         = the surface flux
C    S          = the soil water extraction
C    SWC        = the specific water capacity
C    SWCT       = table of specific water capacities
C    TIME       = the current simulation time
C    TOUT       = the times as which the outputs should occur
C    TOD        = the time of day
C    WC         = The water content
C    WCNT       = table of water contents
C-----------------------------------------------------------------
      PARAMETER (IZ=50,IR=16,IB=IR*2+1,MAX=IZ*IR)
      IMPLICIT REAL  (A-H,O-Z)
      INTEGER I, NUM, IOUT,ISTOP,ICOUNT
      CHARACTER*64 MBFILE
      COMMON /PARA/WC(IZ,IR,3),COND(IZ,IR,3),SWC(IZ,IR,3),HEAD(IZ,IR,3),
     $NL,DZ(IZ),DEPTH(IZ),QS(IR),S(IZ,IR),ICONST,NR,DR(IR),R(IR),ILOW
      COMMON/TIM/DT,TIME,TOUT(90),ENDTIME,DTMAX,DTMIN,TOD,ITIME,QM,DTIRR
      COMMON /TABLES/WCNT(120),CONT(120),SWCT(120),HEDT(120)
```

```
     $               ,NDATA,MBFILE,ISOIL
      COMMON /MASB2/DIFF,PSTOR,FLOWIN,EXTRACT,STORAGE,FLOWOUT
      COMMON /WCC/WKEEP,FLOW1(IZ,IR)
      COMMON /CONV/DIF,ITER,MAXITER
      COMMON /QS1/RDF(IZ,IR),WCWP,WCFC,ICF
      COMMON /ET1/TSNR(90),TSNS(90),ETP(90),RAIN(90),DUR,TSTOP
      COMMON /DUMY/IFIELD(25),JFIELD(25),IFS,RTIME,IOPT
     $             ,ITEN,ITF(25),JTF(25),THRES,RRATE,ISCH(90)
      CALL INPUT
      CALL MASBAL(0)
      WRITE(*,*)' THE INITIAL MASS BALANCE IS '
      WRITE(*,90)TIME,DT,DIFF,PSTOR,FLOWOUT
      WRITE(11,*)' THE INITIAL MASS BALANCE IS '
      WRITE(11,90)TIME,DT,DIFF,PSTOR,FLOWOUT
      WRITE(*,91)STORAGE,FLOWIN,EXTRACT
      WRITE(11,91)STORAGE,FLOWIN,EXTRACT
      TNEW = RTIME
      IF(IOPT.EQ.0)WRITE(15,924)TNEW,(WC(IFIELD(I),JFIELD(I),1),I=1,IFS)
C-----------------------------------------------------------------
C          START OF SIMULATION LOOP
C-----------------------------------------------------------------
      ITIME=1
      MITER = 0
      IDAY = TIME / 24.0  + 1.0
88    CONTINUE
      CALL FLUX(ETPFLX, ETP(IDAY),TSNR(IDAY),TSNS(IDAY),TOD)
      CALL QSS( ETPFLX)
      CALL IRRIGATE( IDAY, IRCODE )
C ONE-DIMENSIONAL MODEL
      IF(NR.EQ.1) THEN
          CALL TSTEP1D( IRCODE )
          CALL REDST1D
      END IF
C TWO-DIMENSIONAL MODEL
      IF(NR.GE.3) THEN
          CALL TSTEP2D( IRCODE )
          CALL REDST2D
      END IF
C
      TIME = TIME + DT
      IDAY = TIME / 24.0 +1.0
      TOD  = TOD  + DT
      IF(TOD.GE.24.0) TOD = TOD - 24.0
C
      IF(TIME.EQ.TOUT(ITIME).OR.TIME.EQ.ENDTIME) THEN
C-------- OUTPUT LOOP ----------------------------------------
      ITIME =ITIME+ 1
      WRITE(*,90)TIME,DT,DIFF,PSTOR,FLOWOUT
      WRITE(11,90)TIME,DT,DIFF,PSTOR,FLOWOUT
90    FORMAT(/,
     $' TIME',T25,'= ',F12.5,' (HRS)    DT',9X,'= ',F12.5
     $,' (HRS)',/,
     $' MASS BALANCE --> ERROR = ',E12.5,' (mm3)    %ERROR     = ',
     $    E12.5,/,' DRAINAGE = ',E12.5)
```

```
C
      WRITE(*,91)STORAGE,FLOWIN,EXTRACT
      WRITE(11,91)STORAGE,FLOWIN,EXTRACT
91    FORMAT(' STORAGE = ',E12.5,' CUM_INFIL = ',E12.5,
     $' CUM_EXTRACT = ',E12.5,/)
C
      WRITE(11,9000)TIME
9000  FORMAT(' TIME =',F12.5)
      DO 12 I=1,NL
      WRITE(*,11)  DEPTH(I),(WC(I,J,1),J=1,NR)
      IF(IOPT.EQ.1)WRITE(15,11)(WC(I,J,1),J=NR,1,-1),(WC(I,J,1),J=1,NR)
12    WRITE(11,11)  DEPTH(I),(WC(I,J,1),J=1,NR)
11    FORMAT(10E12.5)
95    FORMAT(E10.4,10X,E10.4,10X,E10.4)
C
            TNEW = RTIME + TIME / 24.0
      IF(IOPT.EQ.0)WRITE(15,924)TNEW,(WC(IFIELD(I),JFIELD(I),1),I=1,IFS)
      IF(IOPT.EQ.3)WRITE(15,924)TNEW,(WC(IFIELD(I),JFIELD(I),1),I=1,IFS)
     $             ,STORAGE,FLOWIN,EXTRACT,FLOWOUT
924   FORMAT(18X,F9.4,20E12.5)
      END IF
C-----------------------------------------------------------------------
C
      MITER = MITER + 1
      IF(MITER/5*5.EQ.MITER) THEN
       OPEN(12,FILE='TIME.OUT1',IOSTAT=IC)
       IF(IC.NE.0) GO TO  9008
        WRITE(12,9005)TIME,MITER
9005    FORMAT(' TIME =',F12.5,' ITER = ',I10)
       CLOSE(12)
9008  END IF
C
      IF(ENDTIME.LE.TIME) GO TO 99
      GO TO 88
99    CONTINUE
      OPEN(17,FILE='FINAL.POT')
      DO 66 I=1,NL
66    WRITE(17,11) ( HEAD(I,J,1),J=1,NR)
      CLOSE(17)
      CLOSE(11)
      END
C-----------------------------------------------------------------
C   SUBROUTINE TO READ IN THE INPUT VALUES FOR THE SIMULATION
C   AND INITIALIZE THE VARIABLES
C-----------------------------------------------------------------
      SUBROUTINE INPUT
      PARAMETER (IZ=50,IR=16,IB=IR*2+1,MAX=IZ*IR)
      IMPLICIT REAL  (A-H,O-Z)
      CHARACTER*64 INPFILE,MBFILE,OUTFILE,WDFILE,DATAFILE
      CHARACTER*1 Z
      REAL  IWCONT,ISTOR,  HE(6,5),EX(6,5)
      INTEGER  II(6),JJ(5)
      COMMON /TABLES/WCNT(120),CONT(120),SWCT(120),HEDT(120)
     $              ,NDATA,MBFILE,ISOIL
```

```
      COMMON /PARA/WC(IZ,IR,3),COND(IZ,IR,3),SWC(IZ,IR,3),HEAD(IZ,IR,3),
     $NL,DZ(IZ),DEPTH(IZ),QS(IR),S(IZ,IR),ICONST,NR,DR(IR),R(IR),ILOW
      COMMON/TIM/DT,TIME,TOUT(90),ENDTIME,DTMAX,DTMIN,TOD,ITIME,QM,DTIRR
      COMMON /MASB/ IWCONT(IZ,IR),AREA(IR),TAREA,ISTOR
      COMMON /DUMY/IFIELD(25),JFIELD(25),IFS,RTIME,IOPT
     $            ,ITEN,ITF(25),JTF(25),THRES,RRATE,ISCH(90)
      COMMON /CONV/DIF,ITER,MAXITER
      COMMON /QS1/RDF(IZ,IR),WCWP,WCFC,ICF
      COMMON /ET1/TSNR(90),TSNS(90),ETP(90),RAIN(90),DUR,TSTOP
      COMMON /WCC/WKEEP,FLOW1(IZ,IR)
      PIE = 3.1415926
      WRITE(*,*)' ENTER THE INPUT DATA FILE'
      READ(*,1000) DATAFILE
      OPEN(8,FILE=DATAFILE)
      READ(8,901)Z
      READ(8,1005)ISOIL,INPFILE
1000  FORMAT(A64)
1005  FORMAT(I1,1X,A64)
      OPEN(9,FILE=INPFILE)
C-----------------------------------------------------------------
C     READ IN AND WRITE THE SOILS DATA
C-----------------------------------------------------------------
      READ(9,11) NDATA
11    FORMAT(I5)
      READ(9,09)(HEDT(I),WCNT(I),SWCT(I),CONT(I),I=1,NDATA)
09    FORMAT(4E12.5)
900   FORMAT(' ')
      CLOSE(9)
C
      READ(8,901) Z
      READ(8,1000)MBFILE
      READ(8,1000)WDFILE
      OPEN(11,FILE=MBFILE)
      READ(8,901) Z
         READ(8,'(I1,1X,A64)')IOPT,OUTFILE
          OPEN(15,FILE=OUTFILE)
         READ(8,*) IFS
         READ(8,*) RTIME,(IFIELD(I),JFIELD(I),I=1,IFS)
      READ(8,901) Z
      READ(8,*)TIME,ENDTIME,TOD
      READ(8,901)Z
      READ(8,*)WKEEP,WCWP,WCFC
      READ(8,901) Z
      READ(8,*)TOUT(1),TOUT(2),TOUT(3),TOUT(4)
      IF(TOUT(2).NE.-99.0) GO TO 9000
      DO 7000 I = 1,90
      IF(TOUT(1)*FLOAT(I).GT.ENDTIME) GO TO 7000
      TOUT(I) = TOUT(1)*FLOAT(I)
7000  CONTINUE
9000  CONTINUE
      READ(8,901) Z
      READ(8,*)DTMAX,DTMIN,MAXITER,DTIRR,DUR
      WRITE(*,710)MBFILE,TIME,TOUT(1),ENDTIME,DTMAX,DTMIN,MAXITER
      WRITE(11,710)MBFILE,TIME,TOUT(1),ENDTIME,DTMAX,DTMIN,MAXITER
```

```
710   FORMAT(/,' THE MASS BALANCE DATA IS IN FILE ',A40,/,
     $' THE STARTING SIMULATION TIME IS ',E12.5,/,
     $' THE OUTPUTS WILL BE AT INTERVALS ',E12.5,/,
     $' THE ENDING TIME WILL BE          ',E12.5,/,
     $' THE MAXIMUM TIME STEP IS         ',E12.5,/,
     $' THE MINIMUM TIME STEP IS         ',E12.5,/,
     $' THE NUMBER OF ITERATIONS         ',I12,/)
C-----------------------------------------------------------------
C    READ IN THE NUMBER OF GRIDS AND THE GRID SIZES
C-----------------------------------------------------------------
      READ(8,901) Z
      READ(8,*) NL ,DZ(1), NR, DR(1)
      WRITE(*,720)NL,DZ(1),NR,DR(1)
720   FORMAT(' THE NUMBER OF VERTICAL INCREMENTS ',I10,/,
     $       ' THE VERICAL SPACING IS            ',E12.5,/,
     $       ' THE NUMBER OF RADIAL INCREMENTS   ',I10,/,
     $       ' THE RADIAL SPACING  IS            ',E12.5,/)
C
      DEPTH(1) = - DZ(1) / 2
      DO 200 I = 2,NL
         DZ(I) = DZ(I-1)
         DEPTH(I) = DEPTH(I-1) - ( DZ(I) + DZ(I-1) ) / 2
200   CONTINUE
C
      IF(NR.EQ.2)  NR = 1
         AREA(1) = 1.0
         TAREA   = 1.0
      IF(NR.GE.3)  THEN
         R(1) = DR(1) / 2
         AREA(1) = PIE * (R(1)+DR(1)/2)**2
         DO 210 I = 2, NR
            DR(I) = DR(I-1)
            R(I)  = R(I-1) + ( DR(I) + DR(I-1) ) / 2
            AREA(I)= PIE*( (R(I)+DR(I)/2)**2 -(R(I)-DR(I)/2)**2)
210      CONTINUE
         TAREA = PIE * ( DR(1) * NR    )**2
         WRITE(*,735)
735      FORMAT(/,' THE RADIUS AND AREAS  ',/)
         WRITE(*,740)(I,R(I),AREA(I),I=1,NR)
740      FORMAT(' RADIUS(',I3,') = ',E12.5,10X,' AREA = ',E12.5)
      END IF
C
C  INPUT THE INITIAL POTENTIALS FOR THE SYSTEM
C
      READ(8,901)Z
C     READ(8,910)    (( HEAD(I,J,1),J=1,IR),I=1,IZ)
C
      READ(8,*) NLN,NRN,INV
      READ(8,*) ( II(I),I=1,NLN )
      READ(8,*) ( JJ(J),J=1,NRN )
      DO 1010 I=1,NLN
1010  READ(8,*) ( HE(I,J),J=1,NRN)
      READ(8,901)Z
C
```

```
C READ IN THE INFILTRATION RATE
C
C     READ(8,910)   (QS(J),J=1,IR)
      READ(8,901) Z
      READ(8,901)Z
      READ(8,*)      ICONST
      READ(8,901)Z
C
C  READ IN THE CONDITION OF THE LOWER BOUNDRY CONDITION
C  AND THE STATUS OF THE CORRECTION FACTOR
C
      READ(8,*)ILOW, ICF
      READ(8,901) Z
C READ IN THE ROOT DISTRIBUTION FUNCTION
C
C     READ(8,910)  ((RDF(I,J),J=1,IR),I=1,IZ)
      DO 1011 I=1,NLN
1011  READ(8,*)     ( EX(I,J),J=1,NRN)
C
      DO 811 K=1,3
      DO 811 I=1,IZ
      DO 811 J=1,IR
      HEAD(I,J,K)=0.0
      RDF(I,J) = 0.0
      S(I,J)   = 0.0
811   CONTINUE
C
      N = 0
      DO 400 I=1,NLN
      DO 400 L=1,II(I)
           N = N + 1
           M = 0
           DO 400 J=1,NRN
           DO 400 K=1,JJ(J)
                M = M + 1
                HEAD(N,M,1) = HE(I,J)
                HEAD(N,M,2) = HE(I,J)
                HEAD(N,M,3) = HE(I,J)
                K1 = M
                IF(INV.EQ.1) K1 = NR + 1 - M
                AAA = FLOAT(K1**2 - (K1-1)**2) / FLOAT( NR**2)
                IF(NR.EQ.1) AAA = 1.0
                RDF(N,M)  = EX(I,J) /  II(I) * AAA
400   CONTINUE
C
910   FORMAT(5F10.0)
901   FORMAT(A1)
775   FORMAT(10E12.5)
C
      CALL UPDATE (1)
      ISTOR = 0.0
        DO 310 I=1,NL
        DO 310 J=1,NR
          IWCONT(I,J)=WC(I,J,1)
```

```
          ISTOR = ISTOR + WC(I,J,1)*DZ(I)*AREA(J)
310     CONTINUE
C
110   FORMAT(I7,3X,4(E12.5,3X) )
      READ(8,*) ITEN, THRES, RRATE, ISC
      READ(8,*) ( ITF(I),JTF(I),I=1,ITEN )
      DO 1015 I=1,IDAY
1015  ISCH(I) = ISC
      CLOSE(8)
C-----------------------------------------------------------------
C        READ IN WEATHER DATA
C-----------------------------------------------------------------
      OPEN(10,FILE=WDFILE)
      IDAY = ENDTIME / 24.0 + 1.0
      READ(10,1001,END=1002)( ETP(I),TSNR(I),TSNS(I),RAIN(I),I=1,IDAY)
1002  WRITE(11,1003)
      WRITE(11,1001)( ETP(I),TSNR(I),TSNS(I),RAIN(I),I=1,IDAY)
1001  FORMAT(4F10.2)
      CLOSE(10)
1003  FORMAT(/,' THE WEATHER DATA  ',/)
C
      RETURN
      END
C-----------------------------------------------------------------
      SUBROUTINE FLUX (ETPFLX, ETP, TSNR,TSNS,TOD)
C-----------------------------------------------------------------
C   PROGRAM TO CALCULATE THE DISTRIBUTION OF POTENTIAL
C   ET DURING THE DAY.  THE DISTRIBUTION IS ASSUMED TO
C   BE A SINE FUNCTION.
C-----------------------------------------------------------------
C     DEFINITIONS
C     TSNR = TIME OF SUNRISE
C     TSNS = TIME OF SUNSET
C     ETP = POTENTIAL ET MM
C     ETPRMX = MAXIMUM ET RATE MM/HR
C     DAYL = DAY LENGTH HOURS
C     ETPFLX = CURRENT ET FLUX MM/HR
C-----------------------------------------------------------------
      IMPLICIT REAL  (A-H,O-Z)
      PI = 3.141592654
      DAYL = TSNS - TSNR
      ETPRMX = 2 * ETP / DAYL
      OMEGA = 2 * PI / DAYL
      TD = TOD - TSNR
      TI = TOD
      IF(TI.LT.TSNR.OR.TI.GT.TSNS) TD = 0.0
      ETPFLX = (ETPRMX/2)*SIN((OMEGA*TD) - PI/2.) + ETPRMX/2
      END
C-----------------------------------------------------------------
C   SUBROUTINE TO CALCULATE THE WATER UPTAKE RATE FOR THE
C   ONEDIMENSIONAL SOIL PROFILE
C-----------------------------------------------------------------
      SUBROUTINE QSS(TRANS)
      PARAMETER (IZ=50,IR=16,IB=IR*2+1,MAX=IZ*IR)
```

```
      IMPLICIT REAL  (A-H,O-Z)
      REAL  TRANS,RASW(IZ,IR),A(IZ,IR),K1,ISTOR,IWCONT
      COMMON /PARA/WC(IZ,IR,3),COND(IZ,IR,3),SWC(IZ,IR,3),HEAD(IZ,IR,3),
     $NL,DZ(IZ),DEPTH(IZ),QS(IR),S(IZ,IR),ICONST,NR,DR(IR),R(IR),ILOW
      COMMON /MASB/IWCONT(IZ,IR),AREA(IR),TAREA,ISTOR
      COMMON /QS1/RDF(IZ,IR),WCWP,WCFC,ICF
C
      IF(TRANS.EQ.0.0) THEN
         DO 30 I= 1,NL
         DO 30 J= 1,NR
30          S(I,J) = 0.0
         RETURN
      END IF
        K1 = 10.0
        SUM = 0.0
      DO 10 I=1,NL
      DO 10 J=1,NR
         RASW(I,J) = ( WC(I,J,1) - WCWP ) / ( WCFC - WCWP )
         IF(RASW(I,J).GT.1.0) RASW(I,J) = 1.0
            IF(RASW(I,J).LE.0.0) THEN
               RASW(I,J) = 0.0
               A(I,J) = 0.0
               GO TO 100
            END IF
      A(I,J) = TRANS * TAREA * RASW(I,J) ** ( TRANS /(RASW(I,J)*K1))
100   S(I,J) = A(I,J) * RDF(I,J)
      SUM = SUM + S(I,J)
10    CONTINUE
C
      IF( SUM.EQ.0.0.OR.ICF.EQ.1) THEN
           CF = 1.0
      ELSE
           CF = TRANS * TAREA / SUM
      END IF
         SUM2 = 0.0
      DO 20 I=1,NL
      DO 20 J=1,NR
         S(I,J) = S(I,J) / DZ(I) / AREA(J) * CF
         SUM2 = SUM2 + S(I,J)*DZ(I)*AREA(J)
20    CONTINUE
      RETURN
      END
C-----------------------------------------------------------------
      SUBROUTINE TRID(NG,IF,A,B,C,D,V)
C-----------------------------------------------------------------
C      THIS SUBROUTINE SOLVES THE TRIDIAGONAL COEFFICIENT MATRIX
C      WHICH RESULTS FROM A SET OF SIMULTANEOUS EQUATIONS WHICH
C      CAN BE PUT INTO THE FOLLOWING FORM
C             - A*V1 + B*V2 - C*V3 = D
C-----------------------------------------------------------------
      PARAMETER (IZ=50)
      IMPLICIT REAL   (A-H,O-Z)
      DIMENSION A(IZ),B(IZ),C(IZ),D(IZ),V(IZ),BETA(IZ),GAMMA(IZ)
      IFP1 = IF+1
```

```
C     NGM1 = NG-1
C-----------------------------------------------------------------------
C      COMPUTE INTERMEDIATE ARRAYS BETA AND GAMMA
C-----------------------------------------------------------------------
      BETA(IF) = B(IF)
      GAMMA(IF) = D(IF)/BETA(IF)
           DO 100 I = IFP1,NG
           BETA(I) = B(I)-A(I)*C(I-1)/BETA(I-1)
           GAMMA(I) = (D(I)+A(I)*GAMMA(I-1))/BETA(I)
  100      CONTINUE
C-----------------------------------------------------------------------
C      COMPUTE FINAL SOLUTION VECTOR V
C-----------------------------------------------------------------------
      V(NG) = GAMMA(NG)
      LAST = NG-IF
           DO 200 K = 1,LAST
           I = NG-K
           V(I) = GAMMA(I)+C(I)*V(I+1)/BETA(I)
  200      CONTINUE
      RETURN
      END
C-----------------------------------------------------------------------
C   SUBROUTINE TO CALCULATE A MASS BALANCE OF THE SYSTEM SIMULATED
C-----------------------------------------------------------------------
      SUBROUTINE MASBAL(IRESET)
      PARAMETER (IZ=50,IR=16,IB=IR*2+1,MAX=IZ*IR)
      IMPLICIT REAL  (A-H,O-Z)
      REAL  IWCONT,ISTORAGE
      COMMON /PARA/WC(IZ,IR,3),COND(IZ,IR,3),SWC(IZ,IR,3),HEAD(IZ,IR,3),
     $NL,DZ(IZ),DEPTH(IZ),QS(IR),S(IZ,IR),ICONST,NR,DR(IR),R(IR),ILOW
      COMMON/TIM/DT,TIME,TOUT(90),ENDTIME,DTMAX,DTMIN,TOD,ITIME,QM,DTIRR
      COMMON /MASB/ IWCONT(IZ,IR),AREA(IR),TAREA,ISTORAGE
      COMMON /MASB2/DIFF,PSTORAGE,FLOWIN,EXTRACT,STORAGE,FLOWOUT
C
C  INITIALIZE THE CUMULATIVE INFILTRATION AND EXTRACTION
C
      IF(IRESET.EQ.0) THEN
                      FLOWIN = 0.0
                      FLOWOUT = 0.0
                      EXTRACT = 0.0
                      DIFF=0.0
                      STORAGE=0.0
                      DO 20 J=1,NR
                      DO 20 I=1,NL
20                     STORAGE = STORAGE + WC(I,J,1)*DZ(I)*AREA(J)
                      DIFF = STORAGE - ISTORAGE
                      PSTORAGE = DIFF / ISTORAGE * 100.0
                      RETURN
      END IF
      DIFF=0.0
      STORAGE=0.0
C
      DO 10 J=1,NR
      FLOWIN = FLOWIN + DT*QS(J)*AREA(J)
```

```
      IF(ILOW.EQ.1) FLOWOUT = FLOWOUT + DT*(COND(NL,J,1) )
      DO 10 I=1,NL
      STORAGE = STORAGE + WC(I,J,1)*DZ(I)*AREA(J)
      EXTRACT = EXTRACT + S(I,J)*DZ(I)*AREA(J)*DT
10    CONTINUE
      DIFF = STORAGE - (ISTORAGE + FLOWIN - EXTRACT -FLOWOUT )
      PSTORAGE = DIFF / (ISTORAGE + FLOWIN - EXTRACT - FLOWOUT) * 100.0
      RETURN
      END
C-----------------------------------------------------------------
      SUBROUTINE IRRIGATE( IDAY, IRCODE )
C-----------------------------------------------------------------
C  SUBROUTINE TO CALCULATE THE AMOUNT OF IRRIGATION REQUIRED
C  FOR THE MODEL BASED ON THE MAXIMUM SOIL WATER POTENTIAL ALLOWED
C-----------------------------------------------------------------
      PARAMETER (IZ=50,IR=16,IB=IR*2+1,MAX=IZ*IR)
      IMPLICIT REAL  (A-H,O-Z)
      COMMON /PARA/WC(IZ,IR,3),COND(IZ,IR,3),SWC(IZ,IR,3),HEAD(IZ,IR,3),
     $NL,DZ(IZ),DEPTH(IZ),QS(IR),S(IZ,IR),ICONST,NR,DR(IR),R(IR),ILOW
      COMMON/TIM/DT,TIME,TOUT(90),ENDTIME,DTMAX,DTMIN,TOD,ITIME,QM,DTIRR
      COMMON /ET1/TSNR(90),TSNS(90),ETP(90),RAIN(90),DUR,TSTOP
      COMMON /QS1/RDF(IZ,IR),WCWP,WCFC,ICF
      COMMON /DUMY/IFIELD(25),JFIELD(25),IFS,RTIME,IOPT
     $            ,ITEN,ITF(25),JTF(25),THRES,RRATE,ISCH(90)
      COMMON /MASB/ IWCONT(IZ,IR),AREA(IR),TAREA,ISTORAGE
C
      AMOUNT = 0.0
      DEFICIT = 0.0
      IF(ISCH(IDAY).EQ.0) THEN
        DO 10 J=1,NR
        DO 10 I=1,NL
          DEFICIT = DEFICIT + ( WCFC - WC(I,J,1) ) * DZ(I) * AREA(J)
10      CONTINUE
        AMOUNT = DEFICIT / TAREA
        DO 20 I= 1,ITEN
           IF (ABS(HEAD(ITF(I),JTF(I),1)).GE.ABS(THRES)) THEN
               RAIN(IDAY)=AMOUNT
               ISCH(IDAY)= 1
           END IF
20      CONTINUE
      END IF
C
      IF( RAIN(IDAY).LE.0.0) THEN
            DO 100 I=1,NR
               QS(I) = 0.0
100         CONTINUE
            IRCODE = 0
            RETURN
      END IF
C
      IF( IRCODE.EQ.0) THEN
            TSTART = TIME
C             DUR    = RAIN(IDAY) / RRATE
              RAIN(IDAY) = RRATE
```

```
            TSTOP  = TSTART + DUR
C
            IRCODE = 1
            DO 200 I=1,NR
               QS(I) = RAIN( IDAY )
200         CONTINUE
      END IF
C
      IF( TIME.GE. TSTOP )  THEN
            IRCODE = 0
            DO 300 I=1,NR
               QS(I)  = 0.0
300         CONTINUE
            RAIN(IDAY) = 0.0
      END IF
      RETURN
      END
C-----------------------------------------------------------------
C  SUBROUTINE TO CALCULATE THE TIME STEP BASED ON THE
C  MAXIMUM ALLOWABLE CHANGE IN WATER CONTENT
C  FOR THE ONE-DIMENSIONAL MODEL
C-----------------------------------------------------------------
      SUBROUTINE TSTEP1D( IRCODE )
      PARAMETER (IZ=50,IR=16,IB=IR*2+1,MAX=IR*IZ)
      REAL K1,K2
      COMMON/PARA/WC(IZ,IR,3),COND(IZ,IR,3),SWC(IZ,IR,3),HEAD(IZ,IR,3),
     $NL,DZ(IZ),DEPTH(IZ),QS(IR),S(IZ,IR),ICONST,NR,DR(IR),R(IR),ILOW
      COMMON/TIM/DT,TIME,TOUT(90),ENDTIME,DTMAX,DTMIN,TOD,ITIME,QM,DTIRR
      COMMON /WCC/WKEEP,FLOW1(IZ,IR)
      COMMON /ET1/TSNR(90),TSNS(90),ETP(90),RAIN(90),DUR,TSTOP
C-----------------------------------------------------------------
C  CALCULATE THE MAXIMUM FLUX FROM THE INFILTRATION AND EXTRACTION
C-----------------------------------------------------------------
      RATE = ABS(QS(1))
      EXT  = ABS(S(1,1)*DZ(1))
      DO 10 I=1,NL
      IF(EXT.LT.ABS(S(I,1)*DZ(I))) EXT  = ABS( S(I,1)*DZ(I) )
10    CONTINUE
C
      IF(RATE.LT.EXT) RATE = EXT
      QM = RATE
C
      DO 100 I=1,NL
      FLOW1(I,1)=0.0
C
      IF(I.EQ.1)  THEN
       FLOW1(I,1)  =   QS(1)
     $  + ( COND(I,1,1) + COND(I+1,1,1) ) / 2
     $       *((HEAD(I+1,1,1)-HEAD(I,1,1))/DZ(I)-1.0)
       GO TO 900
      END IF
C
      IF(I.EQ.NL) THEN
      FLOW1(I,1) =
```

```
     $ -1.0*( COND(I,1,1) + COND(I-1,1,1) ) / 2
     $       *((HEAD(I,1,1)-HEAD(I-1,1,1))/DZ(I)-1.0)
        IF(ILOW.EQ.1) FLOW1(I,1) = FLOW1(I,1) - COND(I,1,1)
      GO TO 900
      END IF
C
      FLOW1(I,1) =
     $ -1.0*( COND(I,1,1) + COND(I-1,1,1) ) / 2
     $       *((HEAD(I,1,1)-HEAD(I-1,1,1))/DZ(I)-1.0)
     $  + ( COND(I,1,1) + COND(I+1,1,1) ) / 2
     $       *((HEAD(I+1,1,1)-HEAD(I,1,1))/DZ(I)-1.0)
C
900   IF(ABS(FLOW1(I,1)).GT.QM) GO TO 200
      GO TO 100
200   QM = ABS(FLOW1(I,1))
100   CONTINUE
C
      IF(QM.LE.0.0) GO TO 400
      DT = WKEEP * DZ(1)  / QM
      GO TO 500
400   DT = DTMAX
500   IF(DT.GT.DTMAX) DT = DTMAX
      IF(DT.LT.DTMIN) DT = DTMIN
      IF(IRCODE.EQ.1) DT = AMIN1( DTIRR, DT )
      IF(DT+TIME.GT.TOUT(ITIME).AND.TOUT(ITIME).GT.0.0)
     $ DT = TOUT(ITIME) - TIME
      IF(DT+TIME.GT.ENDTIME)       DT = ENDTIME - TIME
      IF(DT+TIME.GT.TSTOP.AND.IRCODE.EQ.1) DT = TSTOP - TIME
      IF(DT.LT.0.0) DT = DTMIN
C     WRITE(*,191) DT,QM
191   FORMAT(/,'*****   DT  = ',F10.8,'   QM = ',E12.5)
      RETURN
      END
C-----------------------------------------------------------------
C          SUBROUTINE TO CALCULATE THE NEW WATER POTENTIALS
C                FOR THE ONE-DIMENSIONAL MODEL
C-----------------------------------------------------------------
      SUBROUTINE REDST1D
      PARAMETER (IZ=50,IR=16,IB=IR*2+1,MAX=IR*IZ)
      IMPLICIT REAL   (A-H,O-Z)
      REAL   K1,K2,D(IZ),A(IZ),B(IZ),C(IZ),V(IZ)
      REAL   CONTAB(120),WCCTAB(120),SPCTAB(120),PRTAB(120)
      CHARACTER*64 MBFILE
      COMMON /TABLES/WCCTAB,CONTAB,SPCTAB,PRTAB,NDATA,MBFILE,ISOIL
      COMMON/PARA/WC(IZ,IR,3),COND(IZ,IR,3),SWC(IZ,IR,3),HEAD(IZ,IR,3),
     $NL,DZ(IZ),DEPTH(IZ),QS(IR),S(IZ,IR),ICONST,NR,DR(IR),R(IR),ILOW
      COMMON/TIM/DT,TIME,TOUT(90),ENDTIME,DTMAX,DTMIN,TOD,ITIME,QM,DTIRR
      COMMON /CONV/DIF,ITER,MAXITER
C-----------------------------------------------------------------
C  SET UP THE INTERIOR GRID POINTS
C-----------------------------------------------------------------
      DO 10 KL=2,NL-1
      K1=( COND(KL,1,1) + COND(KL-1,1,1) ) / 2
      K2=( COND(KL+1,1,1) + COND(KL,1,1) ) / 2
```

```
      C1 = SWC(KL,1,1)
      CONST1 = DT / DZ(KL)**2/C1
C
      A(KL) =  CONST1  * K1
      C(KL) =  CONST1  * K2
      B(KL) =  1.0 + A(KL) + C(KL)
      D(KL) =   HEAD(KL,1,1) + DT/DZ(KL)/C1*( K1 - K2 )
     $      - DT * S(KL,1)/C1
10    CONTINUE
C-----------------------------------------------------------------
C  SET UP THE BOUNDRY CONDITIONS
C-----------------------------------------------------------------
      IF(ICONST.EQ.2) GO TO 800
C-----------------------------------------------------------------
C  NO FLUX  BOUNDRY CONDITION AT THE SURFACE
C-----------------------------------------------------------------
      KL = 1
      K2=( COND(KL+1,1,1) + COND(KL,1,1) ) /  2
      K1 = 0.0
      C1 = SWC(KL,1,1)
      CONST1 =  DT / DZ(KL)**2/C1
C
      A(KL) = 0.0
      C(KL) =  CONST1  * K2
      B(KL) =   1.0 +  C(KL)
      D(KL) =  HEAD(KL,1,1) + DT/DZ(KL)/C1*( QS(1) - K2 )
     $      - DT * S(KL,1)/C1
      GO TO 900
C-----------------------------------------------------------------
C  CONSTANT POTENTIAL BOUNDRY CONDITION AT THE SURFACE
C-----------------------------------------------------------------
800   KL = 1
      K2=( COND(2,1,1) + COND(1,1,1) ) /  2
      K1 = COND(1,1,1)
      C1 = SWC(1,1,1)
      CONST1 =  DT / DZ(1)**2/C1
C
      A(1) =  CONST1  * K1
      C(1) =  CONST1  * K2
      B(1) =   1.0 + C(1)
      D(1) =  HEAD(1,1,1) + DT/DZ(1)/C1*( K1 - K2 )
     $      - DT * S(1,1)/C1
C-----------------------------------------------------------------
C  NO FLUX  BOUNDRY CONDITION  AT LOWER BOUNDRY
C-----------------------------------------------------------------
900   KL = NL
      K1=( COND(KL,1,1) + COND(KL-1,1,1) ) /  2
      K2=  0.0
      IF(ILOW.EQ.1) K2 = COND(KL,1,1)
      C1 = SWC(KL,1,1)
      CONST1 =  DT / DZ(KL)**2/C1
C
      A(KL) =  CONST1 * K1
      B(KL) =  1.0 + A(KL)
```

```
      D(KL) =  HEAD(KL,1,1) + DT/DZ(KL)/C1*( K1 - K2 )
     $      - DT * S(KL,1)/C1
C-----------------------------------------------------------------
C  CALCULATE THE NEW VALUES FOR THE HEADS
C-----------------------------------------------------------------
      IF = 1
C     IF(ICONST.EQ.2) IF = 2
      CALL TRID(NL,IF,A,B,C,D,V)
      DO 700 KL = ICONST,NL
      HEAD(KL,1,3)=V(KL)
700   CONTINUE
C
      IF(HEAD(1,1,3).GT.PRTAB(1).AND.ICONST.EQ.1) ICONST = 2
      IF (ICONST.EQ.1) GO TO 2000
         Q  = 0.0
         Q  = AMAX1( QS(1), QM )
C
2000  CONTINUE
      CALL UPDATE (3)
      DO 5000 I=1,NL
        HEAD(I,1,1)=HEAD(I,1,3)
        HEAD(I,1,2)=HEAD(I,1,3)
        WC(I,1,1)  =WC(I,1,3)
        WC(I,1,2)  =WC(I,1,3)
        COND(I,1,1)=COND(I,1,3)
        COND(I,1,2)=COND(I,1,3)
        SWC(I,1,1) =SWC(I,1,3)
        SWC(I,1,2) =SWC(I,1,3)
5000  CONTINUE
      CALL MASBAL(1)
C
      RETURN
      END
C-----------------------------------------------------------------------
C     SUBROUTINE TO CALCULATE THE TIME STEP BASED ON THE MAXIMUM
C                  NET FLOW RATE INTO EACH GRID
C                  FOR THE TWO-DIMENSIONAL MODEL
C-----------------------------------------------------------------------
      SUBROUTINE TSTEP2D( IRCODE )
      PARAMETER (IZ=50,IR=16,IB=IR*2+1,MAX=IZ*IR)
      IMPLICIT REAL  (A-H,O-Z)
      REAL  K1,K2,K4,K5,NFR
      COMMON /WCC/WKEEP,FLOW1(IZ,IR)
      COMMON /ET1/TSNR(90),TSNS(90),ETP(90),RAIN(90),DUR,TSTOP
      COMMON /PARA/WC(IZ,IR,3),COND(IZ,IR,3),SWC(IZ,IR,3),HEAD(IZ,IR,3),
     $NL,DZ(IZ),DEPTH(IZ),QS(IR),S(IZ,IR),ICONST,NR,DR(IR),R(IR),ILOW
      COMMON/TIM/DT,TIME,TOUT(90),ENDTIME,DTMAX,DTMIN,TOD,ITIME,QM,DTIRR
C
      NFR = 0.0
      DO 100 I=1,NL
      DO 100 J =1,NR
        IF(I.EQ.1) THEN
           Q1 = QS(J)
        ELSE
```

```
            Q1 = -1.0 * (( COND(I,J,1) + COND(I-1,J,1) ) / 2)
     $           *((HEAD(I,J,1)-HEAD(I-1,J,1))/DZ(I)-1.0)
         END IF
            IF(I.EQ.NL) THEN
               Q2 = 0.0
               IF(ILOW.EQ.1) Q2 = COND(I,J,1)
            ELSE
               Q2= -1.0 * (( COND(I+1,J,1) + COND(I,J,1) ) / 2)
     $              *((HEAD(I+1,J,1)-HEAD(I,J,1))/DZ(I)-1.0)
            END IF
                 IF(J.EQ.1) THEN
                    Q3 = 0.0
                 ELSE
                    Q3= -1.0 * (( COND(I,J,1) + COND(I,J-1,1) ) / 2)
     $                *((HEAD(I,J,1)-HEAD(I,J-1,1))/(R(J)-R(J-1)) )
                 END IF
            IF(J.EQ.NR) THEN
               Q4 = 0.0
            ELSE
               Q4 = -1.0 * (( COND(I,J,1) + COND(I,J+1,1))/ 2)
     $             *((HEAD(I,J+1,1)-HEAD(I,J,1))/(R(J+1)-R(J)) )
            END IF
          FLOW1(I,J) = (Q1 - Q2)/DZ(I) + (Q3 - Q4)/DR(J) - S(I,J)
          IF(ABS(FLOW1(I,J)).GT.NFR) GO TO 200
          GO TO 100
200       NFR = ABS(FLOW1(I,J))
100       CONTINUE
C
          IF(NFR.LE.0.0) GO TO 400
          DT = WKEEP /  NFR
          GO TO 500
400       DT = DTMAX
500       IF(DT.GT.DTMAX) DT = DTMAX
          IF(DT.LT.DTMIN) DT = DTMIN
          IF(IRCODE.EQ.1) DT = AMIN1( DTIRR, DT )
          IF( DT+TIME.GE.TOUT(ITIME).AND.TOUT(ITIME).GT.0.0)
     $     DT= TOUT(ITIME) - TIME
          IF(DT+TIME.GT.TSTOP.AND.IRCODE.EQ.1) DT = TSTOP - TIME
          IF( DT+TIME.GE.ENDTIME) DT = ENDTIME - TIME
          IF( DT.LE.0.0 ) DT = DTMIN
          RETURN
          END
C***
C-----------------------------------------------------------------------
C     ADI SOLUTION METHOD OF RICHARDS EQUATION
C-----------------------------------------------------------------------
          SUBROUTINE REDST2D
          PARAMETER (IZ=50,IR=16,IB=IR*2+1,MAX=IZ*IR)
          IMPLICIT REAL  (A-H,O-Z)
          REAL  K1,K2,K3,K4,V(IZ),A(IZ),B(IZ),C(IZ),D(IZ),HSTAR(IZ,IR)
          COMMON/PARA/WC(IZ,IR,3),COND(IZ,IR,3),SWC(IZ,IR,3),HEAD(IZ,IR,3),
         $NL,DZ(IZ),DEPTH(IZ),QS(IR),S(IZ,IR),ICONST,NR,DR(IR),R(IR),ILOW
          COMMON/TIM/DT,TIME,TOUT(90),ENDTIME,DTMAX,DTMIN,TOD,ITIME,QM,DTIRR
          COMMON /CONV/DIF,ITER,MAXITER
```

```
C-----------------------------------------------------------------
C  SET UP THE INTERIOR GRID POINTS FOR THE FIRST HALF CYCLE
C              SOLVE IN THE RADIAL DIRECTION
C-----------------------------------------------------------------
      ITER=0
700   DO 20 KL = 1,NL
         IF(KL.EQ.1) GO TO 25
         IF(KL.EQ.NL)GO TO 35
      DO 10 J=2,NR-1
         I = J
      K1=( COND(KL,J,1) + COND(KL-1,J,1) ) / 2
      K2=( COND(KL+1,J,1) + COND(KL,J,1) ) / 2
      K4=( COND(KL,J+1,2) + COND(KL,J,2) ) / 2
      K3=( COND(KL,J,2) + COND(KL,J-1,2) ) / 2
      C1=( SWC(KL,J,1) + SWC(KL,J,3) ) / 2
      R1=( R(J+1) + R(J) ) / 2
      R2=( R(J) + R(J-1) ) / 2
      CONST1 = -1.0 * DT / DZ(KL)**2 / C1
      CONST2 = -1.0 * DT / DR(J)**2  / C1 / R(J)
      A(I) = -1.0*  CONST2 * R2 * K3 / 2
      C(I) = -1.0*  CONST2 * R1 * K4 / 2
      B(I) =  1.0 + A(I) + C(I)
      D(I) =  HEAD(KL,J,1) + CONST1 * (K2 + K1) * HEAD(KL,J,1) / 2
     $   - CONST1 * ( K1 * HEAD(KL-1,J,1) + K2 * HEAD(KL+1,J,1) ) / 2
     $   + DT/DZ(KL)/C1*( K1 - K2 )/2 + DT/DZ(KL)/C1*( K1 - K2 ) / 4
     $   - DT/C1 * S(KL,J) / 2
10    CONTINUE
C-----------------------------------------------------------------
C  NO FLUX BOUNDRY CONDITION AT INNER RADIUS
C-----------------------------------------------------------------
      J = 1
      I = J
      K1 = (COND(KL,J,1)+COND(KL-1,J,1))/ 2
      K2=( COND(KL+1,J,1) + COND(KL,J,1) ) /  2
      K4=( COND(KL,J+1,2) + COND(KL,J,2) ) /  2
      K3=  K4
      C1 =( SWC(KL,J,1) + SWC(KL,J,3) ) / 2
      CONST1 = -1.0 * DT / DZ(KL)**2 / C1
      CONST2 = -1.0 * DT / DR(J)**2  / C1
      A(I) = 0.0
      C(I) = -1.0*  CONST2 * K4 / 2
      B(I) =  1.0 + C(I)
      D(I) = HEAD(KL,J,1) + CONST1*(K2+K1) * HEAD(KL,J,1) / 2
     $   - CONST1*K1*HEAD(KL-1,J,1)/2 - CONST1*K2*HEAD(KL+1,J,1)/2
     $   + DT/DZ(KL)/C1*( K1 - K2 )/2 + DT/DZ(KL)/C1*( K1 - K2 ) / 4
     $             - DT/C1 * S(KL,J) / 2
C
C-----------------------------------------------------------------
C  NO FLUX BOUNDRY CONDITION AT OUTER RADIUS
C-----------------------------------------------------------------
      J=NR
      I = NR
      K1=( COND(KL,J,1) + COND(KL-1,J,1) ) /  2
      K2=(COND(KL+1,J,1) + COND(KL,J,1) ) /  2
```

```
      K3=( COND(KL,J,2) + COND(KL,J-1,2) ) /  2
      K4 = 0.0
      C1 =( SWC(KL,J,1) + SWC(KL,J,3) ) / 2
      CONST1 = -1.0 * DT / DZ(KL)**2 / C1
      CONST2 = -1.0 * DT / DR(J)**2  / C1
C
      A(I) = -1.0*  CONST2 * K3 / 2
      C(I) = 0.0
      B(I) =  1.0 + A(I)
      D(I) = HEAD(KL,J,1) + CONST1*(K2+K1) * HEAD(KL,J,1) / 2
     $     - CONST1*K1*HEAD(KL-1,J,1)/2 - CONST1*K2*HEAD(KL+1,J,1)/2
     $     + DT/DZ(KL)/C1*( K1 - K2 )/2 + DT/DZ(KL)/C1*( K1 - K2 )/4
     $     - DT/C1 * S(KL,J) / 2
      GO TO 50
C-----------------------------------------------------------------------
C    NO FLUX  BOUNDRY CONDITION AT THE SURFACE
C-----------------------------------------------------------------------
25    DO 30 J=1,NR
         I = J
      K2=( COND(KL+1,J,1) + COND(KL,J,1) ) /  2
      K1 = QS(J)
      IF(J.NE.NR) K4=( COND(KL,J+1,2) + COND(KL,J,2) ) /  2
      IF(J.EQ.NR) K4 = 0.0
      IF(J.NE.NR) R1 = ( R(J+1) + R(J) ) /  2
      IF(J.NE.1) K3 = ( COND(KL,J,2) + COND(KL,J-1,2) ) / 2
      IF(J.EQ.1) K3 = 0.0
      IF(J.NE.1) R2 = ( R(J) + R(J-1) ) / 2
      C1=( SWC(KL,J,1) + SWC(KL,J,3) ) / 2
      CONST1 = -1.0 * DT / DZ(KL)**2 / C1
      IF(J.NE.1.AND.J.NE.NR) CONST2 = -1.0 * DT / DR(J)**2  / C1 / R(J)
      IF(J.EQ.1.OR.J.EQ.NR)  CONST2 = -1.0 * DT / DR(J)**2 / C1
      A(I) = -1.0*  CONST2 * R2 * K3 / 2
      IF(J.EQ.1) A(I) = -1.0* CONST2 * K3 / 2
      C(I) = -1.0*  CONST2 * R1 * K4 / 2
      IF(J.EQ.NR) C(I) = -1.0* CONST2 * K4 / 2
      B(I) =  1.0 + A(I) + C(I)
      D(I) =  HEAD(KL,J,1) + CONST1 * K2 * HEAD(KL,J,1) / 2
     $     - CONST1  * K2 * HEAD(KL+1,J,1) / 2
     $     + DT/DZ(KL)/C1*(K1 - K2)/2 + DT/DZ(KL)/C1*(K1 - K2)/4
     $     - DT/C1 * S(KL,J)  / 2
30    CONTINUE
      GO TO 50
C-----------------------------------------------------------------------
C  NO FLUX  BOUNDRY CONDITION  AT LOWER BOUNDRY
C-----------------------------------------------------------------------
35    DO 40 J=1,NR
         I =  J
      K1=( COND(KL,J,1) + COND(KL-1,J,1) ) /  2
      K2=  0.0
      IF(J.NE.NR) K4=( COND(KL,J+1,2) + COND(KL,J,2) ) /  2
      IF(J.EQ.NR) K4=0.0
      IF(J.NE.NR) R1 = (R(J+1) + R(J) ) /  2
      IF(J.NE.1)  K3=( COND(KL,J,2) + COND(KL,J-1,2) ) /  2
      IF(J.EQ.1)  K3 = 0.0
```

```
      IF(J.NE.1)  R2=( R(J) + R(J-1) ) /  2
      C1 =  ( SWC(KL,J,1) + SWC(KL,J,3) ) / 2
      CONST1 = -1.0 * DT / DZ(KL)**2 / C1
      IF(J.NE.1.AND.J.NE.NR) CONST2 = -1.0 * DT / DR(J)**2  / C1 / R(J)
      IF(J.EQ.1.OR.J.EQ.NR)  CONST2 = -1.0 * DT / DR(J)**2 / C1
      A(I) = -1.0*  CONST2 * R2 * K3 / 2
      IF(J.EQ.1) A(I) = -1.0* CONST2 * K3 / 2
      C(I) = -1.0*  CONST2 * R1 * K4 / 2
      IF(J.EQ.NR) C(I) = -1.0* CONST2 * K4 / 2
      B(I) =  1.0 + A(I) + C(I)
      D(I) =  HEAD(KL,J,1) + CONST1 * K1 * HEAD(KL,J,1) / 2
     $     -  CONST1  * K1 * HEAD(KL-1,J,1) / 2
     $     +  DT/DZ(KL)/C1*(K1 - K2)/2 + DT/DZ(KL)/C1*(K1 - K2)/4
     $     - DT/C1 * S(KL,J)  / 2
40    CONTINUE
C--------**************************************----------
50        IF = 1
      CALL TRID( NR,IF,A, B, C, D, V )
            DO 55 J=1,NR
               HEAD(KL,J,2)= V(J)
55          CONTINUE
20    CONTINUE
C-------------------------------------------------------------------
C  SET UP THE INTERIOR GRID POINTS  FOR THE SECOND HALF
C              IN THE VERTICAL DIRECTION
C-------------------------------------------------------------------
      DO 60 J=1,NR
         IF(J.EQ.1) GO TO 12
         IF(J.EQ.NR)GO TO 14
      DO 70 KL=2,NL-1
         I = KL
      K1=( COND(KL,J,3) + COND(KL-1,J,3) ) / 2
      K2=( COND(KL+1,J,3) + COND(KL,J,3) ) / 2
      K4=( COND(KL,J+1,2) + COND(KL,J,2) ) / 2
      K3=( COND(KL,J,2) + COND(KL,J-1,2) ) / 2
      R1=( R(J+1) + R(J) ) / 2
      R2=( R(J) + R(J-1) ) / 2
      C1 = ( SWC(KL,J,1) + SWC(KL,J,3) ) / 2
      CONST1 = -1.0 * DT / DZ(KL)**2 / C1
      CONST2 = -1.0 * DT / DR(J)**2  / C1 / R(J)
      A(I) = -1.0*  CONST1 * K1 / 2
      C(I) = -1.0*  CONST1 * K2 / 2
      B(I) =  1.0 + A(I) + C(I)
      D(I) =  DT/DZ(KL)/C1*( K1 - K2 ) / 4.0
     $ - CONST2*R2*K3*HEAD(KL,J-1,2)/2 - CONST2*R1*K4*HEAD(KL,J+1,2)/2
     $ + HEAD(KL,J,2) + CONST2 * ( R2*K3 + R1*K4 ) * HEAD(KL,J,2) / 2
     $ - DT/C1 * S(KL,J) / 2
70    CONTINUE
C-------------------------------------------------------------------
C  SET UP THE BOUNDRY CONDITIONS
C-------------------------------------------------------------------
C  NO FLUX  BOUNDRY CONDITION AT THE SURFACE
C-------------------------------------------------------------------
      KL = 1
```

```
      I = KL
      K2=( COND(KL+1,J,3) + COND(KL,J,3) ) /  2
      K1 = QS(J)
      K4=( COND(KL,J+1,2) + COND(KL,J,2) ) /  2
      R1=( R(J+1) + R(J) ) /  2
      K3=( COND(KL,J,2) + COND(KL,J-1,2) ) / 2
      R2=( R(J) + R(J-1) ) / 2
      C1 = ( SWC(KL,J,1) + SWC(KL,J,3) ) / 2
      CONST1 = -1.0 * DT / DZ(KL)**2 / C1
      CONST2 = -1.0 * DT / DR(J)**2  / C1 / R(J)
      A(I) = 0.0
      C(I) = -1.0*  CONST1 * K2 / 2
      B(I) =  1.0 + C(I)
      D(I) =  DT/DZ(KL)/C1*( K1 - K2 ) / 4
     $ - CONST2*R2*K3*HEAD(KL,J-1,2)/2 - CONST2*R1*K4*HEAD(KL,J+1,2)/2
     $ + HEAD(KL,J,2) + CONST2 * ( R2*K3 + R1*K4 ) * HEAD(KL,J,2) / 2
     $ - DT/C1 * S(KL,J) / 2
C-----------------------------------------------------------------------
C  NO FLUX  BOUNDRY CONDITION  AT LOWER BOUNDRY
C-----------------------------------------------------------------------
      KL = NL
      I = KL
      K1=( COND(KL,J,3) + COND(KL-1,J,3) ) /  2
      K2=  0.0
      K4=( COND(KL,J+1,2) + COND(KL,J,2) ) /  2
      R1 = (R(J+1) + R(J) ) /  2
      K3=( COND(KL,J,2) + COND(KL,J-1,2) ) /  2
      R2=( R(J) + R(J-1) ) /  2
      C1 = ( SWC(KL,J,1) + SWC(KL,J,3) ) / 2
      CONST1 = -1.0 * DT / DZ(KL)**2 / C1
      CONST2 = -1.0 * DT / DR(J)**2  / C1 / R(J)
      A(I) = -1.0*  CONST1 * K1 / 2
      C(I) = 0.0
      B(I) =  1.0 + A(I)
      D(I) =  DT/DZ(KL)/C1*( K1 - K2 ) / 4
     $ - CONST2*R2*K3*HEAD(KL,J-1,2)/2 - CONST2*R1*K4*HEAD(KL,J+1,2)/2
     $ + HEAD(KL,J,2) + CONST2 * ( R2*K3 + R1*K4 ) * HEAD(KL,J,2) / 2
     $ - DT/C1 * S(KL,J) / 2
      GO TO 65
C-----------------------------------------------------------------------
C  NO FLUX BOUNDRY CONDITION AT INNER RADIUS
C-----------------------------------------------------------------------
12    DO 41 KL=1,NL
      I = KL
      IF(KL.NE.1) K1 = (COND(KL,J,3)+COND(KL-1,J,3))/ 2
      IF(KL.EQ.1) K1 =  QS(J)
      IF(KL.NE.NL)K2=( COND(KL+1,J,3) + COND(KL,J,3) ) /  2
      IF(KL.EQ.NL)K2 = 0.0
      K4=( COND(KL,J+1,2) + COND(KL,J,2) ) /  2
      K3=  K4
      C1 = ( SWC(KL,J,1) + SWC(KL,J,3) ) / 2
      CONST1 = -1.0 * DT / DZ(KL)**2 / C1
      CONST2 = -1.0 * DT / DR(J)**2  / C1
      A(I) = -1.0*  CONST1 * K1 / 2
```

```
      IF(KL.EQ.1) A(I) = -1.0* 0.0
      C(I) = -1.0*  CONST1 * K2 / 2
      IF(KL.EQ.NL) C(I) = -1.0* 0.0
      B(I) =  1.0 + A(I) + C(I)
      D(I) =  DT/DZ(KL)/C1*( K1 - K2 ) / 4 - CONST2*K4*HEAD(KL,J+1,2)/2
     $ + HEAD(KL,J,2) + CONST2 * K4 * HEAD(KL,J,2) / 2
     $ - DT/C1 * S(KL,J) / 2
41    CONTINUE
      GO TO 65
C-----------------------------------------------------------------
C  NO FLUX BOUNDRY CONDITION AT OUTER RADIUS
C-----------------------------------------------------------------
14    DO 61 KL=1,NL
      I = KL
      IF(KL.NE.1) K1=( COND(KL,J,3) + COND(KL-1,J,3) ) /  2
      IF(KL.EQ.1) K1= QS(J)
      IF(KL.NE.NL)K2=(COND(KL+1,J,3) + COND(KL,J,3) ) /  2
      IF(KL.EQ.NL)K2 = 0.0
      K3=( COND(KL,J,2) + COND(KL,J-1,2) ) /  2
      K4 = 0.0
      C1 = ( SWC(KL,J,1) + SWC(KL,J,3) ) / 2
      CONST1 = -1.0 * DT / DZ(KL)**2 / C1
      CONST2 = -1.0 * DT / DR(J)**2  / C1
      A(I) = -1.0*  CONST1 * K1 / 2
      IF(KL.EQ.1) A(I) = -1.0* 0.0
      C(I) = -1.0*  CONST1 * K2 / 2
      IF(KL.EQ.NL) C(I) = -1.0* 0.0
      B(I) =  1.0 + A(I) + C(I)
      D(I) =  DT/DZ(KL)/C1*(K1 - K2) /4 - CONST2* K3* HEAD(KL,J-1,2)/2
     $ + HEAD(KL,J,2) + CONST2 * K3 * HEAD(KL,J,2) / 2
     $ - DT/C1 * S(KL,J) / 2
61    CONTINUE
C-----------------------------------------------------------------
65    IF = 1
      CALL TRID(NL,IF, A, B, C, D, V)
         DO 71 KL=1,NL
            HSTAR(KL,J)=  V(KL)
71       CONTINUE
60    CONTINUE
C-----------------------------------------------------------------
      DIF = 0.0
         DO 506 I=1,NL
         DO 506 J=1,NR
            DIF = DIF + ABS((HSTAR(I,J)-HEAD(I,J,3))/HEAD(I,J,3) )
            HEAD(I,J,3)=HSTAR(I,J)
506      CONTINUE
C
      IF(DIF.LT.1.0E-6) GO TO 701
      CALL UPDATE (2)
      ITER= ITER + 1
      IF(ITER.LT.MAXITER) GO TO 700
C-----------------------------------------------------------------
701   CONTINUE
      CALL UPDATE(3)
```

```
          DO 80 I=1,NL
          DO 80 J=1,NR
             HEAD(I,J,1)=HEAD(I,J,3)
             HEAD(I,J,2)=HEAD(I,J,3)
             WC(I,J,1)  =WC(I,J,3)
             WC(I,J,2)  =WC(I,J,3)
             COND(I,J,1)=COND(I,J,3)
             COND(I,J,2)=COND(I,J,3)
             SWC(I,J,1) =SWC(I,J,3)
             SWC(I,J,2) =SWC(I,J,3)
80        CONTINUE
        CALL MASBAL(1)
        RETURN
        END
C-----------------------------------------------------------------------
C   ROUTINE TO UPDATE THE SOIL PROPERTIES
C-----------------------------------------------------------------------
        SUBROUTINE UPDATE ( ILOOP )
        PARAMETER (IZ=50,IR=16,IB=IR*2+1,MAX=IZ*IR)
        IMPLICIT REAL  (A-H,O-Z)
        CHARACTER*64 MBFILE
        REAL  WCNT(120),CONT(120),SWCT(120),HEDT(120)
        COMMON /TABLES/WCNT,CONT,SWCT,HEDT,NDIM,MBFILE,ISOIL
        IF(ISOIL.EQ.1) CALL TBLARR ( ILOOP )
        IF(ISOIL.EQ.2) CALL TBLREH ( ILOOP )
        IF(ISOIL.EQ.3) CALL TBLOAM ( ILOOP )
        IF(ISOIL.EQ.4) CALL TBLOAM ( ILOOP )
        IF(ISOIL.EQ.5) CALL TBLYOL ( ILOOP )
        IF(ISOIL.EQ.6) CALL LINEAR ( ILOOP )
        RETURN
        END
C-----------------------------------------------------------------------
        SUBROUTINE TBLARR ( ILOOP )
C-----------------------------------------------------------------------
C       THIS SUBROUTINE USES AN INDEX ROUTING TECHNIQUE WITH
C       TABULATED DATA TO FIND THE CORRESPONDING VALUES OF
C       WATER CONTENT, SPECIFIC WATER CAPACITY AND HYDRAULIC
C       CONDUCTIVITY FOR A GIVEN VALUE OF SOIL MATRIC POTENTIAL
C       FOR ARREDONDO FINE SAND.
C-----------------------------------------------------------------------
        PARAMETER (IZ=50,IR=16,IB=IR*2+1,MAX=IZ*IR)
        IMPLICIT REAL  (A-H,O-Z)
        CHARACTER*64 MBFILE
        REAL  WCNT(120),CONT(120),SWCT(120),HEDT(120)
        COMMON/PARA/WCN(IZ,IR,3),CON(IZ,IR,3),SWC(IZ,IR,3),HED(IZ,IR,3),
       $ NL,DZ(IZ),DEPTH(IZ),QS(IR),S(IZ,IR),ICONST,NR,DR(IR),R(IR),ILOW
        COMMON/TABLES/WCNT,CONT,SWCT,HEDT,NDIM,MBFILE,ISOIL
C-----------------------------------------------------------------------
        HEDSML = HEDT(118)
        HEDLGE = HEDT(1)
          DO 100 J=ILOOP,3
          DO 100 K=1,NR
             DO 100 I = 1,NL
             IF (HED(I,K,J) .LE. HEDSML) HED(I,K,J) = HEDSML
```

```
            IF (HED(I,K,J) .GE. HEDLGE) HED(I,K,J) = HEDLGE
            RINDEX = ALOG10(-1.*HED(I,K,J))*4.E01-8.1E01
            INDEX = RINDEX
            IF(INDEX.LT.1) INDEX = 1
            IF (HED(I,K,J) .LT. HEDT(INDEX+1)) INDEX = INDEX+1
            IF (HED(I,K,J) .GT. HEDT(INDEX)) INDEX = INDEX-1
            IF(INDEX.LT.1) INDEX = 1
            IF (INDEX .GE. 118) INDEX = 118
            RM = RINDEX-INDEX
            RATIO = ALOG10(HED(I,K,J)/HEDT(INDEX))/ALOG10(HEDT(INDEX+1)/
     +           HEDT(INDEX))
            WCN(I,K,J) = WCNT(INDEX)+RATIO*(WCNT(INDEX+1)-WCNT(INDEX))
            SWC(I,K,J) = SWCT(INDEX)*1.E01**(RATIO*ALOG10(SWCT(INDEX+1)/
     +           SWCT(INDEX)))
            CON(I,K,J) = CONT(INDEX)*1.E01**(RATIO*ALOG10(CONT(INDEX+1)/
     +           CONT(INDEX)))
  100       CONTINUE
      RETURN
      END
C-----------------------------------------------------------------------
      SUBROUTINE TBLOAM ( ILOOP )
C-----------------------------------------------------------------------
C      THIS SUBROUTINE USES AN INDEX ROUTING TECHNIQUE WITH
C      TABULATED DATA TO FIND THE CORRESPONDING VALUES OF
C      WATER CONTENT, SPECIFIC WATER CAPACITY AND HYDRAULIC
C      CONDUCTIVITY FOR A GIVEN VALUE OF SOIL MATRIC POTENTIAL
C      FOR EITHER OF THE LOAMS.
C-----------------------------------------------------------------------
      PARAMETER (IZ=50,IR=16,IB=IR*2+1,MAX=IZ*IR)
      IMPLICIT REAL  (A-H,O-Z)
      CHARACTER*64 MBFILE
      REAL  WCNT(120),CONT(120),SWCT(120),HEDT(120)
      COMMON/PARA/WCN(IZ,IR,3),CON(IZ,IR,3),SWC(IZ,IR,3),HED(IZ,IR,3),
     $ NL,DZ(IZ),DEPTH(IZ),QS(IR),S(IZ,IR),ICONST,NR,DR(IR),R(IR),ILOW
      COMMON/TABLES/WCNT,CONT,SWCT,HEDT,NDIM,MBFILE,ISOIL
C-----------------------------------------------------------------------
      HEDSML = HEDT(49)
      HEDLGE = HEDT(1)
        DO 100 J = ILOOP ,3
        DO 100 K = 1,NR
           DO 100 I = 1,NL
           IF (HED(I,K,J) .LE. HEDSML) HED(I,K,J) = HEDSML
           IF (HED(I,K,J) .GE. HEDLGE) HED(I,K,J) = HEDLGE
           RINDEX = ALOG10(-1.*HED(I,K,J))*1.E01-2.0E01
           INDEX = RINDEX
           IF (HED(I,K,J) .LT. HEDT(INDEX+1)) INDEX = INDEX+1
           IF (HED(I,K,J) .GT. HEDT(INDEX)) INDEX = INDEX-1
           IF (INDEX .GE. 49) INDEX = 49
           IF (INDEX .LE. 1) INDEX = 1
           RM = RINDEX-INDEX
           RATIO = ALOG10(HED(I,K,J)/HEDT(INDEX))/ALOG10(HEDT(INDEX+1)/
     +          HEDT(INDEX))
           WCN(I,K,J) = WCNT(INDEX)+RATIO*(WCNT(INDEX+1)-WCNT(INDEX))
           SWC(I,K,J) = SWCT(INDEX)*1.E01**(RATIO*ALOG10(SWCT(INDEX+1)/
```

```
     +          SWCT(INDEX)))
           CON(I,K,J) = CONT(INDEX)*1.E01**(RATIO*ALOG10(CONT(INDEX+1)/
     +          CONT(INDEX)))
  100      CONTINUE
      RETURN
      END
C-----------------------------------------------------------------------
      SUBROUTINE TBLREH ( ILOOP )
C-----------------------------------------------------------------------
C      THIS SUBROUTINE USES AN INDEX ROUTING TECHNIQUE WITH
C      TABULATED DATA TO FIND THE CORRESPONDING VALUES OF
C      WATER CONTENT, SPECIFIC WATER CAPACITY AND HYDRAULIC
C      CONDUCTIVITY FOR A GIVEN VALUE OF SOIL MATRIC POTENTIAL
C      FOR REHOVOT SAND
C-----------------------------------------------------------------------
      PARAMETER (IZ=50,IR=16,IB=IR*2+1,MAX=IZ*IR)
      IMPLICIT REAL  (A-H,O-Z)
      CHARACTER*64 MBFILE
      REAL  WCNT(120),CONT(120),SWCT(120),HEDT(120)
      COMMON/PARA/WCN(IZ,IR,3),CON(IZ,IR,3),SWC(IZ,IR,3),HED(IZ,IR,3),
     $ NL,DZ(IZ),DEPTH(IZ),QS(IR),S(IZ,IR),ICONST,NR,DR(IR),R(IR),ILOW
      COMMON/TABLES/WCNT,CONT,SWCT,HEDT,NDIM,MBFILE,ISOIL
C-----------------------------------------------------------------------
      HEDSML = HEDT(59)
      HEDLGE = HEDT(1)
        DO 100 J = ILOOP ,3
        DO 100 K = 1,NR
           DO 100 I = 1,NL
           IF (HED(I,K,J) .LE. HEDSML) HED(I,K,J) = HEDSML
           IF (HED(I,K,J) .GE. HEDLGE) HED(I,K,J) = HEDLGE
           RINDEX = ALOG10(-1.*HED(I,K,J))*1.E01-1.1E01
           INDEX = RINDEX
           IF (HED(I,K,J) .LT. HEDT(INDEX+1)) INDEX = INDEX+1
           IF (HED(I,K,J) .GT. HEDT(INDEX)) INDEX = INDEX-1
           IF (INDEX .GE. 59) INDEX = 59
           IF (INDEX .LE. 1) INDEX = 1
           RM = RINDEX-INDEX
           RATIO = ALOG10(HED(I,K,J)/HEDT(INDEX))/ALOG10(HEDT(INDEX+1)/
     +          HEDT(INDEX))
           WCN(I,K,J) = WCNT(INDEX)+RATIO*(WCNT(INDEX+1)-WCNT(INDEX))
           SWC(I,K,J) = SWCT(INDEX)*1.E01**(RATIO*ALOG10(SWCT(INDEX+1)/
     +          SWCT(INDEX)))
           CON(I,K,J) = CONT(INDEX)*1.E01**(RATIO*ALOG10(CONT(INDEX+1)/
     +          CONT(INDEX)))
  100      CONTINUE
      RETURN
      END
C
      SUBROUTINE TBLYOL ( ILOOP )
C-----------------------------------------------------------------------
C      THIS SUBROUTINE USES AN INDEX ROUTING TECHNIQUE WITH
C      TABULATED DATA TO FIND THE CORRESPONDING VALUES OF
C      WATER CONTENT, SPECIFIC WATER CAPACITY AND HYDRAULIC
C      CONDUCTIVITY FOR A GIVEN VALUE OF SOIL MATRIC POTENTIAL
```

```
C      FOR YOLO LIGHT CLAY.
C-----------------------------------------------------------------------
      PARAMETER (IZ=50,IR=16,IB=IR*2+1,MAX=IZ*IR)
      IMPLICIT REAL  (A-H,O-Z)
      CHARACTER*64 MBFILE
      REAL  WCNT(120),CONT(120),SWCT(120),HEDT(120)
      COMMON/PARA/WCN(IZ,IR,3),CON(IZ,IR,3),SWC(IZ,IR,3),HED(IZ,IR,3),
     $ NL,DZ(IZ),DEPTH(IZ),QS(IR),S(IZ,IR),ICONST,NR,DR(IR),R(IR),ILOW
      COMMON/TABLES/WCNT,CONT,SWCT,HEDT,NDIM,MBFILE,ISOIL
      HEDSML = HEDT(49)
      HEDLGE = HEDT(1)
        DO 100 J = ILOOP ,3
        DO 100 K = 1,NR
           DO 100 I = 1,NL
           IF (HED(I,K,J) .LE. HEDSML) HED(I,K,J) = HEDSML
           IF (HED(I,K,J) .GE. HEDLGE) HED(I,K,J) = HEDLGE
           RINDEX = ALOG10(-1.*HED(I,K,J))*1.E01-1.1E01
           INDEX = RINDEX
           IF (HED(I,K,J) .LT. HEDT(INDEX+1)) INDEX = INDEX+1
           IF (HED(I,K,J) .GT. HEDT(INDEX)) INDEX = INDEX-1
           IF (INDEX .GE. 49) INDEX = 49
           IF (INDEX .LE. 1) INDEX = 1
           RM = RINDEX-INDEX
           RATIO = ALOG10(HED(I,K,J)/HEDT(INDEX))/ALOG10(HEDT(INDEX+1)/
     +          HEDT(INDEX))
           WCN(I,K,J) = WCNT(INDEX)+RATIO*(WCNT(INDEX+1)-WCNT(INDEX))
           SWC(I,K,J) = SWCT(INDEX)*1.E01**(RATIO*ALOG10(SWCT(INDEX+1)/
     +          SWCT(INDEX)))
           CON(I,K,J) = CONT(INDEX)*1.E01**(RATIO*ALOG10(CONT(INDEX+1)/
     +          CONT(INDEX)))
  100      CONTINUE
      RETURN
      END
C
      SUBROUTINE LINEAR ( ILOOP )
      PARAMETER (IZ=50,IR=16,IB=IR*2+1,MAX=IZ*IR)
      IMPLICIT REAL  (A-H,O-Z)
      CHARACTER*64 MBFILE
      REAL  WCNT(120),CONT(120),SWCT(120),HEDT(120)
      COMMON /TABLES/WCNT,CONT,SWCT,HEDT,NDIM,MBFILE,ISOIL
      COMMON/PARA/WCN(IZ,IR,3),CON(IZ,IR,3),SWC(IZ,IR,3),HED(IZ,IR,3),
     $ NL,DZ(IZ),DEPTH(IZ),QS(IR),S(IZ,IR),ICONST,NR,DR(IR),R(IR),ILOW
C
      DO 100 K= ILOOP, 3
      DO 100 J=1,NR
         DO 100 I = 1,NL
         IF(HED(I,J,K).GT.0.0) HED(I,J,K) = 0.0
      CALL INTPL(HED(I,J,K),CON(I,J,K),SWC(I,J,K),WCN(I,J,K))
100   CONTINUE
      RETURN
      END
CCCCCCCCCCCCCCCCCCCCCCCCCCCCCCCCCCCCCCCCCCCCCCCCCCCCCCCCCCCCCCCCCCCCCCC
C
      SUBROUTINE INTPL (W,X,Y,Z)
```

```
      IMPLICIT REAL  (A-H,O-Z)
C     THIS SUBROUTINE INTERPOLATES LINEARLY BETWEEN TWO SETS OF DATA
C     POINTS.  DATA IS INPUT AS TABULAR FUNCTIONS
C
      CHARACTER*64 MBFILE
      REAL  WTAB(120),XTAB(120),YTAB(120),ZTAB(120)
      COMMON /TABLES/ZTAB,XTAB,YTAB,WTAB,NDIM,MBFILE,ISOIL
      X=XTAB(1)
C     Y=YTAB(1)
      Z=ZTAB(1)
      N=2
      IF(ABS(W).LE.ABS(WTAB(1) )) GO TO 50
      X=XTAB(NDIM)
C     Y=YTAB(NDIM)
      Z=ZTAB(NDIM)
      N=NDIM
      IF(ABS(W).GE.ABS(WTAB(NDIM) )) GO TO 50
C
      DO 10 I=2,NDIM
      N=I
      IF(ABS(W).LE.ABS(WTAB(I))) GO TO 50
10    CONTINUE
50    X=XTAB(N-1)-ABS((W-WTAB(N-1))/(WTAB(N)-WTAB(N-1))*
     +(XTAB(N)-XTAB(N-1)))
      Y=YTAB(N-1)-ABS((W-WTAB(N-1))/(WTAB(N)-WTAB(N-1))*
     +(YTAB(N)-YTAB(N-1)))
      Z=ZTAB(N-1)-ABS((W-WTAB(N-1))/(WTAB(N)-WTAB(N-1))*
     +(ZTAB(N)-ZTAB(N-1)))
100   RETURN
      END
```

REFERENCES

Amerman, C.R. 1969. Finite difference solutions of unsteady, two-dimensional, partially saturated porous media flow. Volumes I and II. Ph.D. Dissertation, Purdue University, W. Lafayette, Ind.

Amerman, C.R., and E.J. Monke. 1977. Soil water modeling II: On sensitivity to finite difference grid spacing. Trans. Amer. Soc. Agr. Eng. 20(3):478-484,488.

Aribi, K., A.G. Smajstrla, F.S. Zazueta, and S.F. Shih. 1985. Accuracies of neutron probe water content measurements for sandy soils. Soil and Crop Sci. Soc. Fla. Proc. 44:44-49.

Armstrong, C.F., and T.V. Wilson. 1983. Computer model for moisture distribution in stratified soils under a trickle source. Trans. Amer. Soc. Agr. Eng. 26(6):1704-1709.

Bottcher, A.B., and L.W. Miller. 1982. Automatic tensiometer scanner for rapid measurements. Trans. Amer. Soc. Agr. Eng. 15:1338-1342.

Brandt, A., E. Bresler, N. Diner, I. Ben-Asher, J. Heller, and D. Goldberg. 1971. Infiltration from a trickle source: I. mathematical models. Soil Sci. Soc. Amer. Proc. 35:675-682.

Bresler, E., J. Heller, N. Diner, I. Ben-Asher,A. Brandt, and D. Goldberg. 1971. Experimental data and theoretical predictions. Soil Sci. Soc. Amer. Proc. 35:683-689.

Clark, G.A. 1982. Simulation of the sensivity of water movement and storage in sandy soils to irrigation application rate and depth. Unpublished Master's Thesis. University of Florida, Gainesville, FL.

Clark, G., and A.G. Smajstrla. 1983. Water distributions in soils as influenced by irrigation depths and intensities. Soil and Crop Sci. Soc. Fla. Proc. 42:157-165.

Denmead, O.T., and R.H. Shaw. 1962. Availability of soil water water to plants as affected by soil moisture content and meteorological conditions. Agron. J. 45:385-390.

Enfield, C.G., and C.V. Gillaspy. 1980. Pressure transducer for remote data acquisition. Trans. Amer. Soc. Agr. Eng. 23(5):1195-1200.

Feddes, R.A., P.J. Kowalik, and H. Zaradny. 1978. Simulation of field water use and crop yield. Halsted Press. New York.

Fitzsimmons, D.W., and N.C. Young. 1972. Tensiometer-pressure transducer system for studying unsteady flow through soils. Trans. Amer. Soc. Agr. Eng. 15:272-275.

Fletcher, J.E. 1939. A dielectric method of measuring soil moisture. Soil Sci. Soc. Amer. Proc. 4:84-88.

Gardner, W.R. 1960. Dynamic aspects of water availability to plants. Soil Sci. 89(2):63-73.

Gardner, W.R., and C.F. Ehling. 1962. Some observations on the movement of water to plant roots. Agron. J. 54:453-456.

Gradmann, H. 1928. Untersuchungen uber die wasserverhaltnisse des bodens als grundlage des pflanzenwachstums. Jahrb. Wiss. Bot., 69:1-100.

Hanks, R.J., and S.A. Bowers. 1962. Numerical solution of the moisture flow equation for infiltration into layered soils. Soil Sci. Soc. Amer. Proc. 26:530-534.

Harrison, D.S., A.G. Smajstrla, R.E. Choate, and G.W. Isaacs. 1983. Irrigation in Florida agriculture in the '80s. Bulletin 196, Fla. Coop. Ext. Serv., Univ. of Fla.

Haverkamp, R., M. Vauclin, J. Touma, P.J. Wierenga, and G. Vachaud. 1977. A compairison of numerical simulation models for one-dimensional infiltration. Soil Sci. Soc. Amer. Proc. 41:285-294.

Hiler, E.A., and S.I. Bhuiyan. 1971. Dynamic simulation of unsteady flow of water in unsaturated soils and its application to subirrigation system design. Technical Report TR-40. Texas Water Resources Institute. College Station, TX.

Hillel, D. 1980. Fundamentals of soil physics. Academic Press, New York.

Hornberger, G.M., I. Remson, and A.A. Fungaroli. 1969. Numeric studies of a composite soil moisture ground-water system. Water Resour. Res. 5:797-802.

Long, F.L., and M.G. Hulk. 1980. An automated system for measuring soil water potential gradients in a rhizotron soil profile. Soil Sci. 129:305-310.

Marthaler, H.P., W. Vogelsanger, F. Richard, and P.J. Wierenga. 1983. A pressure transducer for field tensiometers. Soil Sci Soc. Amer. Proc. 47:624-627.

Molz, F.J., and J. Remson. 1970. Extraction term models of soil moisture use of transpiring plants. Water Resour. Res. 6:1346-1356.

Nimah, M.N., and R.J. Hanks. 1973a. Model for estimating soil water, plant and atmospheric interrelations: I. description and sensitivity. Soil Sci. Soc. Amer. Proc. 37:522-527.

Nimah, M.N., and R.J. Hanks. 1973b. Model for estimating soil water, plant and atmospheric interrelations: II field test of model. Soil Sci. Soc. Amer. Proc. 37:528-532.

Perrens, S.J., and K.K. Watson. 1977. Numerical analysis of two-dimensional infiltration and redistribution. Water Resour. Res. 13(4):781-790.

Phene, C.J., G.J. Hoffman, and S.L. Rawlins. 1971. Measuring soil matric potential in situ by sensing heat dissipation within a porous body: I. Theory and sensor construction. Soil Sci. Soc. Amer. Proc. 35:27-33.

Phene, C.J., S.L. Rawlins, and G.J. Hoffman. 1971. Measuring soil matric potential in situ by sensing heat dissipation within a porous body: II. Experimental Results. Soil Sci. Soc. Amer. Proc. 35:225-229.

Phillip, J.R. 1968. Steady infiltration from buried point sources and spherical cavities. Water Resour. Res. 4:1039-1047.

Ritchie, J.T. 1973. Influence of soil water status and meteorological conditions on evaporation from a corn canopy. Agron. J. 65:893-897.

Reddell, D.L., and D.K. Sunada. 1970. Numerical simulation of dispersion in groundwater aquifers. Hydrology paper 41, Colorado State University, Fort Collins, Colorado.

Rubin, J., and R. Steinhardt. 1963. Soil water relations during rain infiltration: 1. Theory. Soil Sci. Soc. Amer. Proc. 27:246-251.

Rubin, J. 1967. Numerical method for analyzing hysteresis-affected, post-infiltration redistribution of soil moisture. Soil Sci. Soc. Amer. Proc. 31:13-20.

Rubin, J. 1968. Theoretical analysis of two-dimensional, transient flow of water in unsaturated and partly unsaturated soils. Soil Sci. Soc. Amer. Proc. 32:607-615.

Saxton, K.E., H.P. Johnson, and R.H. Shaw. 1974. Modeling evapotranspiration and soil moisture. Trans. Amer. Soc. Agr. Eng. 17:673-677.

Slack, D.C., C.T. Haan, and L.G. Wells. 1977. Modeling soil water movement into plant roots. Trans. Amer. Soc. Agr. Eng. 20:919-927,933.

Smajstrla, A.G. 1973. Simulation of Miscible displacement in soils and sensitivity to the dispersion coefficient. Master's Thesis. Texas A & M University.

Smajstrla, A.G. 1982. Irrigation management for the conservation of limited water resources. Office of Water Research and Technology of the department of Interior Water Conservation Research Program (WRC-80).

Smajstrla, A.G., 1985. A field lysimeter system for crop water use and water stress studies in humid regions. Soil and Crop Sci. Soc. Fla. Proc. 44:53-59.

Smajstrla, A.G., L.R. Parsons, F.S. Zazueta, G. Vellidis, and K. Aribi. 1986. Water use and growth of young citrus trees. ASAE Paper No. 86-2069, Amer. Soc. of Agr. Eng. St. Joseph, MI.

Taylor, G.S., and J.N. Luthin. 1969. Computer methods for transient analysis of water-table aquifers. Water Resour. Res. 5:144-152.

Thomson, S.J., E.D. Threadgill, and J.R. Stansell. 1982. Field test of a microprocessor based center pivot irrigation controller. ASAE Paper No. 82-2535, Amer. Soc. of Agr. Eng. St. Joseph, MI.

Thurnau, D.H. 1963. Algorithm 195, bandsolve. Communications of the Association for Computing Machinery, 6(8):441.

Tollner, E.W., and F.J. Molz. 1983. Simulating plant water uptake in moist, lighter textured soils. Trans. Amer. Soc. Agr. Eng. 26(1):87-91.

Van Bavel, C.H.M., G.B. Strik, and K.J. Burst. 1968. Hydraulic properties of a clay loam soil and the field measurement of water uptake by roots. I. Interpretation of water content and pressure profiles. Soil Sci. Soc. Amer. Proc. 32:310-317.

Van den Honert, T.H. 1948. Water transport in plants as a catenary process. Discuss. Faraday Soc. 3:146-153.

Wooding, R.A. 1968. Steady infiltration with a shallow circular pond. Water Resour. Res. 4:1259-1273.

Zazueta, F.S., A.G. Smajstrla, and D.S. Harrison. 1984. Microcomputer control of irrigation systems I: Hardware and software considerations. Soil and Crop Sci. Soc. Fla. Proc. 43:123-129.

Zazueta, F.S., A.G. Smajstrla, and D.S. Harrison. 1985. A simple numerical model for the prediction of soil-water movement from trickle sources. Soil and Crop Sci. Soc. Fla. Proc. 44:72-76.

Zur, B., and J.W. Jones. 1981. A model for the water relations, photosynthesis , and expansive growth of crops. Water Resour. Res. 17:311-320.

BIOGRAPHICAL SKETCH

Kenneth Coy Stone was born June 25, 1959, in Tifton, Georgia. He graduated from Tiftarea Academy, Chula, Georgia, in June 1977. He then attended Abraham Baldwin Agricultural College in Tifton, Georgia, from which he received an Associate in Science degree in mathematics in June of 1979. In September of 1979 he began his undergraduate studies in agricultural engineering at the University of Georgia. He graduated from the University of Georgia with a Bachelor of Science in Agricultural Engineering degree in June 1981. He then began his graduate studies at the University of Georgia and received his Master of Science (agricultural engineering) degree in March 1985. He enrolled in the University of Florida in May 1983 to pursue the Ph.D. degree in agricultural engineering.

I certify that I have read this study and that in my opinion it conforms to acceptable standards of scholarly presentation and is fully adequate, in scope and quality, as a dissertation for the degree of Doctor of Philosophy.

Allen G. Smajstrla, Chairman
Associate Professor of
Agricultural Engineering

I certify that I have read this study and that in my opinion it conforms to acceptable standards of scholarly presentation and is fully adequate, in scope and quality, as a dissertation for the degree of Doctor of Philosophy.

James W. Jones
Professor of
Agricultural Engineering

I certify that I have read this study and that in my opinion it conforms to acceptable standards of scholarly presentation and is fully adequate, in scope and quality, as a dissertation for the degree of Doctor of Philosophy.

Fedro R. Zazueta
Assistant Professor of
Agricultural Engineering

I certify that I have read this study and that in my opinion it conforms to acceptable standards of scholarly presentation and is fully adequate, in scope and quality, as a dissertation for the degree of Doctor of Philosophy.

T. Gray Curtis
Assistant Professor of
Civil Engineering

This dissertation was submitted to the Graduate Faculty of the College of Engineering and to the Graduate School and was accepted as partial fulfillment of the requirements for the degree of Doctor of Philosophy.

May 1987

Herbert A. Bewis
Dean, College of Engineering

Dean, Graduate School

UNIVERSITY OF FLORIDA
3 1262 08554 0135